

PREPARED FOR SUBMISSION TO JHEP

# Electric Dipole Moments in 5+3 Flavor Weak Effective Theory

---

**Jacky Kumar, Emanuele Mereghetti**

*Theoretical Division, Los Alamos National Laboratory, Los Alamos, NM 87545, USA*

*E-mail:* [jacky.kumar@lanl.gov](mailto:jacky.kumar@lanl.gov), [emereghetti@lanl.gov](mailto:emereghetti@lanl.gov)

**ABSTRACT:** A fully generic treatment of electric dipole moments (EDMs) is presented in the CP-violating and flavor-conserving weak effective field theory (WET) with five flavors of quarks and three flavors of leptons. We systematically analyze leading contributions to EDMs originating from QCD and QED renormalization group running between the electroweak scale and low energy scales of about 2 GeV. We include the full one-loop anomalous dimension and a subset of two-loop corrections, as well as threshold corrections at the bottom, charm and  $\tau$  masses. This allows us to derive master formulae in the space of generic WET for the neutron and proton EDMs, for EDMs of diamagnetic atoms, and for the precession frequencies constrained in molecular EDM experiments, from which bounds on the electron EDM are extracted. In particular, our master formulae capture the contributions of WET CP-violating operators with heavy quark and lepton flavors. As an application, we study EDM constraints on the Yukawa couplings of the Higgs boson, in both the linear and non-linear realizations of electroweak symmetry breaking.

---

## Contents

<b>1</b>	<b>Introduction</b>	<b>1</b>
<b>2</b>	<b>Flavor-conserving CP-violation in WET</b>	<b>3</b>
2.1	Operator Basis for 3+1 Flavors	4
2.1.1	Dipole Operators	5
2.1.2	Weinberg Operator	5
2.1.3	Four-fermion operators with 3+1 Flavors	5
2.2	Four-fermion Operators with 5+3 Flavors	8
<b>3</b>	<b>Electric dipole moments</b>	<b>8</b>
3.1	Integrating out heavy flavors	9
3.2	Leptonic EDMs	10
3.3	ThO, YbF, and HfF Frequencies	10
3.4	Nucleon EDMs	11
3.4.1	Pion nucleon couplings	13
3.5	Diamagnetic Atomic EDMs	16
<b>4</b>	<b>Renormalization group running and threshold effects</b>	<b>18</b>
4.1	Leading-log 1-loop RG running	19
4.2	1-loop Matching	22
4.2.1	Matching to Weinberg operators	22
4.2.2	Matching to dipole operators	22
4.3	Two-step operator mixing	23
4.4	2-loop anomalous dimension	24
4.4.1	$C_{\substack{uddu \\ prrp}}^{V1,LR}, C_{\substack{uddu \\ prrp}}^{V8,LR}$ onto dipoles	26
4.4.2	$C_{\substack{uu \\ prrp}}^{V1,LR}, C_{\substack{uu \\ prrp}}^{V8,LR}$ onto dipoles	27
4.4.3	$C_{\substack{dd \\ prrp}}^{V1,LR}, C_{\substack{dd \\ prrp}}^{V8,LR}$ onto dipoles	27
4.4.4	$C_{\substack{ee \\ prrp}}^{V,LR}$ onto dipole	28
4.5	Numerical solution for the RGEs	30
<b>5</b>	<b>EDM Master Formulae in WET</b>	<b>31</b>
5.1	Theoretical uncertainties	32
5.2	$\omega_{\text{HfF}}$	32
5.3	$d_{\text{Hg}}$	33
5.4	$d_n$	34

<b>6</b>	<b>Non-standard Higgs Couplings</b>	<b>35</b>
6.1	Matching at the EW scale	37
6.2	Constraints on flavor-violating Higgs couplings	39
6.3	EDM constraints on flavor-conserving Higgs couplings	40
6.4	LHC constraints on flavor-conserving Higgs couplings	41
6.5	SMEFT Interpretation	45
<b>7</b>	<b>Summary and Outlook</b>	<b>46</b>
<b>A</b>	<b>Additional Formulae</b>	<b>49</b>
	<b>References</b>	<b>51</b>

---

## 1 Introduction

The origin of the baryon asymmetry in the Universe (BAU) is one of the most pressing open problems in particle physics. While the Standard Model (SM) satisfies the three Sakharov conditions [1] for the dynamical generation of an asymmetry, for a Higgs mass of  $m_h = 125$  GeV the electroweak (EW) phase transition does not provide sufficient deviation from thermal equilibrium to explain the observed BAU. Even if the SM were able to induce a first-order phase transition, the violation of the symmetry under a charge conjugation and parity (CP) transformation induced by the phase of the Cabibbo-Kobayashi-Maskawa (CKM) matrix would be far too weak, underpredicting the BAU by several orders of magnitude [2–5]. The generation of the BAU thus quite generally requires physics beyond the Standard Model (BSM) to have new sources of CP violation. Permanent electric dipole moments (EDMs) of leptons, nucleons, atoms, and molecules are extremely sensitive probes of flavor-diagonal CP-violation, as they can be constrained very accurately and receive negligible contributions from the phase of the CKM matrix. For example, the current bound on the neutron EDM is  $|d_n| < 1.8 \cdot 10^{-26}$  e cm, naively probing BSM physics at scales far above 10 TeV. On the other hand, this bound is five to six orders of magnitude away from the contribution of the SM [6–10]. An observation of a neutron EDM in the next generation of experiments would then be a clear indication of CP violation beyond the CKM paradigm, and observations in multiple systems will be able to rule out a QCD  $\bar{\theta}$  term and demonstrate the existence of BSM CP violation. For this reason, a rich experimental program is in place, with ongoing and planned searches in different systems, from the muon and tau leptons to the neutron, to atomic and molecular systems, aiming at improving current bounds by at least one or two orders of magnitude [11, 12].

Because of the strength of existing and upcoming constraints, it is important to address the question of what existing EDM experiments teach us about CP violation in generic BSM scenarios. In addition, assuming multiple observations of non-zero EDMs in the next generation of experiments, we will be faced with the “inverse problem” of identifying the

fundamental mechanism of CP violation from a set of low-energy measurements. Effective Field Theories (EFT) provide the theoretical tools to answer these questions with minimal reliance on specific models of BSM physics [13]. First of all, EFTs such as the Weak EFT (WET) [14, 15] allow one to organize all possible flavor-diagonal ( $\Delta F = 0$ ) CP-violating operators of a given dimension. Secondly, in WET it is possible to systematically consider loop effects, such as renormalization group (RG) evolution and matching corrections induced by heavy quark thresholds, and to connect low-scale observables with physics at the electroweak scale. Here one can match WET onto other EFTs, such as the Standard Model EFT (SMEFT) [16, 17] or the Higgs EFT (HEFT) [18, 19], and study collider phenomenology. This tower of EFTs provides a general and model-independent link between EDMs, other precision flavor observables, and collider experiments, which will be necessary to solve the aforementioned inverse problem.

The advantages of parameterizing EDMs in terms of a minimal set of low-energy operators have long been recognized [10, 20], and there is a vast literature on EDM calculations in specific BSM models (see [10, 11, 21] and references therein). In EFTs, EDMs in the SMEFT at tree level and the matching onto hadronic EFTs were considered in Ref. [22]. Beyond the tree level, the contributions to EDMs induced by classes of SMEFT operators, including in the Yukawa [13, 23–28], top [29, 30], heavy flavor [31, 32], Higgs-gauge [33–35], right-handed charged current [36] and flavor [37, 38] sectors, have been studied in a mostly piecemeal approach. A more systematic analysis of the 1-loop contributions to EDMs in SMEFT was carried out in Ref. [39], but mostly with a focus on the electron and nucleon EDMs. This paper is a first step towards a complete study of  $\Delta F = 0$  CP violation in EFT extensions of the SM, and its correlations with other sectors of the theory (such as the Higgs and flavor sectors). We focus here on CP-violating (CPV)  $\Delta F = 0$  WET operators, with  $n_f = 5$  quark flavors and  $n_\ell = 3$  lepton flavors. The main new results of this work are:

- We derive master formulae for the neutron, proton, and diamagnetic EDMs, and for the precession frequencies in molecular EDM experiments, in terms of the full set of  $\Delta F = 0$  WET operators at the electroweak scale. The master formulae for  $\omega_{\text{HFF}}$ , and  $\omega_{\text{ThO}}$ ,  $\omega_{\text{YbF}}$  are given in Tables 7 and 15, respectively. Contributions to  $d_{\text{Hg}}$  are listed in Tables 8 and 9, while the neutron and proton EDMs,  $d_n$  and  $d_p$ , are given in Tables 10 and 16, respectively.
- The expressions use up-to-date hadronic and nuclear matrix elements, which are however still affected by large and often uncontrolled theoretical uncertainties. For hadronic matrix elements, including the neutron and proton EDMs and CPV pion-nucleon couplings, we rely as much as possible on information from Lattice QCD, using either direct EDM calculations or indirect calculations (such as Lattice QCD calculations of mesonic matrix elements which contribute to pion-nucleon couplings). The implementation of the master formulae in the package `flavio` [40] allows for a quick implementation of new matrix elements, as soon as they become available.
- For WET operators involving only the  $u$ ,  $d$  and  $s$  quark flavors ( $n_f = 3$ ) and the

electron ( $n_\ell = 1$ ), our formulae have leading logarithmic accuracy. We present master formulae in the Jenkins, Manohar, and Stoffer (JMS) basis for WET [14, 15], which can be easily connected to the SMEFT.

- We consider the contributions of operators with heavy quark ( $c$  and  $b$ ) and lepton ( $\mu$  and  $\tau$ ) flavors, where renormalization group mixing and matching at the heavy fermion thresholds are crucial. In the case of scalar four-quark operators, all operators with two heavy and two light quarks contribute to EDMs at leading logarithmic accuracy. Scalar operators with four heavy quarks do not contribute at the leading log. In this case, we identify next-to-leading logarithmic contributions, arising from 1-loop running and 1-loop matching at the heavy flavor threshold. Since the renormalization group mixing is mostly driven by QCD,  $d_n$  and  $d_{\text{Hg}}$  provide strong constraints even on scalar operators with only heavy quarks.
- Four-quark vector operators with two heavy and two light quarks also contribute at the next-to-leading log. In this case, the dominant contributions arise from 2-loop running and 1-loop matching. Four-quark vector operators with two  $b$  and two  $c$  quarks contribute at the next-to-next-to-leading log. EDM contributions from scalar and vector operators with the same flavors are comparable.
- Leptonic operators with two heavy leptons and two electrons contribute to the electron EDM at the leading log and next-to-leading log for scalar and vector operators, respectively. We also find that all semileptonic operators with two muons or  $\tau$  leptons contribute to EDMs of diamagnetic atoms at the order we are working. Since the mixing is driven by QED and proportional to the lepton masses, however, some of the constraints are weak, especially for muonic operators.

As we illustrate in Section 6, the WET master formulae can be easily adapted to EFTs at the electroweak scale, by calculating the matching coefficients in SMEFT, HEFT, or in any given BSM model.

The paper is organized as follows. In Section 2 we introduce the WET basis of  $\Delta F = 0$  CPV operators. In Section 3 we provide expressions for the neutron, atomic, and molecular EDMs in terms of WET operators at low energy. In Section 4 we discuss the renormalization group evolution and threshold effects and in Section 5 we provide master formulae for EDMs in terms of WET coefficients at the electroweak scale. In Section 6 we discuss one example of application of the master formulae, EDM constraints on non-standard Higgs couplings. We conclude in Section 7.

## 2 Flavor-conserving CP-violation in WET

There are numerous sources of CP-violation in WET at the dim-4, 5, and 6 levels. Since our main goal is to study EDMs, we will restrict ourselves to flavor-conserving WET operators. We can identify two kinds of contributions. Operators constructed out of light fermion flavors, like  $u, d$ , or  $s$  quarks or electrons, generate EDMs at the tree level. As we will see, they will receive the strongest constraints. Operators that contain heavier

quark and lepton generations can also contribute via loop effects originating either from the renormalization group running or from threshold effects. Below we consider the full list of WET operators with five quark and three lepton flavors that can contribute to EDMs. Very schematically, WET Wilson coefficients at low energy are obtained by solving renormalization group equations (RGEs), which give rise to expressions of the form

$$C(\mu) = \left[ \sum_{n=0} \left( \frac{g^2}{(4\pi)^2} \right)^n \log^n \frac{\mu}{\mu_{ew}} + \sum_{n=1} \left( \frac{g^2}{(4\pi)^2} \right)^n \log^{n-1} \frac{\mu}{\mu_{ew}} + \dots \right] \times C(\mu_{ew}), \quad (2.1)$$

where  $g$  here stands for any coupling in WET, and  $\mu_{ew}$  is a scale close to the electroweak. The first and second terms in the bracket on the r.h.s of Eq. (2.1) denote the leading logarithmic (LL) and next-to-leading logarithmic (NLL) series. As we will discuss, the great majority of  $\Delta F = 0$  CPV operators feeds into light flavor operators at LL. These contributions are captured by the solution of the WET 1-loop RGEs, which are known [15, 41, 42]. Certain classes of operators, including, for example, vector left-right operators, do not contribute at LL. In these cases, we identify NLL corrections, arising from 2-loop running and 1-loop matching at the heavy quark threshold. A summary of the order in which each WET operator contributes is given in Table 1, where operators contributing at LL, NLL, and next-to-next-to-leading log (NNLL) are indicated by no asterisk, or single and double asterisks, respectively. We stress that, while the logarithmic series expansion in Eq. (2.1) provides useful guidance to organize WET contributions to EDMs, and we will therefore use it throughout the paper, the RGEs involve small couplings (e.g. the QED coupling), for which the suppression from additional loops is not fully offset by the large logarithms. In these cases, it is possible that higher loop corrections to matching and running will be more important than those included here. These can only be captured by pushing the calculations of WET anomalous dimensions and matching corrections to higher order. For the sake of generality, we also include the operators that cannot be generated in SMEFT at leading order, i.e. the ones that violate the hypercharge quantum number.

In the JMS basis complete 1-loop anomalous dimension matrices (ADMs) are known [14, 15]. Moreover, the complete 1-loop matching conditions of WET onto SMEFT has been recently worked out [43] in the JMS basis. Given these developments, it is useful to express the EDMs in terms of the Wilson coefficients (WCs) of the JMS basis so that their connection to UV physics can be easily established. The translation of the JMS WCs into several other popular WET bases or vice versa can be numerically carried out using the `wilson` [44] program, which we also use to perform the LL component of the RG running. Moreover, throughout this paper, we will follow the WCxf conventions for WET and SMEFT [45].

## 2.1 Operator Basis for 3+1 Flavors

At dim-4 in WET, CP can be violated by a complex quark mass term and by the QCD  $\bar{\theta}$  term. We choose to work in a basis in which the quark mass matrices are diagonal and real, so that, at dim-4, the only CP-odd interactions is

$$\mathcal{L}_\theta = \bar{\theta} \frac{g_s^2}{32\pi^2} \tilde{G}_{\mu\nu}^A G^{A\mu\nu}, \quad (2.2)$$

where  $g_s$  is the strong coupling constant,  $G_{\mu\nu}^A$  is the gluon field strength and  $\tilde{G}_{\mu\nu}^A = \frac{1}{2}\varepsilon_{\mu\nu\alpha\beta}G^{A\alpha\beta}$ . Throughout this paper, we assume that the contribution of the  $\bar{\theta}$  term to EDMs is canceled by the Peccei-Quinn (PQ) mechanism [46, 47].

In a  $n_f = 3 + 1$  flavor theory, the dipole operators can contribute to EDMs at the dim-5 level. At dim-6, there are contributions from the Weinberg three-gluon operator and various four-fermion operators.

### 2.1.1 Dipole Operators

The flavor-conserving QCD and QED dipole operators are given by

$$\begin{aligned} [O_{u\gamma}]_{ii} &= (\bar{u}_i\sigma^{\mu\nu}P_Ru_i)F_{\mu\nu}, & [O_{d\gamma}]_{ii} &= (\bar{d}_i\sigma^{\mu\nu}P_Rd_i)F_{\mu\nu}, \\ [O_{uG}]_{ii} &= (\bar{u}_i\sigma^{\mu\nu}T^AP_Ru_i)G_{\mu\nu}^A, & [O_{dG}]_{ii} &= (\bar{d}_i\sigma^{\mu\nu}T^AP_Rd_i)G_{\mu\nu}^A, \\ [O_{e\gamma}]_{ii} &= (\bar{e}_i\sigma^{\mu\nu}P_Re_i)F_{\mu\nu}. \end{aligned} \quad (2.3)$$

Here  $ii$  indicates the flavor index and  $T^A$  are the  $SU(3)_c$  generators. Down-type type operators having  $ii = 11, 22$ , and up-type quarks with  $ii = 11$  directly contribute to the neutron and atomic EDMs. Dipole operators with  $b$  and  $c$  quarks contribute via loops. In the leptonic sector,  $ii = 11, 22$ , and  $33$  contribute directly to electron, muon, and  $\tau$  EDMs, respectively. Since the limits on  $d_\mu$  and  $d_\tau$  are much weaker than on the electron EDM, it is important also to consider the matching and running of heavier leptons into leptonic and semileptonic operators that contribute to molecular EDMs.

### 2.1.2 Weinberg Operator

The CPV Weinberg operator has the form

$$[O_{\tilde{G}}] = f^{ABC}\tilde{G}_\mu^{A\nu}G_\nu^{B\rho}G_\rho^{C\mu}. \quad (2.4)$$

Here  $f^{ABC}$  are the structure constants of the  $SU(3)_c$  group. Note that the WC  $[C_{\tilde{G}}]$  is real by definition.

### 2.1.3 Four-fermion operators with 3+1 Flavors

In this section, we give a complete list of four-fermion WET operators with  $n_f = 3 + 1$  quark and lepton flavors. All of these operators enter directly into the EDM expressions, hence these are the leading operators. A four-fermion basis in terms of scalar-pseudoscalar and tensor operators was presented in Ref. [48], where the 1-loop matching to the gradient flow scheme used in Lattice QCD calculations is also provided. Here, to facilitate the renormalization group evolution and the matching to EFTs at the electroweak scale, we adopt the JMS basis. In the first category, we consider vector operators having  $(LL)(RR)$  chiralities of the fermion currents. These are given by

$$\begin{aligned} [O_{uddu}^{V1,LR}]_{ijkl} &= (\bar{u}_i\gamma^\mu P_Ld_j)(\bar{d}_k\gamma_\mu P_Ru_l), \\ [O_{uddu}^{V8,LR}]_{ijkl} &= (\bar{u}_i\gamma^\mu P_LT^Ad_j)(\bar{d}_k\gamma_\mu P_RT^Au_l), \\ [O_{dd}^{V1,LR}]_{ijkl} &= (\bar{d}_i\gamma^\mu P_Ld_j)(\bar{d}_k\gamma_\mu P_Rd_l), \\ [O_{dd}^{V8,LR}]_{ijkl} &= (\bar{d}_i\gamma^\mu P_LT^Ad_j)(\bar{d}_k\gamma_\mu P_RT^Ad_l). \end{aligned} \quad (2.5)$$

These lead to six flavor structures that are CP-violating and directly contribute to EDMs:

$$[O_{uddu}^{V1,LR}]_{1111}, [O_{uddu}^{V1,LR}]_{1221}, [O_{uddu}^{V8,LR}]_{1111}, [O_{uddu}^{V8,LR}]_{1221}, [O_{dd}^{V1,LR}]_{1221}, [O_{dd}^{V8,LR}]_{1221}. \quad (2.6)$$

In the next category, there are various scalar operators. First we have  $(LR)(LR)$  up-type operators

$$\begin{aligned} [O_{uu}^{S1,RR}]_{ijkl} &= (\bar{u}_i P_R u_j)(\bar{u}_k P_R u_l), \\ [O_{uu}^{S8,RR}]_{ijkl} &= (\bar{u}_i P_R T^A u_j)(\bar{u}_k P_R T^A u_l). \end{aligned} \quad (2.7)$$

The following two operators are CP-violating and enter at the tree-level

$$[O_{uu}^{S1,RR}]_{1111}, [O_{uu}^{S8,RR}]_{1111}. \quad (2.8)$$

The down-type operators are given by

$$\begin{aligned} [O_{dd}^{S1,RR}]_{ijkl} &= (\bar{d}_i P_R d_j)(\bar{d}_k P_R d_l), \\ [O_{dd}^{S8,RR}]_{ijkl} &= (\bar{d}_i P_R T^A d_j)(\bar{d}_k P_R T^A d_l). \end{aligned} \quad (2.9)$$

Here the following eight operators directly contribute

$$\begin{aligned} [O_{dd}^{S1,RR}]_{1111}, [O_{dd}^{S8,RR}]_{1111}, [O_{dd}^{S1,RR}]_{2222}, [O_{dd}^{S8,RR}]_{2222}, \\ [O_{dd}^{S1,RR}]_{1122}, [O_{dd}^{S8,RR}]_{1122}, [O_{dd}^{S1,RR}]_{1221}, [O_{dd}^{S8,RR}]_{1221}. \end{aligned} \quad (2.10)$$

Then the operators containing both up and down-quark come in two sub-categories. The first one is

$$\begin{aligned} [O_{ud}^{S1,RR}]_{ijkl} &= (\bar{u}_i P_R u_j)(\bar{d}_k P_R d_l), \\ [O_{ud}^{S8,RR}]_{ijkl} &= (\bar{u}_i P_R T^A u_j)(\bar{d}_k P_R T^A d_l). \end{aligned} \quad (2.11)$$

The following four flavor structures can contribute

$$[O_{ud}^{S1,RR}]_{1111}, [O_{ud}^{S8,RR}]_{1111}, [O_{ud}^{S1,RR}]_{1122}, [O_{ud}^{S8,RR}]_{1122}. \quad (2.12)$$

In the second sub-category, we have the operators

$$\begin{aligned} [O_{uddu}^{S1,RR}]_{ijkl} &= (\bar{u}_i P_R d_j)(\bar{d}_k P_R u_l), \\ [O_{uddu}^{S8,RR}]_{ijkl} &= (\bar{u}_i P_R T^A d_j)(\bar{d}_k P_R T^A u_l). \end{aligned} \quad (2.13)$$

The following four operators contribute

$$[O_{uddu}^{S1,RR}]_{1111}, [O_{uddu}^{S8,RR}]_{1111}, [O_{uddu}^{S1,RR}]_{1221}, [O_{uddu}^{S8,RR}]_{1221}. \quad (2.14)$$

In total, there are 24 four-quark operators with  $n_f = 3$ , in agreement with Ref. [48]. Semileptonic operators contribute to molecular and atomic EDMs at the tree level

$$\begin{aligned} [O_{eu}^{S,RL}]_{ijkl} &= (\bar{e}_i P_R e_j)(\bar{u}_k P_L u_l), & [O_{ed}^{S,RL}]_{ijkl} &= (\bar{e}_i P_R e_j)(\bar{d}_k P_L d_l), \\ [O_{eu}^{S,RR}]_{ijkl} &= (\bar{e}_i P_R e_j)(\bar{u}_k P_R u_l), & [O_{ed}^{S,RR}]_{ijkl} &= (\bar{e}_i P_R e_j)(\bar{d}_k P_R d_l), \\ [O_{eu}^{T,RR}]_{ijkl} &= (\bar{e}_i \sigma^{\mu\nu} P_R e_j)(\bar{u}_k \sigma_{\mu\nu} P_R u_l), & [O_{ed}^{T,RR}]_{ijkl} &= (\bar{e}_i \sigma^{\mu\nu} P_R e_j)(\bar{d}_k \sigma_{\mu\nu} P_R d_l). \end{aligned} \quad (2.15)$$



Four-fermion Operators for EDMs with $n_q + n_\ell$ flavors					
$u, d, s, e$ operators in 3+1 flavor WET					
$[O_{uddu}^{V1,LR}]_{1111}$	$[O_{uddu}^{V8,LR}]_{1111}$	$[O_{uddu}^{V1,LR}]_{1221}$	$[O_{uddu}^{V8,LR}]_{1221}$	$[O_{dd}^{V1,LR}]_{1221}$	$[O_{dd}^{V8,LR}]_{1221}$
$[O_{uu}^{S1,RR}]_{1111}$	$[O_{uu}^{S8,RR}]_{1111}$	$[O_{dd}^{S1,RR}]_{1111}$	$[O_{dd}^{S8,RR}]_{1111}$	$[O_{dd}^{S1,RR}]_{2222}$	$[O_{dd}^{S8,RR}]_{2222}$
$[O_{dd}^{S1,RR}]_{1122}$	$[O_{dd}^{S8,RR}]_{1122}$	$[O_{dd}^{S1,RR}]_{1221}$	$[O_{dd}^{S8,RR}]_{1221}$	$[O_{ud}^{S1,RR}]_{1111}$	$[O_{ud}^{S8,RR}]_{1111}$
$[O_{ud}^{S1,RR}]_{1122}$	$[O_{ud}^{S8,RR}]_{1122}$	$[O_{uddu}^{S1,RR}]_{1111}$	$[O_{uddu}^{S8,RR}]_{1111}$	$[O_{uddu}^{S1,RR}]_{1221}$	$[O_{uddu}^{S8,RR}]_{1221}$
$[O_{eu}^{S,RL}]_{1111}$	$[O_{eu}^{S,RR}]_{1111}$	$[O_{ed}^{S,RL}]_{1111}$	$[O_{ed}^{S,RR}]_{1111}$	$[O_{ed}^{S,RL}]_{1122}$	$[O_{ed}^{S,RR}]_{1122}$
$[O_{eu}^{T,RR}]_{1111}$	$[O_{ed}^{T,RR}]_{1111}$	$[O_{ed}^{T,RR}]_{1122}$	$[O_{ee}^{S,RR}]_{1111}^*$		
$c$ operators $\subset$ 4+1 flavor WET					
$[O_{uu}^{S1,RR}]_{2222}^*$	$[O_{uu}^{S8,RR}]_{2222}^*$	$[O_{ud}^{S1,RR}]_{1122}$	$[O_{uu}^{S8,RR}]_{1122}$	$[O_{ud}^{S1,RR}]_{2211}$	$[O_{ud}^{S8,RR}]_{2211}$
$[O_{ud}^{S1,RR}]_{2222}$	$[O_{ud}^{S8,RR}]_{2222}$	$[O_{uddu}^{S1,RR}]_{2112}$	$[O_{uddu}^{S8,RR}]_{2112}$	$[O_{uddu}^{S1,RR}]_{2222}$	$[O_{uddu}^{S8,RR}]_{2222}$
$[O_{uu}^{S1,RR}]_{1221}$	$[O_{uu}^{S8,RR}]_{1221}$	$[O_{uddu}^{V1,LR}]_{2112}^*$	$[O_{uddu}^{V8,LR}]_{2112}^*$	$[O_{uddu}^{V1,LR}]_{2222}^*$	$[O_{uddu}^{V8,LR}]_{2222}^*$
$[O_{uu}^{V1,LR}]_{1221}^*$	$[O_{uu}^{V8,LR}]_{1221}^*$				
$[O_{eu}^{S,RR}]_{1122}$	$[O_{eu}^{T,RR}]_{1122}$				
$b, \mu, \tau$ operators $\subset$ 5+3 flavor WET					
$[O_{dd}^{S1,RR}]_{3333}^*$	$[O_{dd}^{S8,RR}]_{3333}^*$	$[O_{dd}^{S1,RR}]_{1133}$	$[O_{dd}^{S8,RR}]_{1133}$	$[O_{dd}^{S1,RR}]_{2233}$	$[O_{dd}^{S8,RR}]_{2233}$
$[O_{dd}^{S1,RR}]_{1331}$	$[O_{dd}^{S8,RR}]_{1331}$	$[O_{dd}^{S1,RR}]_{2332}$	$[O_{dd}^{S8,RR}]_{2332}$	$[O_{ud}^{S1,RR}]_{1133}$	$[O_{ud}^{S8,RR}]_{1133}$
$[O_{uddu}^{S1,RR}]_{1331}$	$[O_{uddu}^{S8,RR}]_{1331}$	$[O_{ud}^{S1,RR}]_{2233}^*$	$[O_{ud}^{S8,RR}]_{2233}^*$	$[O_{uddu}^{S1,RR}]_{2332}^*$	$[O_{uddu}^{S8,RR}]_{2332}^*$
$[O_{uddu}^{V1,LR}]_{1331}^*$	$[O_{uddu}^{V8,LR}]_{1331}^*$	$[O_{dd}^{V1,LR}]_{1331}^*$	$[O_{dd}^{V8,LR}]_{1331}^*$	$[O_{dd}^{V1,LR}]_{2332}^*$	$[O_{dd}^{V8,LR}]_{2332}^*$
$[O_{uddu}^{V1,LR}]_{2332}^{**}$	$[O_{uddu}^{V8,LR}]_{2332}^{**}$				
$[O_{ed}^{T,RR}]_{1133}$	$[O_{ed}^{T,RR}]_{2211}$	$[O_{ed}^{T,RR}]_{2222}$	$[O_{ed}^{T,RR}]_{2233}^*$	$[O_{ed}^{T,RR}]_{3311}$	$[O_{ed}^{T,RR}]_{3322}$
$[O_{ed}^{T,RR}]_{3333}^*$	$[O_{eu}^{T,RR}]_{2211}$	$[O_{eu}^{T,RR}]_{2222}^*$	$[O_{eu}^{T,RR}]_{3311}$	$[O_{eu}^{T,RR}]_{3322}^*$	
$[O_{ed}^{S,RR}]_{1133}$	$[O_{ed}^{S,RR}]_{2211}$	$[O_{ed}^{S,RR}]_{2222}$	$[O_{ed}^{S,RR}]_{2233}^*$	$[O_{ed}^{S,RR}]_{3311}$	$[O_{ed}^{S,RR}]_{3322}$
$[O_{ed}^{S,RR}]_{3333}^*$	$[O_{eu}^{S,RR}]_{2211}$	$[O_{eu}^{S,RR}]_{2222}^*$	$[O_{eu}^{S,RR}]_{3311}$	$[O_{eu}^{S,RR}]_{3322}^*$	
$[O_{ee}^{V,LR}]_{1221}^*$	$[O_{ee}^{V,LR}]_{1331}^*$	$[O_{ee}^{S,RR}]_{1221}$	$[O_{ee}^{S,RR}]_{1331}$	$[O_{ee}^{S,RR}]_{1122}$	$[O_{ee}^{S,RR}]_{1133}$

**Table 1:** The complete list of four-fermion flavor conserving CP-violating operators relevant for EDMs in  $n_q + n_\ell = 5+3$  Flavor WET below the EW scale. Here the LL, NLL, and NNLL operators are marked by no asterisk, single asterisk, and double asterisk signs, respectively.

The relevant flavor structures for semi-leptonic operators are

$$\begin{aligned}
& [O_{eu}^{S,RL}]_{1111}, [O_{eu}^{S,RR}]_{1111}, [O_{ed}^{S,RL}]_{1111}, [O_{ed}^{S,RR}]_{1111}, \\
& [O_{ed}^{S,RL}]_{1122}, [O_{ed}^{S,RR}]_{1122}, [O_{eu}^{T,RR}]_{1111}, [O_{ed}^{T,RR}]_{1111}, \\
& [O_{ed}^{T,RR}]_{1122}.
\end{aligned} \tag{2.16}$$

Finally, we note that there are no leptonic operators that can contribute at the tree-level to any of the EDMs. As we will see, the purely leptonic operator can contribute at one loop. In particular, the scalar operator

$$[O_{ee}^{S,RR}]_{ijkl} = (\bar{e}_i P_R e_j)(\bar{e}_k P_R e_l) \tag{2.17}$$

can mix onto the electron EDM. In the 3 + 1 theory, the relevant flavor structure is

$$[O_{ee}^{S,RR}]_{1111}. \tag{2.18}$$

## 2.2 Four-fermion Operators with 5+3 Flavors

In this section, we list the leading heavy flavor (5+3) four-fermion operators that contribute up to the 2-loop level via matching and running effects. The only new Lorentz structure appearing due to loop effects is the pure leptonic operator

$$[O_{ee}^{V,LR}]_{ijkl} = (\bar{e}_i \gamma^\mu P_L e_j)(\bar{e}_k \gamma_\mu P_R e_l). \tag{2.19}$$

This operator can break CP if  $i \neq j$ , so that the CP-odd coefficients are

$$[O_{ee}^{V,LR}]_{1221}, [O_{33}^{V,LR}]_{1331}. \tag{2.20}$$

These two operators contribute to the electron EDM at the 2-loop QED level. Otherwise, only new flavor structures are added to the EDM basis for the 5+3 theory. The complete list of relevant WET operators containing 3+1, 4+1, and 5+3 quark and lepton flavors ( $n_q + n_\ell$ ) is given in Table 1. In this table, the operators are categorized based on their contributions to the EDMs at the LL, NLL, and NNLL order in RG improved perturbation theory. The order is indicated by the asterisk signs.

## 3 Electric dipole moments

Electric dipole moments are an extremely sensitive probe of  $\Delta F = 0$  CP-violation at low energy. The strongest constraints currently come from measurements in ThO [49], HfF [50], and YbF [51], which can be interpreted as bounds on the electron EDM, and from bounds on the neutron EDM [52] and on the EDM of  $^{199}\text{Hg}$  [53]. Experiments looking for the EDM of  $^{129}\text{Xe}$  [54] and  $^{225}\text{Ra}$  [55] are at the moment weaker, but they provide constraints on independent combinations of hadronic parameter and Wilson coefficients [56]. A summary of current EDM bounds is shown in Table 2. In the future, the limits on the electron EDM are expected to improve by at least a factor of ten, while new molecular EDM experiments sensitive to nuclear Schiff moments could lead to a large

	$d_e$	$d_n$	$d_{\text{Hg}}$	$d_p$	$d_{\text{Xe}}$	$d_{\text{Ra}}$
current limit	$4.0 \cdot 10^{-30}$	$1.8 \cdot 10^{-26}$	$6.2 \cdot 10^{-30}$	x	$1.4 \cdot 10^{-27}$	$4.2 \cdot 10^{-22}$
expected limit	$4.0 \cdot 10^{-29}$	$1.0 \cdot 10^{-28}$	$6.2 \cdot 10^{-30}$	$1.0 \cdot 10^{-29}$	$1.4 \cdot 10^{-28}$	$1.0 \cdot 10^{-27}$
	$\omega_{\text{ThO}}$	$\omega_{\text{HfF}}$	$\omega_{\text{YbF}}$			
current limit	1.3 mrad/s	0.17 mrad/s	23.5 mrad/s			

**Table 2:** Current limits on the electron [50], neutron [52], and mercury [53, 63] EDMs in units of  $e$  cm (90% confidence level). We also show an indication of their prospective limits [12, 56, 64] as well as those of the proton, xenon [54], and radium [55] EDMs, which could provide interesting constraints in the future. The electron EDM bound is extracted from CPV precession frequencies in molecular EDM experiments and thus depends on the assumptions that no other CPV operator contributes. In our analysis, we will use directly the constraints on the precession frequencies in HfF [50], ThO [49], and YbF [51], which are shown in the bottom part of the table. In the future, the precession frequencies are expected to improve by one order.

improvement in the constraints on hadronic CPV interactions [57]. Several experimental collaborations, including n2EDM at the Paul Scherrer Institute [58], PanEDM [59] at the Institute Laue Langevin, TUCAN EDM at Triumf [60], and LANL EDM at Los Alamos National Laboratory [61], aim at improving the bound on the neutron EDM by one order of magnitude. Finally, EDMs of light ions such as the proton, deuteron, or  $^3\text{He}$  could be measured in storage ring experiments [62]. To estimate future EDM sensitivities, we will use the projection on the second row of Table 2. In the following subsections, we will express the EDMs of charged leptons, the neutron and proton EDMs, atomic EDMs, and the CPV precession frequencies measured in molecular experiments in terms of WET operators at low energy, while in Section 4 we will show how these operators are generated from WET operators at the EW scale, via running and matching effects.

### 3.1 Integrating out heavy flavors

In this paper, we integrate out heavy quarks and leptons at, or close to, their mass threshold. In particular, we integrate out the  $b$  quark at  $\mu_b = m_b^{\overline{\text{MS}}} = 4.18$  GeV, and the charm quark at  $\mu_c = 2$  GeV. We thus do not consider nonperturbative matrix elements of operators with  $b$  and  $c$  quarks between nucleons or nucleons and pions, but take their effects into account in perturbation theory, via renormalization group mixing or matching at the threshold. For the  $b$  quark, with  $\alpha_s(m_b^{\overline{\text{MS}}})$  well in the perturbative regime, this approach is fully justified. Since the  $c$  quark lies at the boundary between the perturbative and nonperturbative regimes, in this case one could pursue the alternative approach of not integrating out the  $c$ , and evaluating charm matrix elements in Lattice QCD. While most Lattice QCD collaborations use actions with dynamical charm quarks, calculations of nucleon charm matrix elements are very preliminary in the case of quark bilinears [65], and non-existing for more complicated operators, such as the charm quark chromoelectric dipole moment or four-fermion operators. One would thus have to rely on models, which

come with uncontrolled uncertainties. As Lattice QCD calculations improve, it will become interesting to compare the perturbative and nonperturbative treatment of heavy quarks.

### 3.2 Leptonic EDMs

For the electron, muon, and  $\tau$  EDMs, there is a direct connection between the WET dipole operators  $C_{e\gamma}$  and the electric dipole moment. In addition, the semileptonic tensor operators  $[C_{eq}^{T,RR}]$  with light quark flavors induce charged lepton dipole operator non-perturbatively [66, 67], with a contribution proportional to the correlator of the vector and tensor currents  $\Pi_{VT}(\mathbf{q})$  [68]

$$\begin{aligned} d_\ell &= -2\text{Im} \left[ C_{e\gamma} - 2i\Pi_{VT}(0) \left( q_u [C_{eu}^{T,RR}]_{1111} + q_d [C_{ed}^{T,RR}]_{1111} + q_s [C_{ed}^{T,RR}]_{1122} \right) \right]_{\ell\ell} \\ &= -1.3 \cdot 10^{-16} \left[ C_{e\gamma} - 2.5 \cdot 10^{-5} \text{TeV} \left( 2 [C_{eu}^{T,RR}]_{1111} - [C_{ed}^{T,RR}]_{1111} - [C_{ed}^{T,RR}]_{1122} \right) \right]_{\ell\ell} \text{TeV } e \text{ cm}, \end{aligned} \quad (3.1)$$

with  $q_u = 2/3$  and  $q_d = q_s = -1/3$ . In Eq. (3.1), and in the rest of this section, the WET couplings are understood to be evaluated at the scale of  $\mu = 2$  GeV. Here we use a resonance model for  $\Pi_{VT}$  and write [68–71]

$$i\Pi_{VT}(0) = \frac{B_0 F_\pi^2}{M_\rho^2}, \quad (3.2)$$

with the quark condensate  $B_0 = 2.7$  GeV at the renormalization scale  $\mu = 2$  GeV,  $F_\pi = 92.2$  MeV and  $M_\rho = 0.770$  GeV. The above estimate is based on large  $N_C$  considerations, and on the truncation of the resonance spectrum to the first state, and it is therefore affected by large theoretical uncertainties, which were estimated to be at least 50% [68–71].

The limit on the electron EDM, as extracted from HfF and ThO measurements [49, 50], is shown in Table 2. Direct limits exist on the muon EDM, from  $g - 2$  storage ring experiments [72], and on the EDM of the tau lepton, from the measurement of spin-momentum correlations in  $\tau$  decays at  $e^+e^-$  machines [73]. The current limits are [74]

$$|d_\mu| < 1.8 \cdot 10^{-19} e \text{ cm}, \quad -0.185 \cdot 10^{-16} e \text{ cm} < d_\tau < 0.061 \cdot 10^{-16} e \text{ cm}. \quad (3.3)$$

These are much weaker than the electron EDM bound so running effects of  $\mu$  and  $\tau$  flavor operators onto electron operators can be important.

### 3.3 ThO, YbF, and HfF Frequencies

The best limit on the electron EDM currently comes from experiments with polar molecules. In this case, the observables are the parity ( $P$ ) and time-reversal ( $T$ ) odd frequency shifts  $\omega$ , which receive contributions from the electron EDM and semileptonic scalar operators. The frequency shifts are expressed in terms of an isospin invariant and an isospin-breaking electron-nucleon coupling, captured by the Lagrangian

$$\mathcal{L} = -\frac{G_F}{\sqrt{2}} \bar{e} i \gamma_5 e \bar{N} \left( C_S^{(0)} + \tau_3 C_S^{(1)} \right) N, \quad (3.4)$$

with  $N = (p, n)$  the nucleon doublet and  $\tau_3$  a Pauli matrix in isospin space. The nucleon-level scalar couplings can be expressed in terms of WET four-fermion operators as

$$C_S^{(0)} = -\frac{v^2}{2} \left( \text{Im}[C_{eu}^{\text{SRL}}]_{1111} + \text{Im}[C_{eu}^{\text{SRR}}]_{1111} + \text{Im}[C_{ed}^{\text{SRL}}]_{1111} + \text{Im}[C_{ed}^{\text{SRR}}]_{1111} \right) \frac{\sigma_{\pi N}}{\bar{m}} - v^2 \left( \text{Im}[C_{ed}^{\text{SRL}}]_{1122} + \text{Im}[C_{ed}^{\text{SRR}}]_{1122} \right) \frac{\sigma_s}{m_s} \quad (3.5)$$

$$C_S^{(1)} = -\frac{v^2}{2} \left( \text{Im}[C_{eu}^{\text{SRL}}]_{1111} + \text{Im}[C_{eu}^{\text{SRR}}]_{1111} - \text{Im}[C_{ed}^{\text{SRL}}]_{1111} - \text{Im}[C_{ed}^{\text{SRR}}]_{1111} \right) g_S^{u-d}, \quad (3.6)$$

where  $2\bar{m} = m_u + m_d$ , and  $v = 246$  GeV. For the nucleon  $\sigma_{\pi N}$  term, we use the extraction from  $\pi$ -nucleon scattering data [75]

$$\sigma_{\pi N} = 59.0 \pm 3.5 \text{ MeV}. \quad (3.7)$$

For the strange  $\sigma$  term and the isovector scalar charge, we use the FLAG lattice averages [76]

$$\sigma_s = 52.9 \pm 7.0 \text{ MeV}, \quad g_S^{u-d} = 1.02 \pm 0.10, \quad (3.8)$$

where the scalar charge is evaluated at the renormalization scale  $\mu = 2$  GeV. With these definitions, we can express the frequency measured in the HfF, ThO, and YbF experiments as [11, 77, 78]

$$\omega_{\text{HfF}} = \left[ (34.9 \pm 1.4) \left( \frac{d_e}{10^{-27} e \text{ cm}} \right) + (32_{-2}^{+1}) \left( \frac{C_S}{10^{-7}} \right) \right] (\text{mrad/s}) \quad (3.9)$$

$$\omega_{\text{ThO}} = - \left[ (121_{-39}^{+5}) \left( \frac{d_e}{10^{-27} e \text{ cm}} \right) + (182_{-27}^{+42}) \left( \frac{C_S}{10^{-7}} \right) \right] (\text{mrad/s}) \quad (3.10)$$

$$\omega_{\text{YbF}} = - \left[ (19.6 \pm 1.5) \left( \frac{d_e}{10^{-27} e \text{ cm}} \right) + (17.6 \pm 2.0) \left( \frac{C_S}{10^{-7}} \right) \right] (\text{mrad/s}) \quad (3.11)$$

where

$$C_S = C_S^{(0)} + \frac{Z - N}{Z + N} C_S^{(1)}. \quad (3.12)$$

Here  $(Z, A) = (72, 106), (90, 142), (70, 103)$  for HfF, ThO, and YbF, respectively.

### 3.4 Nucleon EDMs

The interpretation of neutron and proton EDMs is complicated by the need to match quark-level operators onto hadronic couplings. This matching requires nonperturbative techniques and it has been carried out with different levels of sophistication for different WET operators. In the case of the quark dipole operators  $[C_{u\gamma}]_{11}$  and  $[C_{d\gamma}]_{11,22}$ , the hadronic input is captured by the quark tensor charges, which have been computed on the lattice [65, 76, 79].

$$d_n = -1.3 \cdot 10^{-16} \left( g_T^d \text{Im}[C_{u\gamma}]_{11} + g_T^u \text{Im}[C_{d\gamma}]_{11} + g_T^s \text{Im}[C_{d\gamma}]_{22} \right) \text{ TeV } e \text{ cm}, \quad (3.13)$$

$$d_p = -1.3 \cdot 10^{-16} \left( g_T^u \text{Im}[C_{u\gamma}]_{11} + g_T^d \text{Im}[C_{d\gamma}]_{11} + g_T^s \text{Im}[C_{d\gamma}]_{22} \right) \text{ TeV } e \text{ cm}, \quad (3.14)$$

with [76]

$$g_T^u = 0.784 \pm 0.030, \quad g_T^d = -0.204 \pm 0.015, \quad g_T^s = -0.0027 \pm 0.0016 \quad (3.15)$$

at the renormalization scale  $\mu = 2$  GeV. The  $u$  and  $d$  tensor charges have better than 10% uncertainties, while the  $s$  tensor charge is harder to compute and zero within two sigma. The  $c$  tensor charge has been considered in Ref. [65], but it is even more uncertain,

$$g_T^c = -(10 \pm 19) \cdot 10^{-5}. \quad (3.16)$$

For this reason, will not consider directly charm matrix elements, but integrate out the charm quark.

Lattice QCD calculations of the nucleon EDM induced by the quark chromoelectric dipole moment (qCEDM) operators  $[C_{uG}]_{11}$ ,  $[C_{dG}]_{11,22}$  are at the moment only preliminary [80–82]. Currently, the best estimates come from QCD sum rules [10, 83–85]. In Refs. [10, 83, 84], the  $u$  and  $d$  qCEDM contribution to the neutron and proton EDMs was estimated to be

$$d_n = -\frac{4.3 \cdot 10^{-17}}{g_s} \times (1 \pm 0.5) (\text{Im} [C_{dG}]_{11} + 0.5 \text{Im} [C_{uG}]_{11}) \text{ TeV } e \text{ cm}, \quad (3.17)$$

$$d_p = +\frac{5.2 \cdot 10^{-17}}{g_s} \times (1 \pm 0.5) (0.5 \text{Im} [C_{dG}]_{11} + \text{Im} [C_{uG}]_{11}) \text{ TeV } e \text{ cm}, \quad (3.18)$$

with roughly 50% uncertainty. Here  $g_s$  is the strong coupling constant. We will use the estimates in Eq. (3.17) for our numerics. Ref. [85] finds a larger value and a substantial contribution from the strange qCEDM

$$d_n = -\frac{9.8 \cdot 10^{-17}}{g_s} (\text{Im} [C_{dG}]_{11} + 1.2 \text{Im} [C_{uG}]_{11} + 0.2 \text{Im} [C_{dG}]_{22}) \text{ TeV } e \text{ cm}. \quad (3.19)$$

Estimates based on the dominance of long-distance contributions mediated by pion-nucleon couplings end up in a similar range [86, 87], though, of course, they are affected by uncontrolled systematic errors. The above matrix elements are given in the assumption that a PQ mechanism cancels the  $\bar{\theta}$  term, including the shift in the  $\bar{\theta}$  term induced by the chromoelectric operators [10]. The scale dependence of  $g_s$  and of the WET coefficients should in principle be compensated by the scale dependence of the hadronic matrix elements. In the sum rule calculations, such scale dependence is not explicitly tracked, and thus, at the moment, the choice of  $\mu$  introduces some arbitrariness. Since the conversion between Lattice QCD schemes and  $\overline{\text{MS}}$  is known [88, 89], this issue will be overcome once Lattice QCD calculations will become available. The contribution of the Weinberg three-gluon operator  $C_{\tilde{G}}$  has been estimated in Refs. [90, 91]. The two evaluations are in good agreement, and here we use the results of Ref. [91]

$$d_n = 1.5 \cdot 10^{-21} (1 \pm 0.5) [C_{\tilde{G}}] \text{ TeV}^2 e \text{ cm}, \quad (3.20)$$

$$d_p = -2.1 \cdot 10^{-21} (1 \pm 0.5) [C_{\tilde{G}}] \text{ TeV}^2 e \text{ cm}. \quad (3.21)$$

Also in this case, Lattice QCD calculations are preliminary [92], even though progress has been achieved on the matching between Lattice QCD and  $\overline{\text{MS}}$  schemes [93, 94]. The

estimates in Eq. (3.17), (3.19) and (3.20) clearly show that hadronic matrix elements are affected by large theoretical uncertainties, which need to be considered in any realistic analysis of EDM bounds.

The situation for four-fermion operators is even less well-developed. The matching between gradient flow and  $\overline{\text{MS}}$  renormalization at one loop has been derived in Ref. [48]. Robust calculations of the nucleon EDM currently do not exist. Here we will use the expression derived at next-to-next-to-leading order (N<sup>2</sup>LO) in two-flavor chiral perturbation theory [86]

$$d_n = -\frac{eg_A}{8\pi^2 F_\pi^2} \left[ \left( \bar{g}_0 - \frac{\bar{g}_2}{3} \right) \left( \ln \frac{m_\pi^2}{m_N^2} - \frac{\pi m_\pi}{2 m_N} \right) + \frac{\bar{g}_1}{4} (\kappa_1 - \kappa_0) \frac{m_\pi^2}{m_N^2} \ln \frac{m_\pi^2}{m_N^2} \right] + e\bar{d}_n \quad (3.22)$$

$$d_p = \frac{eg_A}{8\pi^2 F_\pi^2} \left[ \left( \bar{g}_0 - \frac{\bar{g}_2}{3} \right) \left( \ln \frac{m_\pi^2}{m_N^2} - 2\pi \frac{m_\pi}{m_N} \right) - \frac{\bar{g}_1}{4} \left( \frac{2\pi m_\pi}{m_N} + \left( \frac{5}{2} + \kappa_1 + \kappa_0 \right) \frac{m_\pi^2}{m_N^2} \ln \frac{m_\pi^2}{m_N^2} \right) \right] + e\bar{d}_p. \quad (3.23)$$

with  $g_A = 1.27$ .  $\kappa_{1,0}$  are the nucleon isovector and isoscalar anomalous magnetic moments,  $\kappa_1 = 3.7$ ,  $\kappa_0 = -0.12$ .  $\bar{g}_0$ ,  $\bar{g}_1$ ,  $\bar{d}_n$ , and  $\bar{d}_p$  are  $PT$ -odd low-energy couplings in the nucleon EFT, which implicitly depend on WET Wilson coefficients. In the following, we will provide a recipe to estimate  $\bar{g}_{0,1}$  in the case of four-fermion operators.

### 3.4.1 Pion nucleon couplings

$P$  and  $T$ -odd pion-nucleon ( $\pi N$ ) couplings play an important role for both nucleon and nuclear EDMs. In the case of the nucleon EDM,  $\pi N$  couplings induce logarithmically-enhanced contributions [95], as can be seen in Eqs. (3.22) and (3.23). Since they are accompanied by unknown low-energy constants,  $\pi N$  couplings cannot completely determine the leading contributions to the nucleon EDM, and thus expressions as Eq. (3.22) will be eventually superseded by Lattice QCD calculations. Knowing the strength of  $\bar{g}_{0,1}$ , however, can provide guidance for the chiral and momentum extrapolation [96] and for the removal of excited state contamination [97] in Lattice QCD calculations. Depending on the chiral properties of the WET operators,  $\pi N$  couplings furthermore provide one of the leading contributions to the  $PT$ -odd potential [22, 98, 99], which then feeds into the calculation of Schiff moments and thus atomic EDMs [100, 101].

We focus here on the most important  $\pi N$  couplings and refer for a more detailed discussion to Ref. [99]. We define the  $PT$ -odd  $\pi N$  Lagrangian as

$$\mathcal{L}_{\pi N} = \bar{N} \left[ \frac{\bar{g}_0}{F_\pi} \boldsymbol{\tau} \cdot \boldsymbol{\pi} + \frac{\bar{g}_1}{F_\pi} \pi_0 + \frac{\bar{g}_2}{F_\pi} \left( \pi_0 \tau_3 - \frac{1}{3} \boldsymbol{\tau} \cdot \boldsymbol{\pi} \right) \right] N, \quad (3.24)$$

where  $\boldsymbol{\tau}$  are Pauli matrices in isospin space. The couplings in Eq. (3.24) break chiral symmetry and are thus mostly important for chiral-symmetry-breaking WET operators. These usually come in chiral multiplets, with the CP-even components inducing corrections to the baryon spectrum while the CP-odd components contribute to  $\pi N$  couplings. At leading order in chiral perturbation theory, chiral symmetry then provides a relation between corrections to the baryon spectrum and  $\pi N$  couplings [22], which survives higher

order corrections [87, 102]. It can be shown that  $\bar{g}_2$  only arises at higher order in isospin breaking [22]. The couplings  $\bar{g}_0$  and  $\bar{g}_1$  receive a “direct” contribution, proportional to the shift in the baryon masses induced by dim-6 operators, and “indirect” contributions, arising from “vacuum alignment” [103], i.e. from imposing the condition that  $\pi_0$  and  $\eta$  mesons do not disappear into the vacuum in the presence of  $PT$ -odd interactions. We will thus write

$$\bar{g}_i = \bar{g}_i|_{\text{dir}} + \bar{g}_i|_{\text{ind}}. \quad (3.25)$$

The indirect contributions depend on meson matrix elements, which are more controlled.

For the qCEDM, the  $\pi N$  couplings were extracted using QCD sum rules [104],

$$\frac{\bar{g}_0}{F_\pi} = -1.97 \cdot 10^{-3} \frac{(1 \pm 2)}{g_s} (\text{Im} [C_{uG}]_{11} + \text{Im} [C_{dG}]_{11}) \text{ TeV}, \quad (3.26)$$

$$\frac{\bar{g}_1}{F_\pi} = -1.97 \cdot 10^{-3} \frac{(4^{+8}_{-2})}{g_s} (\text{Im} [C_{uG}]_{11} - \text{Im} [C_{dG}]_{11}) \text{ TeV}. \quad (3.27)$$

Again, we are neglected contributions proportional to  $\bar{\theta}_{\text{ind}}$ , which are canceled if a PQ mechanism is active. In chiral perturbation theory, the indirect part of the coupling is given by [87]

$$\left. \frac{\bar{g}_0}{F_\pi} \right|_{\text{ind}} = \frac{r g_S^{u-d}}{F_\pi g_s} (\text{Im} [C_{uG}]_{11} + \text{Im} [C_{dG}]_{11}) = -\frac{4.4 \cdot 10^{-3}}{g_s} (\text{Im} [C_{uG}]_{11} + \text{Im} [C_{dG}]_{11}), \quad (3.28)$$

$$\left. \frac{\bar{g}_1}{F_\pi} \right|_{\text{ind}} = \frac{r \sigma_{\pi N}}{\bar{m} F_\pi g_s} (\text{Im} [C_{uG}]_{11} - \text{Im} [C_{dG}]_{11}) = -\frac{7.4 \cdot 10^{-2}}{g_s} (\text{Im} [C_{uG}]_{11} - \text{Im} [C_{dG}]_{11}), \quad (3.29)$$

where  $r$  is the ratio of chromomagnetic and  $\bar{q}q$  condensates, for which we used [104]

$$r = -\frac{1}{2} \frac{\langle 0 | \bar{q} g_s \sigma G q | 0 \rangle}{\langle 0 | \bar{q} q | 0 \rangle} = -(0.4 \pm 0.1) \text{ GeV}^2. \quad (3.30)$$

The ratio between  $\bar{g}_1/\bar{g}_0$  is determined by the ratio of isoscalar and isovector charges, which, for the value of the sigma term we adopt, is about 17. The assumption of the dominance of the indirect piece leads to larger values compared to the QCD sum rules calculations, especially in the case of  $\bar{g}_1$ . For the qCEDM operators we will just use the sum rules results, while for the four-fermion operators, where only the indirect pieces can be estimated, we will capture these effects by assigning a large uncertainty. Plugging Eqs. (3.26) and (3.27) or Eqs. (3.28) and (3.29) in the chiral perturbation theory expression for the nucleon EDM we recover estimates that agree in magnitude with Eqs. (3.17)–(3.19).

We discussed in some detail various estimates for the qCEDM operators to justify our choices for four-fermion operators, for which complete evaluations of the couplings, either on the Lattice or from QCD sum rules are not available. The structure of the couplings is very similar to qCEDM, with a direct piece that could be extracted from dim-6 corrections to the baryon spectrum and an indirect piece determined by the ratio of vacuum matrix



elements [105, 106]. The operators constructed in Section 2.1.3 belong to the  $\mathbf{8} \times \mathbf{8}$ ,  $\mathbf{6} \times \bar{\mathbf{6}}$  and  $\mathbf{3} \times \bar{\mathbf{3}}$  representations of the  $SU(3)$  flavor group [106]. The indirect components of the  $\pi N$  couplings are given by

$$\begin{aligned} \bar{g}_0|_{\text{ind}} = & -\frac{F_\pi^2 \bar{m} g_S^{u-d}}{m_\pi^2} \left[ \mathcal{A}_{\mathbf{8} \times \mathbf{8}} C_{\mathbf{8} \times \mathbf{8}}^{(1,0)} + \bar{\mathcal{A}}_{\mathbf{8} \times \mathbf{8}} C_{\mathbf{8} \times \mathbf{8}}^{(8,0)} + \mathcal{A}_{\mathbf{6} \times \mathbf{6}} C_{\mathbf{6} \times \mathbf{6}}^{(1,0)} + \bar{\mathcal{A}}_{\mathbf{6} \times \mathbf{6}} C_{\mathbf{6} \times \mathbf{6}}^{(8,0)} \right. \\ & \left. + \mathcal{A}_{\mathbf{3} \times \mathbf{3}} C_{\mathbf{3} \times \mathbf{3}}^{(1,0)} + \bar{\mathcal{A}}_{\mathbf{3} \times \mathbf{3}} C_{\mathbf{3} \times \mathbf{3}}^{(8,0)} \right], \end{aligned} \quad (3.31)$$

$$\begin{aligned} \bar{g}_1|_{\text{ind}} = & -\frac{F_\pi^2 \sigma_{\pi N}}{m_\pi^2} \left[ \mathcal{A}_{\mathbf{8} \times \mathbf{8}} C_{\mathbf{8} \times \mathbf{8}}^{(1,1)} + \bar{\mathcal{A}}_{\mathbf{8} \times \mathbf{8}} C_{\mathbf{8} \times \mathbf{8}}^{(8,1)} + \mathcal{A}_{\mathbf{6} \times \mathbf{6}} C_{\mathbf{6} \times \mathbf{6}}^{(1,1)} + \bar{\mathcal{A}}_{\mathbf{6} \times \mathbf{6}} C_{\mathbf{6} \times \mathbf{6}}^{(8,1)} \right. \\ & \left. + \mathcal{A}_{\mathbf{3} \times \mathbf{3}} C_{\mathbf{3} \times \mathbf{3}}^{(1,1)} + \bar{\mathcal{A}}_{\mathbf{3} \times \mathbf{3}} C_{\mathbf{3} \times \mathbf{3}}^{(8,1)} \right]. \end{aligned} \quad (3.32)$$

The operators in the  $LLRR$  class belong to the  $\mathbf{8} \times \mathbf{8}$  representation, and we have

$$C_{\mathbf{8} \times \mathbf{8}}^{(1,0)} = \frac{1}{2} \left( \text{Im} \left[ C_{uddu}^{V1,LR} \right]_{1221} + \text{Im} \left[ C_{dd}^{V1,LR} \right]_{1221} \right), \quad (3.33)$$

$$C_{\mathbf{8} \times \mathbf{8}}^{(8,0)} = \frac{1}{2} \left( \text{Im} \left[ C_{uddu}^{V8,LR} \right]_{1221} + \text{Im} \left[ C_{dd}^{V8,LR} \right]_{1221} \right), \quad (3.34)$$

$$C_{\mathbf{8} \times \mathbf{8}}^{(1,1)} = \text{Im} \left[ C_{uddu}^{V1,LR} \right]_{1111} + \frac{1}{2} \text{Im} \left[ C_{uddu}^{V1,LR} \right]_{1221} - \frac{1}{2} \text{Im} \left[ C_{dd}^{V1,LR} \right]_{1221}, \quad (3.35)$$

$$C_{\mathbf{8} \times \mathbf{8}}^{(8,1)} = \text{Im} \left[ C_{uddu}^{V8,LR} \right]_{1111} + \frac{1}{2} \text{Im} \left[ C_{uddu}^{V8,LR} \right]_{1221} - \frac{1}{2} \text{Im} \left[ C_{dd}^{V8,LR} \right]_{1221}. \quad (3.36)$$

The first superscript indicates whether the operators are color singlet or octet, while the second superscript whether they are isospin 0 or isospin 1. The  $LRLL$  operators, on the other hand, belong to the  $\mathbf{6} \times \bar{\mathbf{6}}$  and  $\mathbf{3} \times \bar{\mathbf{3}}$  representations. The  $\mathbf{6} \times \bar{\mathbf{6}}$  coefficients are given by

$$\begin{aligned} C_{\mathbf{6} \times \mathbf{6}}^{(1,0)} = & \text{Im} \left[ C_{uu}^{S1,RR} \right]_{1111} + \text{Im} \left[ C_{dd}^{S1,RR} \right]_{1111} + \frac{1}{2} \left( \text{Im} \left[ C_{uddu}^{S1,RR} \right]_{1111} + \text{Im} \left[ C_{ud}^{S1,RR} \right]_{1111} \right) \\ & + \frac{1}{4} \left( \text{Im} \left[ C_{uddu}^{S1,RR} \right]_{1221} + \text{Im} \left[ C_{ud}^{S1,RR} \right]_{1122} + \text{Im} \left[ C_{dd}^{S1,RR} \right]_{1221} + \text{Im} \left[ C_{dd}^{S1,RR} \right]_{1122} \right), \end{aligned} \quad (3.37)$$

$$\begin{aligned} C_{\mathbf{6} \times \mathbf{6}}^{(1,1)} = & \text{Im} \left[ C_{uu}^{S1,RR} \right]_{1111} - \text{Im} \left[ C_{dd}^{S1,RR} \right]_{1111} \\ & + \frac{1}{4} \left( \text{Im} \left[ C_{uddu}^{S1,RR} \right]_{1221} + \text{Im} \left[ C_{ud}^{S1,RR} \right]_{1122} - \text{Im} \left[ C_{dd}^{S1,RR} \right]_{1221} - \text{Im} \left[ C_{dd}^{S1,RR} \right]_{1122} \right), \end{aligned} \quad (3.38)$$

with the same expressions for the color octet operators, with  $S1 \rightarrow S8$ . For the  $\mathbf{3} \times \bar{\mathbf{3}}$  coefficients we have

$$\begin{aligned} C_{\mathbf{3} \times \mathbf{3}}^{(1,0)} = & \frac{1}{2} \left( -\text{Im} \left[ C_{uddu}^{S1,RR} \right]_{1111} + \text{Im} \left[ C_{ud}^{S1,RR} \right]_{1111} \right) \\ & + \frac{1}{4} \left( -\text{Im} \left[ C_{uddu}^{S1,RR} \right]_{1221} + \text{Im} \left[ C_{ud}^{S1,RR} \right]_{1122} - \text{Im} \left[ C_{dd}^{S1,RR} \right]_{1221} + \text{Im} \left[ C_{dd}^{S1,RR} \right]_{1122} \right) \end{aligned} \quad (3.39)$$

$$C_{\mathbf{3} \times \mathbf{3}}^{(1,1)} = \frac{1}{4} \left( -\text{Im} \left[ C_{uddu}^{S1,RR} \right]_{1221} + \text{Im} \left[ C_{ud}^{S1,RR} \right]_{1122} + \text{Im} \left[ C_{dd}^{S1,RR} \right]_{1221} - \text{Im} \left[ C_{dd}^{S1,RR} \right]_{1122} \right), \quad (3.40)$$

and again the color octet coefficients are obtained by  $S1 \rightarrow S8$ .

The  $\mathbf{8} \times \mathbf{8}$  and  $\mathbf{6} \times \bar{\mathbf{6}}$  are related by  $SU(3)$  chiral symmetry to operators that contribute to  $K-\bar{K}$  oscillations,  $K \rightarrow \pi\pi$  and to short-distance contributions to neutrinoless double beta decay [107]. Here we determine the LECs from calculations of neutrinoless double beta decay matrix elements [108] and write

$$\mathcal{A}_{\mathbf{8} \times \mathbf{8}} = -g_4^{\pi\pi}, \quad \bar{\mathcal{A}}_{\mathbf{8} \times \mathbf{8}} = -\left[\frac{1}{2}g_5^{\pi\pi} - \frac{1}{2N_c}g_4^{\pi\pi}\right] \quad (3.41)$$

$$\mathcal{A}_{\mathbf{6} \times \mathbf{6}} = -g_2^{\pi\pi}, \quad \bar{\mathcal{A}}_{\mathbf{6} \times \mathbf{6}} = -\left[\frac{1}{2}g_3^{\pi\pi} - \frac{1}{2N_c}g_2^{\pi\pi}\right], \quad (3.42)$$

with

$$g_2^{\pi\pi} = 2.0(2) \text{ GeV}^2, \quad g_3^{\pi\pi} = -0.62(6) \text{ GeV}^2, \quad (3.43)$$

$$g_4^{\pi\pi} = -1.9(2) \text{ GeV}^2, \quad g_5^{\pi\pi} = -8.0(6) \text{ GeV}^2, \quad (3.44)$$

in the  $\overline{\text{MS}}$  scheme, at  $\mu = 2 \text{ GeV}$ . The LECs for  $\mathcal{A}_{\mathbf{3} \times \mathbf{3}}$  and  $\bar{\mathcal{A}}_{\mathbf{3} \times \mathbf{3}}$  are at the moment unknown. We will set them to zero but stress that this is an uncontrolled assumption.

$$\mathcal{A}_{\mathbf{3} \times \mathbf{3}} = 0 \text{ GeV}^2 \quad \bar{\mathcal{A}}_{\mathbf{3} \times \mathbf{3}} = 0 \text{ GeV}^2 \quad (3.45)$$

### 3.5 Diamagnetic Atomic EDMs

We finally consider EDMs of diamagnetic atoms. The strongest bound is currently on the EDM of  $^{199}\text{Hg}$  [53, 63], followed by  $^{129}\text{Xe}$  [54]. We will also consider  $^{225}\text{Ra}$ , which has enhanced sensitivity to the nuclear Schiff moment [101, 109] and could provide important constraints in the future [12]. We can write the EDM of diamagnetic atoms as a term induced by the nuclear Schiff moment, plus contributions from semileptonic operators

$$d_{AX} = d_{\text{Schiff}} + \sum_{N=n,p} \left( \alpha_S^N C_S^{(N)} + \alpha_P^N C_P^{(N)} + \alpha_T^N C_T^{(N)} \right). \quad (3.46)$$

The Schiff moment component is sensitive to the neutron and proton EDM and to  $PT$ -odd nucleon-nucleon interactions. These have been classified in phenomenological one-meson-exchange models [101, 110, 111], and in chiral EFT and pionless EFT [22, 98, 99, 112, 113]. For chiral-symmetry breaking operators, such as the qCEDM and the four-quark operators,  $\bar{g}_{0,1}$  give the leading contribution to the  $PT$ -odd nucleon-nucleon potential [22, 98], even though short-range operators in the  $^3P_0-^1S_0$  channel are required for renormalization [114]. For chiral-invariant operators, such as the Weinberg three-gluon operator,  $\pi N$  couplings and short-range isospin-invariant  $NN$  couplings contribute at the same order [22, 98]. Since little can be said about the size of the  $NN$  CP-odd short-range interactions induced by WET operators, we focus here on the contributions to the Schiff moment from  $\bar{g}_{0,1}$ . With progress from Lattice QCD and nuclear theory, the Schiff moment expressions could in the future be extended to include additional operators.

We write

$$d_{\text{Schiff}} = A_{\text{Schiff}} \left( \alpha_n d_n + \alpha_p d_p + a_0 \frac{\bar{g}_0}{F_\pi} + a_1 \frac{\bar{g}_1}{F_\pi} + a_2 \frac{\bar{g}_2}{F_\pi} \right). \quad (3.47)$$

	$A_{\text{Schiff}}$	$\alpha_n$	$\alpha_p$	$a_0$ (e fm)	$a_1$ (e fm)	$a_2$ (e fm)
$^{199}\text{Hg}$	$-(2.40 \pm 0.24) \cdot 10^{-4}$	$1.9 \pm 0.1$	$0.20 \pm 0.06$	$0.13_{-0.07}^{+0.5}$	$0.25_{-0.63}^{+0.89}$	$0.09_{-0.04}^{+0.17}$
$^{129}\text{Xe}$	$-(0.364 \pm 0.025) \cdot 10^{-4}$	$-(0.29 \pm 0.10)$	–	$0.10_{-0.037}^{+0.53}$	$0.076_{-0.038}^{+0.55}$	
$^{225}\text{Ra}$	$(6.3 \pm 0.5) \cdot 10^{-4}$	–	–	$2.5 \pm 7.5$	$-65 \pm 40$	$14 \pm 6.5$

**Table 3:** Nuclear and atomic theory input for the EDMs of diamagnetic atoms.

The prefactor  $A_{\text{Schiff}}$  accounts for the Schiff screening, while the coefficients  $\alpha_{n,p}$  and  $a_{0,1,2}$  contain the information on the nuclear structure of the systems of interest. We report them in Table 3. We use the results of Ref. [115] for the screening factors of Hg and Xe, and Ref. [116] for  $^{225}\text{Ra}$ . In the case of  $^{199}\text{Hg}$ ,  $\alpha_{n,p}$  are known with good accuracy [117], while in the case of Xe we use the calculation of  $\alpha_n$  from [118]. The contributions of the CP-odd  $\pi N$  couplings are affected by substantial uncertainties. Here we take the ranges suggested in Refs. [11, 21], which considers results from various nuclear structure calculations.

The contributions from semileptonic operators are usually expressed in terms of nucleon-level operators. In addition to the scalar operators in Eq. (3.4), one can write pseudoscalar and tensor terms. In a relativistic notation

$$\mathcal{L} = -\frac{G_F}{\sqrt{2}} \left( \bar{e} e \bar{N} \left( C_P^{(0)} + \tau_3 C_P^{(1)} \right) i \gamma_5 N - \frac{1}{2} \varepsilon_{\mu\nu\alpha\beta} \bar{e} \sigma^{\mu\nu} e \bar{N} \sigma^{\alpha\beta} \left( C_T^{(0)} + C_T^{(1)} \tau_3 \right) N \right), \quad (3.48)$$

where the isoscalar/isovector couplings are related to proton/neutron couplings by

$$C_X^{(p)} = C_X^{(0)} + C_X^{(1)}, \quad C_X^{(n)} = C_X^{(0)} - C_X^{(1)}. \quad (3.49)$$

As can be more clearly seen in a non-relativistic notation [78], the pseudoscalar operators vanish at zero momentum and are thus proportional to powers of  $Q/\Lambda_{\text{had}}$ , where  $\Lambda_{\text{had}}$  is an hadronic scale. Here we only retain the isovector component, which is dominated by the pion pole contribution and thus relatively large, with  $\Lambda_{\text{had}} \sim m_u + m_d$ .

$$C_P^{(1)} = -\frac{v^2}{2} \left( \text{Im}[C_{eu}^{\text{SRR}}]_{1111} - \text{Im}[C_{eu}^{\text{SRL}}]_{1111} - \text{Im}[C_{ed}^{\text{SRR}}]_{1111} + \text{Im}[C_{ed}^{\text{SRL}}]_{1111} \right) \frac{g_A m_N}{\bar{m}}. \quad (3.50)$$

The isoscalar component is suppressed by the  $\eta$  mass, rather than the pion mass, and thus we neglect it. Its contribution was considered, for example, in Ref. [77]. In terms of WET operators, the tensor coefficients are

$$C_T^{(0)} = -\frac{v^2}{2} \left( \frac{g_T^u + g_T^d}{2} \left( \text{Im}[C_{eu}^{\text{TRR}}]_{1111} + \text{Im}[C_{ed}^{\text{TRR}}]_{1111} \right) + g_T^s \text{Im}[C_{ed}^{\text{TRR}}]_{1122} \right) \quad (3.51)$$

$$C_T^{(1)} = -\frac{v^2}{2} \frac{g_T^u - g_T^d}{2} \left( \text{Im}[C_{eu}^{\text{TRR}}]_{1111} - \text{Im}[C_{ed}^{\text{TRR}}]_{1111} \right). \quad (3.52)$$

The coefficients  $\alpha_S^N$  are given by

$$\alpha_S^p = \mathcal{R}_{\text{SP}} \frac{Z}{A}, \quad \alpha_S^n = \mathcal{R}_{\text{SP}} \frac{N}{A}. \quad (3.53)$$

$(Z, N, A) = (80, 121, 201), (54, 77, 131), (87, 136, 223)$  are the atomic number, number of neutrons, and mass number of Hg, Xe, and Ra, respectively.  $\mathcal{R}_{\text{SP}}$  depends solely on atomic theory, and, for Mercury and Xenon, we use the values [119, 120].

$$\mathcal{R}_{\text{SP}}|_{\text{Hg}} = -(2.8 \pm 0.6) \cdot 10^{-22} e \text{ cm} \quad \mathcal{R}_{\text{SP}}|_{\text{Xe}} = -(0.71 \pm 0.18) \cdot 10^{-23} e \text{ cm}. \quad (3.54)$$

These values are somewhat smaller than in other calculations, especially in the case of xenon [121]. The tensor coefficients can be written as

$$\alpha_T^p = \mathcal{R}_T \langle \sigma_{pz} \rangle, \quad \alpha_T^n = \mathcal{R}_T \langle \sigma_{nz} \rangle, \quad (3.55)$$

where  $\mathcal{R}_T$  is calculated in atomic theory, while  $\langle \sigma_{pz} \rangle$  and  $\langle \sigma_{nz} \rangle$  are nuclear spin matrix elements. We use [119, 120]

$$\mathcal{R}_T|_{\text{Hg}} = -(2.8 \pm 0.6) \cdot 10^{-20} e \text{ cm} \quad \mathcal{R}_T|_{\text{Xe}} = (0.520 \pm 0.049) \cdot 10^{-20} e \text{ cm}, \quad (3.56)$$

and [122, 123]

$$\langle \sigma_{nz} \rangle|_{\text{Hg}} = -0.377, \quad \langle \sigma_{pz} \rangle|_{\text{Hg}} = 0.009 \quad (3.57)$$

$$\langle \sigma_{nz} \rangle|_{\text{Xe}} = +0.658, \quad \langle \sigma_{pz} \rangle|_{\text{Xe}} = 0.020. \quad (3.58)$$

Finally,  $\alpha_P^N$  are related to the tensor contributions by [124]

$$\alpha_P^N = \frac{Z \alpha_{\text{em}}}{5 m_N R} \alpha_T^N \quad (3.59)$$

where  $R = 1.2A^{1/3}$  fm is the nuclear radius.

#### 4 Renormalization group running and threshold effects

The WET operators containing heavier fermions (charm, bottom, muon, and tau) can contribute to the electron, neutron, atomic, and molecular EDMs via renormalization group evolution and threshold effects arising when the heavy particles are integrated out. In this section, we discuss the following three kinds of contributions of WET operators with heavier generations to the EDMs observables given in Sec. 3, focusing only on the leading effects<sup>1</sup>:

- Leading-log QCD+QED RG running from EW scale to  $\mu = 2$  GeV.
- 1-loop threshold effects at  $\mu = m_c$  and  $\mu = m_b$ .
- Next-to-leading-log 2-loop QCD+QED RG running from EW scale to  $\mu = 2$  GeV.

The logarithmic order at which each operator contributes is indicated in Table 1. In the following, we will dissect how these contributions arise.

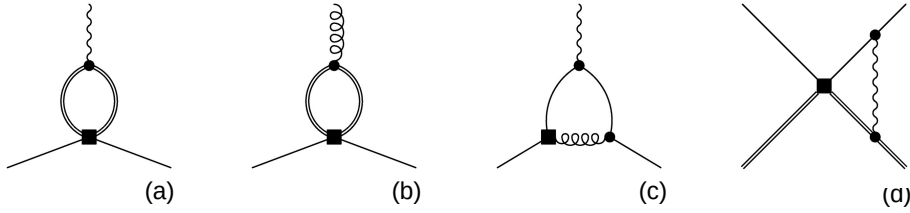


**Figure 1:** Representative diagrams contributing to the 1-loop anomalous dimension, which induces LL contributions to EDMs. Plain and double lines denote light ( $e$  and  $u, d, s$  quarks) and heavy fermions ( $\mu, \tau$  leptons and  $c, b$  quarks), respectively. Wavy and wiggly lines denote photons and gluons. Insertions of WET operators are denoted by squares, while SM vertices by dots. Diagrams (a) and (b) contribute to the mixing of heavy-light four-fermion operators onto photon and gluon dipole operators. Four-quark operators of the type  $\mathcal{O}_{uu}^{S1,RR}$ ,  $\mathcal{O}_{uu}^{S8,RR}$ ,  $\mathcal{O}_{dd}^{S8,RR}$ ,  $\mathcal{O}_{dd}^{S8,RR}$ ,  $\mathcal{O}_{uddu}^{S1,RR}$  and  $\mathcal{O}_{uddu}^{S8,RR}$ , with two heavy and two light quarks, semileptonic tensor operators  $\mathcal{O}_{eu}^{T,RR}$ ,  $\mathcal{O}_{ed}^{T,RR}$  with heavy quarks or heavy leptons, and the leptonic scalar operator  $\mathcal{O}_{ee}^{S,RR}$  with two heavy and two light leptons generate LL EDMs via this path. Diagram (c) denotes the mixing of dipole operators. Diagram (d) denotes the mixing of the semileptonic scalar operators  $\mathcal{O}_{eu}^{S,RR}$  and  $\mathcal{O}_{ed}^{S,RR}$  onto tensor operators. Combined with the running of the tensor into dipoles, these induce corrections to the electron EDM starting at  $\mathcal{O}(L_\mu^2)$ .

#### 4.1 Leading-log 1-loop RG running

The complete 1-loop ADMs in WET including  $\Delta F = 0$  operators have been calculated in [15]. In what follows, we identify all relevant terms in the ADMs and provide the naive solutions for the corresponding RGEs. Through diagrams such as diagram (a) and (c) in Figure 1, the QCD dipole and four-quark scalar operators mix onto the photon dipole. Neglecting the running of the electromagnetic and strong couplings, and the running of the Wilson coefficients, we can denote the solution of the RGEs as

$$\begin{aligned}
[C_{f\gamma}]_{ii} &= 8eg_sq_i C_F [C_{fG}]_{ii} L_\mu, \\
[C_{f\gamma}]_{ii} &= 2eq_j m_j [C_{ff}^{S1,RR}]_{ijji} L_\mu, \\
[C_{f\gamma}]_{ii} &= 2eq_j m_j C_F [C_{ff}^{S8,RR}]_{ijji} L_\mu, \\
[C_{f\gamma}]_{ii} &= -8eq_e m_j [C_{ef}^{T,RR}]_{jjii} L_\mu, \\
[C_{u\gamma}]_{ii} &= eq_j m_j [C_{uddu}^{S1,RR}]_{ijji} L_\mu, \\
[C_{u\gamma}]_{ii} &= eq_j m_j C_F [C_{uddu}^{S8,RR}]_{ijji} L_\mu.
\end{aligned} \tag{4.1}$$

where we define

$$L_\mu = \frac{1}{16\pi^2} \log \frac{\mu_{low}}{\mu_{ew}}. \tag{4.2}$$

<sup>1</sup>Meaning if an operator contributes at the tree-level its 1-loop effects are not discussed in this section, and so on.

Here  $f = u$  or  $d$ , and  $\mu_{low}$  denotes the scale to which we run, which depends on the flavor of the particle in the loop.  $e$  denotes the electric charge, while  $q_j$  is the charge of the quark or lepton  $j$ , with  $q_e = -1$ ,  $q_d = -1/3$  and  $q_u = 2/3$ .  $C_F = (N_c^2 - 1)/(2N_c)$  and  $C_A = N_c$ , with  $N_c$  the number of colors. The mixing of  $[C_{uddu}^{S1(S8),RR}]_{ijji}$  onto  $[C_{d\gamma}]$  is governed the last two equations in (4.1) by replacing  $q_j, m_j$  by  $q_i, m_i$ , respectively. The QCD dipoles mix with the electromagnetic dipoles and four-quark scalar operators

$$\begin{aligned}
[C_{fG}]_{ii} &= 2g_s m_j [C_{ff}^{S1,RR}]_{ijji} L_\mu, \\
[C_{fG}]_{ii} &= 2g_s m_j \left( C_F - \frac{C_A}{2} \right) [C_{ff}^{S8,RR}]_{ijji} L_\mu, \\
[C_{uG}]_{ii} &= g_s m_j [C_{uddu}^{S1,RR}]_{ijji} L_\mu, \\
[C_{uG}]_{ii} &= g_s m_j \left( C_F - \frac{C_A}{2} \right) [C_{uddu}^{S8,RR}]_{ijji} L_\mu.
\end{aligned} \tag{4.3}$$

The mixing of  $[C_{f\gamma}]$  onto  $[C_{fG}]$  follows the exact same relation as the first equation in (4.1). Also, the mixing of  $[C_{uddu}^{S1(S8),RR}]$  onto  $[C_{dG}]$  follows the same relations as the last two equations in (4.3). Eqs. (4.1) and (4.3) show that all scalar operators with two heavy and two light quarks induce light quark EDMs and CEDMs at one loop, leading, as we will see, to strong constraints from neutron and mercury EDM experiments. For the electron EDM, the mixing of the scalar and tensor operators onto the dipole operator is governed by pure QED

$$\begin{aligned}
[C_{e\gamma}]_{ii} &= -8eq_i m_j N_c [C_{ed}^{T,RR}]_{ijji} L_\mu, \\
[C_{e\gamma}]_{ii} &= -8eq_j m_j N_c [C_{eu}^{T,RR}]_{ijji} L_\mu, \\
[C_{e\gamma}]_{ii} &= 2eq_j m_j [C_{ee}^{S,RR}]_{ijji} L_\mu.
\end{aligned} \tag{4.4}$$

The first two relations in (4.4) indicate that semileptonic operators with heavier generations of up and down quarks can mix with the electromagnetic dipole operator for the electron. Similarly, the muon and tau scalar operators can also mix with the dipole operator as indicated by the last relation in (4.4).

Finally, through diagrams such as diagram (d) in Fig. 1, the leptonic operators  $[C_{ee}^{S,RR}]_{1122}$  and  $[C_{ee}^{S,RR}]_{1133}$  mix with  $[C_{e\gamma}^{S,RR}]_{11}$  via the  $[C_{ee}^{S,RR}]_{1221}$  and  $[C_{ee}^{S,RR}]_{1331}$  operators. Similarly, semileptonic scalar operators mix into tensor operators, and scalar operators of the form  $[C_{uu}^{S1(8),RR}]_{ijjj}$ ,  $[C_{dd}^{S1(8),RR}]_{ijjj}$  and  $[C_{ud}^{S1(8),RR}]_{ijjj}$  mix onto  $[C_{uu}^{S1(8),RR}]_{ijji}$ ,  $[C_{dd}^{S1(8),RR}]_{ijji}$  and  $[C_{uddu}^{S1(8),RR}]_{ijji}$ , respectively. In this way, these operators induce LL contribution to the electron and quark dipole operators, which however start at two loops and go as  $L_\mu^2$ .

$$\begin{aligned}
[C_{e\gamma}]_{11} &= 32q_e^3 e^3 m_j [C_{ee}^{S,RR}]_{11jj} \frac{L_\mu^2}{2}, \\
[C_{e\gamma}]_{11} &= 16q_e q_u^2 e^3 m_j N_c [C_{eu}^{S,RR}]_{11jj} \frac{L_\mu^2}{2}, \\
[C_{e\gamma}]_{11} &= 16q_e q_d^2 e^3 m_j N_c [C_{ed}^{S,RR}]_{11jj} \frac{L_\mu^2}{2}.
\end{aligned} \tag{4.5}$$

In the first relation in (4.5),  $jj = 22, 33$ , for the second  $jj = 11, 22$  and for third  $jj = 11, 22$ , or 33. Similarly, the semileptonic operators also mix with the quark dipoles

$$\begin{aligned} [C_{u\gamma}]_{ii} &= 16q_e^2 q_u e^3 m_j [C_{eu}^{S,RR}]_{jjii} \frac{L_\mu^2}{2}, \\ [C_{d\gamma}]_{ii} &= 16q_e^2 q_d e^3 m_j [C_{ed}^{S,RR}]_{jjii} \frac{L_\mu^2}{2}. \end{aligned} \quad (4.6)$$

Here,  $jj = 11, 22$  or 33, however, only 33 cases can induce significant effects. Finally, four-quark scalar operators also generate  $L_\mu^2$  contributions. In the case of  $uu$  and  $dd$  operators, the mixing is given by

$$\begin{aligned} [C_{f\gamma}]_{ii} &= \frac{2eq_f m_j}{N_c} (16e^2 q_u^2 + 16g_s^2 C_F) [C_{ff}^{S1,RR}]_{iiij} \frac{L_\mu^2}{2}, \\ [C_{f\gamma}]_{ii} &= \frac{2eC_F q_f m_j}{N_c} \left( 16e^2 q_u^2 C_F + 2g_s^2 \left( \frac{2}{N_c^2} + N_c^2 - 3 \right) \right) [C_{ff}^{S8,RR}]_{iiij} \frac{L_\mu^2}{2}, \\ [C_{fG}]_{ii} &= \frac{2g_s m_j}{N_c} (16e^2 q_u^2 + 16g_s^2 C_F) [C_{ff}^{S1,RR}]_{iiij} \frac{L_\mu^2}{2}, \\ [C_{fG}]_{ii} &= -\frac{2g_s}{N_c} m_j \left( C_F - \frac{C_A}{2} \right) \left( 16e^2 q_u^2 - 4g_s^2 \left( \frac{2}{N_c} + N_c \right) \right) [C_{ff}^{S8,RR}]_{iiij} \frac{L_\mu^2}{2}, \end{aligned} \quad (4.7)$$

for  $f = u$  or  $d$ .  $[C_{ud}^{S1(8),RR}]$  operators induce both QED and QCD dipoles. For the QED dipoles, one finds

$$\begin{aligned} [C_{u\gamma}]_{ii} &= \frac{eq_d m_j}{N_c} (16e^2 q_u q_d + 16g_s^2 C_F) [C_{ud}^{S1,RR}]_{iiij} \frac{L_\mu^2}{2}, \\ [C_{u\gamma}]_{ii} &= \frac{2eC_F q_d m_j}{N_c} \left( 16e^2 q_u q_d C_F + 2g_s^2 \left( \frac{2}{N_c^2} + N_c^2 - 3 \right) \right) [C_{ud}^{S8,RR}]_{iiij} \frac{L_\mu^2}{2}, \\ [C_{d\gamma}]_{jj} &= \frac{eq_d m_i}{N_c} (16e^2 q_u q_d + 16g_s^2 C_F) [C_{ud}^{S1,RR}]_{iiij} \frac{L_\mu^2}{2}, \\ [C_{d\gamma}]_{jj} &= \frac{2eC_F q_d m_i}{N_c} \left( 16e^2 q_u q_d C_F + 2g_s^2 \left( \frac{2}{N_c^2} + N_c^2 - 3 \right) \right) [C_{ud}^{S8,RR}]_{iiij} \frac{L_\mu^2}{2}, \end{aligned} \quad (4.8)$$

and, for the QCD dipoles,

$$\begin{aligned} [C_{uG}]_{ii} &= \frac{g_s m_j}{N_c} (16e^2 q_u q_d + 16g_s^2 C_F) [C_{ud}^{S1,RR}]_{iiij} \frac{L_\mu^2}{2}, \\ [C_{uG}]_{ii} &= \frac{g_s}{N_c} m_j \left( C_F - \frac{C_A}{2} \right) \left( 16e^2 q_u q_d C_F + 2g_s^2 \left( \frac{2}{N_c^2} + N_c^2 - 3 \right) \right) [C_{ud}^{S8,RR}]_{iiij} \frac{L_\mu^2}{2}, \\ [C_{dG}]_{jj} &= \frac{g_s}{N_c} m_i (16e^2 q_u q_d + 16g_s^2 C_F) [C_{ud}^{S1,RR}]_{iiij} \frac{L_\mu^2}{2}, \\ [C_{dG}]_{jj} &= \frac{g_s}{N_c} m_j \left( C_F - \frac{C_A}{2} \right) \left( 16e^2 q_u q_d C_F + 2g_s^2 \left( \frac{2}{N_c^2} + N_c^2 - 3 \right) \right) [C_{ud}^{S8,RR}]_{iiij} \frac{L_\mu^2}{2}. \end{aligned} \quad (4.9)$$

This exhausts all the operators denoted as LL in Table 1.

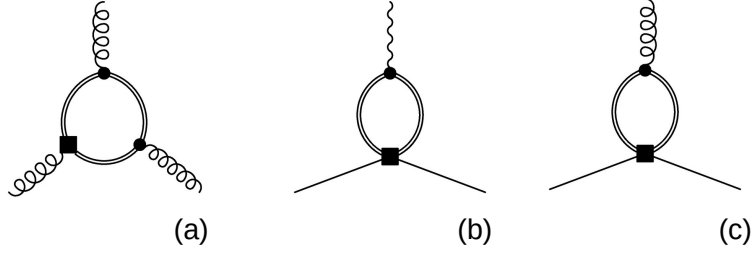


**Figure 2:** Matching contributions arising from integrating out heavy particles. Diagram (a) shows contributions to the Weinberg three-gluon operator from gluon dipole operators with heavy quarks. Diagram (b) and (c) illustrate matching corrections from the four-quark operators  $\mathcal{O}_{uddu}^{V1,LR}$ ,  $\mathcal{O}_{uddu}^{V8,LR}$ ,  $\mathcal{O}_{dd}^{V1,LR}$ ,  $\mathcal{O}_{dd}^{V8,LR}$ ,  $\mathcal{O}_{uu}^{V1,LR}$  and  $\mathcal{O}_{dd}^{V8,LR}$  and from the leptonic vector operators  $\mathcal{O}_{ee}^{V,LR}$  onto dipole operators.

## 4.2 1-loop Matching

In this subsection, we discuss the threshold effects at  $m_c$ ,  $m_b$ ,  $m_\mu$ , and  $m_\tau$  at the 1-loop level.

### 4.2.1 Matching to Weinberg operators

$[C_{dG}]_{33}$  mixes with  $[C_{\tilde{G}}]$  after integrating out  $b$ -quark [125]. After adjusting the normalization of the operators, in the JMS basis, we find

$$[C_{\tilde{G}}](\mu_b^-) = [C_{\tilde{G}}](\mu_b^+) + \frac{1}{3m_b} \frac{\alpha_s}{8\pi} \text{Im}[C_{dG}]_{33}(\mu_b^+). \quad (4.10)$$

The coefficient of second term is  $\approx 7.1 \cdot 10^{-4}$ . The 1-loop Feynman diagram governing this mixing is given in Fig. 2, diagram (a). Similarly, we can integrate out the charm quark leading to

$$[C_{\tilde{G}}](\mu_c^-) = [C_{\tilde{G}}](\mu_c^+) + \frac{1}{3m_c} \frac{\alpha_s}{8\pi} \text{Im}[C_{uG}]_{22}(\mu_c^+). \quad (4.11)$$

The coefficient of second term is  $\approx 5.2 \cdot 10^{-3}$ .

### 4.2.2 Matching to dipole operators

The vector operators with left-right chiral currents match onto dipole operators at one loop [36]. For chromo-dipoles, in the JMS basis, we find

$$\begin{aligned} [C_{uG}]_{ii}(\mu^-) &= [C_{uG}]_{ii}(\mu^+) - \frac{g_s m_j}{16\pi^2} \left( [C_{uddu}^{V1,LR}]_{ijji}(\mu^+) - \frac{1}{6} [C_{uddu}^{V8,LR}]_{ijji}(\mu^+) \right), \\ [C_{dG}]_{jj}(\mu^-) &= [C_{dG}]_{jj}(\mu^+) - \frac{g_s m_i}{16\pi^2} \left( [C_{uddu}^{V1,LR}]_{ijji}(\mu^+) - \frac{1}{6} [C_{uddu}^{V8,LR}]_{ijji}(\mu^+) \right), \\ [C_{uG}]_{ii}(\mu^-) &= [C_{uG}]_{ii}(\mu^+) - \frac{g_s m_j}{16\pi^2} \left( [C_{uu}^{V1,LR}]_{ijji}(\mu^+) - \frac{1}{6} [C_{uu}^{V8,LR}]_{ijji}(\mu^+) \right), \\ [C_{dG}]_{jj}(\mu^-) &= [C_{dG}]_{jj}(\mu^+) - \frac{g_s m_i}{16\pi^2} \left( [C_{dd}^{V1,LR}]_{ijji}(\mu^+) - \frac{1}{6} [C_{dd}^{V8,LR}]_{ijji}(\mu^+) \right), \end{aligned} \quad (4.12)$$



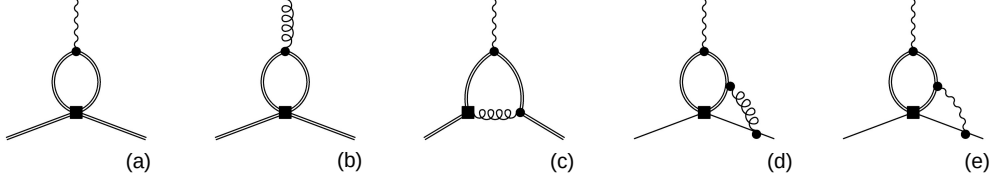


**Figure 3:** Representative diagrams that induce NLL contributions to EDMs. Diagrams (a) and (b) denote the LL mixing of scalar four-fermion operators with four heavy quarks onto heavy flavor dipoles, while diagram (c) the running of heavy flavor dipoles into themselves. At the heavy flavor threshold, the gluonic dipole is integrated out, inducing  $\mathcal{O}((4\pi)^{-2}L_\mu)$  contributions to  $C_{\tilde{G}}$ . Diagrams (d) and (e) contribute to the 2-loop mixing of heavy-light vector operators onto dipoles.

similarly, using the last two equations one can obtain the matching for  $[C_{uG}]_{jj}$  and  $[C_{dG}]_{ii}$ . For the photon dipoles, we have

$$\begin{aligned}
[C_{u\gamma}]_{ii}(\mu^-) &= [C_{u\gamma}]_{ii}(\mu^+) + \frac{eQ_j m_j}{16\pi^2} \left( [C_{uddu}^{V1,LR}]_{ijji}(\mu^+) - \frac{4}{3} [C_{uddu}^{V8,LR}]_{ijji}(\mu^+) \right), \\
[C_{d\gamma}]_{jj}(\mu^-) &= [C_{d\gamma}]_{jj}(\mu^+) + \frac{eQ_i m_i}{16\pi^2} \left( [C_{uddu}^{V1,LR}]_{ijji}(\mu^+) - \frac{4}{3} [C_{uddu}^{V8,LR}]_{ijji}(\mu^+) \right), \\
[C_{u\gamma}]_{ii}(\mu^-) &= [C_{u\gamma}]_{ii}(\mu^+) + \frac{eQ_j m_j}{16\pi^2} \left( [C_{uu}^{V1,LR}]_{ijji}(\mu^+) - \frac{4}{3} [C_{uu}^{V8,LR}]_{ijji}(\mu^+) \right), \\
[C_{d\gamma}]_{jj}(\mu^-) &= [C_{d\gamma}]_{jj}(\mu^+) + \frac{eQ_i m_i}{16\pi^2} \left( [C_{dd}^{V1,LR}]_{ijji}(\mu^+) - \frac{4}{3} [C_{dd}^{V8,LR}]_{ijji}(\mu^+) \right).
\end{aligned} \tag{4.13}$$

In the above relations, the scale  $\mu$  can be set to the appropriate matching scale of either  $m_c$  or  $m_b$ . Finally, for the leptonic dipoles, at  $\mu = m_\tau$ , we obtain [67]

$$[C_{e\gamma}]_{ii}(\mu^-) = [C_{e\gamma}]_{ii}(\mu^+) + \frac{eQ_j m_j}{16\pi^2} [C_{ee}^{V,LR}]_{ijji}(\mu^+). \tag{4.14}$$

### 4.3 Two-step operator mixing

We next consider possible NLL effects, which give rise to the dominant EDM contributions for those operators that do not contribute at LL. As shown in (4.10) and (4.11) the QCD dipoles  $[C_{dG}]_{33}$  and  $[C_{uG}]_{22}$  can mix with the three-gluon operator  $[C_{\tilde{G}}]$  due to 1-loop threshold at the bottom and charm thresholds, respectively. As illustrated in diagram (b) in Fig. 3, the scalar operators  $[C_{uu}^{S1,RR}]_{2222}$  and  $[C_{uu}^{S8,RR}]_{2222}$  mix with  $[C_{uG}]_{22}$  at 1-loop level. Therefore,  $[C_{uu}^{S1,RR}]_{2222}$  and  $[C_{uu}^{S8,RR}]_{2222}$  induce a correction to the three gluon operator of the form

$$\begin{aligned}
[C_{\tilde{G}}](m_c) &= \frac{2}{3} g_s^3 [C_{uu}^{S1,RR}]_{2222}(\mu_{ew}) \frac{L_{\mu_c}}{16\pi^2}, \\
[C_{\tilde{G}}](m_c) &= \frac{2}{3} g_s^3 \left( C_F - \frac{C_A}{2} \right) [C_{uu}^{S8,RR}]_{2222}(\mu_{ew}) \frac{L_{\mu_c}}{16\pi^2},
\end{aligned} \tag{4.15}$$

where, again, the approximate solution in Eq. (4.15) is obtained by neglecting the running of the Wilson coefficients and of the strong coupling constant. Similarly, for the operators containing bottom quarks, it reads

$$\begin{aligned} [C_{\tilde{G}}](m_b) &= \frac{2}{3}g_s^3 [C_{dd}^{S1,RR}]_{3333}(\mu_{ew}) \frac{L_{\mu_b}}{16\pi^2}, \\ [C_{\tilde{G}}](m_b) &= \frac{2}{3}g_s^3 \left( C_F - \frac{C_A}{2} \right) [C_{dd}^{S8,RR}]_{3333}(\mu_{ew}) \frac{L_{\mu_b}}{16\pi^2}. \end{aligned} \quad (4.16)$$

Here we denoted

$$L_{\mu_c} = \frac{1}{16\pi^2} \log \left( \frac{m_c}{\mu_{ew}} \right), \quad L_{\mu_b} = \frac{1}{16\pi^2} \log \left( \frac{m_b}{\mu_{ew}} \right), \quad (4.17)$$

and the appearance of one power of  $L_\mu$  and an additional power of  $(16\pi^2)^{-1}$  is typical of a NLL correction. Eqs. (4.15) and (4.16) are the leading contributions of scalar operators with charm and bottom quarks  $[C_{uu}^{S1(S8),RR}]_{2222}$  and  $[C_{dd}^{S1(S8),RR}]_{3333}$  to EDMs. The operators  $[C_{uddu}^{S1(S8)}]_{2332}$  can also mix with the three-gluon operator by first generating a  $b$  or  $c$  chromoelectric EDM

$$\begin{aligned} [C_{\tilde{G}}](m_c) &= \frac{m_b}{3m_c} g_s^3 [C_{uddu}^{S1,RR}]_{2332}(\mu_{ew}) \frac{L_{\mu_c}}{16\pi^2}, \\ [C_{\tilde{G}}](m_c) &= \frac{m_b}{3m_c} g_s^3 \left( C_F - \frac{C_A}{2} \right) [C_{uddu}^{S8,RR}]_{2332}(\mu_{ew}) \frac{L_{\mu_c}}{16\pi^2}, \\ [C_{\tilde{G}}](m_b) &= \frac{m_c}{3m_b} g_s^3 [C_{uddu}^{S1,RR}]_{2332}(\mu_{ew}) \frac{L_{\mu_b}}{16\pi^2}, \\ [C_{\tilde{G}}](m_b) &= \frac{m_c}{3m_b} g_s^3 \left( C_F - \frac{C_A}{2} \right) [C_{uddu}^{S8,RR}]_{2332}(\mu_{ew}) \frac{L_{\mu_b}}{16\pi^2}. \end{aligned} \quad (4.18)$$

The operators  $[C_{ud}^{S1(8),RR}]_{2233}$  have 1-loop QCD and QED mixing with  $[C_{uddu}^{S1(8),RR}]_{2332}$ , and thus generate contributions to the  $b$  and  $c$  QED and QCD dipoles analogous to Eqs. (4.8) and (4.9). These generate corrections to  $[C_{\tilde{G}}]$  that scale as  $L_\mu^2/(16\pi^2)$ .

#### 4.4 2-loop anomalous dimension

We have seen that four-quark scalar operators in the  $(LR)(LR)$  class contribute to EDM at LL, in the case of operators with four light quarks or two heavy and two light quarks, or NLL, for operators with four heavy quarks. We next analyze vector operators in the  $(LL)(RR)$  class. For heavy-light operators, the first contribution arises at NLL. At this order, we need to consider the 2-loop running between  $\mu_{ew}$  and  $m_b$  or  $m_c$ , and the 1-loop matching contribution discussed in Sec. 4.2.2. Both the anomalous dimension and the matching coefficient are separately scheme-dependent, and the scheme dependence cancels between the two [126]. The 2-loop anomalous dimension can be obtained by generalizing the results of Misiak and Cho [127]. They calculated the mixing between  $\Delta F = 1$  vector left-right and dipole operators in the “standard” basis. Here we generalize their results to the mixing of  $\Delta F = 0$  four-fermion and dipole operators in the JMS basis. A typical

2-loop Feynman diagram governing this mixing is given by diagram (d) in Fig. 3. The  $\Delta F = 1$  effective Lagrangian used in Ref. [127] was

$$\mathcal{L}_{\text{eff}}^{\Delta F=1} = V_{tb}V_{ts}^* \frac{G_F}{\sqrt{2}} \sum_{i \in \{7,8,9,10\}} C_i Q_i, \quad (4.19)$$

with

$$\begin{aligned} Q_7 &= \frac{e}{16\pi^2} m_b (\bar{s}_\alpha \sigma^{\mu\nu} P_R b_\alpha) F_{\mu\nu}, & Q_8 &= \frac{g_s}{16\pi^2} m_b (\bar{s}_\alpha \sigma^{\mu\nu} P_R T_{\alpha\beta}^A b_\beta) G_{\mu\nu}^A, \\ Q_9 &= \frac{m_b}{m_c} (\bar{s}_\alpha \gamma_\mu P_L u_\beta) (\bar{u}_\beta \gamma^\mu P_R b_\alpha), & Q_{10} &= \frac{m_b}{m_c} (\bar{s}_\alpha \gamma_\mu P_L u_\alpha) (\bar{u}_\beta \gamma^\mu P_R b_\beta). \end{aligned} \quad (4.20)$$

The RGE for corresponding WCs can be written as

$$2\mu^2 \frac{d}{d\mu^2} \vec{C}_S(\mu) = \frac{\alpha_s}{4\pi} (\hat{\gamma}_S^u)^T \vec{C}_S(\mu). \quad (4.21)$$

The  $4 \times 4$  ADM for the standard operator vector  $\vec{Q}_S = \{Q_7, Q_8, Q_9, Q_{10}\}$  is given in equation (4.7) of Ref. [127] for  $u = c$ . Keeping the explicit dependence on the electric charges of the  $u$ -type and  $d$ -type quarks, it reads<sup>2</sup>

$$\frac{\hat{\gamma}_S^u}{2} = \begin{pmatrix} \frac{16}{3} & 0 & 0 & 0 \\ -\frac{16}{9} & \frac{14}{3} & 0 & 0 \\ 40q_u & -2 & -8 & 0 \\ 8q_u + \frac{16}{3}q_d & \frac{4}{3} & -3 & 1 \end{pmatrix}. \quad (4.22)$$

The superscript  $u$  indicates that the  $u$ -quarks are closed in diagram (d) in Fig. 3. Since the JMS basis uses the unit normalization for the operators, using (4.24), first we go to an intermediate basis and obtain the ADM for it

$$\vec{Q}' = \{Q'_7, Q'_8, Q'_9, Q'_{10}\}. \quad (4.23)$$

The  $Q'_i$ 's are the same as the operators given in (4.20) but with unit normalization like the JMS operators and follows a JMS like RGEs for the WCs

$$16\pi^2 \mu \frac{d\vec{C}'(\mu)}{d\mu} = \hat{\gamma}' \vec{C}'(\mu). \quad (4.24)$$

The ADM in this basis (when closing  $u$ -quark) comes out to be

$$\hat{\gamma}'^u = \begin{pmatrix} \frac{8}{3}g_s^2 & \frac{-32eg_s}{9} & \frac{5eg_s^2 m_u}{\pi^2} q_u & \frac{eg_s^2 m_u}{8\pi^2} \left(\frac{16q_d}{3} + 8q_u\right) \\ 0 & \frac{-19g_s^2}{3} & \frac{-g_s^3 m_u}{4\pi^2} & \frac{g_s^3 m_u}{6\pi^2} \\ 0 & 0 & -16g_s^2 & -6g_s^2 \\ 0 & 0 & 0 & 2g_s^2 \end{pmatrix}. \quad (4.25)$$

The relation between  $\hat{\gamma}'^u$  and  $\hat{\gamma}_S^u$  is given by

$$\hat{\gamma}'^u = 16\pi^2 \mu \frac{dR(\mu)}{d\mu} R(\mu)^{-1} + R(\mu) g_s^2 (\hat{\gamma}_S^u)^T R(\mu)^{-1}. \quad (4.26)$$

<sup>2</sup>We thank M. Misiak for providing us the expressions of the ADM for generic  $q_u$  and  $q_d$  charges.

The matrix  $R(\mu)$  is the transformation matrix defined by  $C'(\mu) = R(\mu)C_S(\mu)$ . The RGE for  $R(\mu)$  is dictated by the RGEs of  $g_s(\mu)$  and  $m_b(\mu)$

$$16\pi^2\mu\frac{dR(\mu)}{d\mu} = \begin{pmatrix} -8eg_s^2m_b & 0 & 0 & 0 \\ 0 & -\frac{47}{3}g_s^3m_b & 0 & 0 \\ 0 & 0 & 0 & 0 \\ 0 & 0 & 0 & 0 \end{pmatrix}. \quad (4.27)$$

We have used  $16\pi^2\mu(dm_b/d\mu) = -6C_Fg_s^2m_b$  and  $16\pi^2\mu(dg_s/d\mu) = -23g_s^3/3$  for five flavors. The correspondence between the  $Q'$  and the JMS bases is given by

$$\hat{\gamma}_{\text{JMS}} = P\hat{\gamma}'P^{-1}. \quad (4.28)$$

Here the matrix  $P$  defines the transformation between the WCs in the two bases, namely  $C_{\text{JMS}} = PC'$ . In what follows we will derive  $\hat{\gamma}_{\text{JMS}}$  for specific sets of the JMS  $\Delta F = 0$  operators entering the EDMs.

#### 4.4.1 $C_{uddu}^{V1,LR}$ , $C_{uddu}^{V8,LR}$ onto dipoles

In this case, the operators  $C_{uddu}^{V1,LR}$  and  $C_{uddu}^{V8,LR}$  contribute to EDMs, here the index  $p$  can be equal or unequal to  $r$ . At 2-loop order, these two operators can mix with  $\{C_{u\gamma}, C_{uG}\}$ , if one closes the  $d$  quark loop, or  $\{C_{d\gamma}, C_{dG}\}$ , by closing the  $u$  quark loop. Using the color identity  $T_{ij}^A T_{kl}^A = \frac{1}{2}(\delta_{il}\delta_{jk} - \frac{1}{3}\delta_{ij}\delta_{kl})$ , the tree-level transformation matrix between the intermediate basis with properly adjusted down-quark flavors to  $\Delta F = 0$  and the JMS basis  $\vec{C}_u = \{C_{d\gamma}, C_{dG}, C_{uddu}^{V1,LR}, C_{uddu}^{V8,LR}\}$  is found to be

$$P = \begin{pmatrix} 1 & 0 & 0 & 0 \\ 0 & 1 & 0 & 0 \\ 0 & 0 & 1/3 & 1 \\ 0 & 0 & 2 & 0 \end{pmatrix}. \quad (4.29)$$

Using (4.22), (4.27) and (4.29) in (4.26), we obtain <sup>3</sup> the ADMs for  $\vec{C}_u$  when the  $u$ -quark loop is closed<sup>4</sup>

$$\gamma_{\text{JMS}}^u = \begin{pmatrix} \frac{8g_s^2}{3} & -\frac{32eg_s}{9} & \frac{4eg_s^2m_u}{9\pi^2} & \frac{43eg_s^2m_u}{27\pi^2} \\ -\frac{8eg_s}{3} & -\frac{19g_s^2}{3} & \frac{g_s^3m_u}{6\pi^2} & -\frac{11g_s^3m_u}{72\pi^2} \\ 0 & 0 & 0 & -\frac{8g_s^2}{3} \\ 0 & 0 & -12g_s^2 & -14g_s^2 \end{pmatrix}. \quad (4.30)$$

Here  $u = u$  or  $c$ .

<sup>3</sup>Note that one needs to properly adjust the value of electric charge for the case of up-type dipoles in contrast to the original result which is valid for the down-quark dipoles.

<sup>4</sup>Note that in the original result of Misiak and Cho the charm-quark loop was closed.

For down-quark loops we have a four-vector  $\vec{C}_d = \{C_{u\gamma}, C_{uG}, C_{uddu}^{V1,LR}, C_{uddu}^{V8,LR}\}$ . The transformation matrix is the same as given in (4.29). However, in this case, first, we need to make the replacements  $q_u \rightarrow q_d$  and  $q_d \rightarrow q_u$  in the original ADM (4.22). This brings us

$$\gamma_{\text{JMS}}^d = \begin{pmatrix} \frac{8g_s^2}{3} & \frac{64eg_s}{9} & \frac{eg_s^2 m_d}{9\pi^2} & \frac{-23eg_s^2 m_d}{27\pi^2} \\ \frac{16eg_s}{3} & \frac{-19g_s^2}{3} & \frac{g_s^3 m_d}{6\pi^2} & \frac{-11g_s^3 m_d}{72\pi^2} \\ 0 & 0 & 0 & \frac{-8g_s^2}{3} \\ 0 & 0 & -12g_s^2 & -14g_s^2 \end{pmatrix}. \quad (4.31)$$

Here  $d$  represents  $d, s$  or  $b$ . Obviously, only the 1–3 and 1–4 entries corresponding to the mixing of vector left-right operators onto QED dipole operators are modified as compared to  $\gamma_{\text{JMS}}^u$ .

#### 4.4.2 $C_{pp}^{V1,LR}, C_{pp}^{V8,LR}$ onto dipoles

The operators  $C_{pp}^{V1,LR}$  and  $C_{pp}^{V8,LR}$  can contribute to EDMs if  $p \neq r$ . These mix with  $\{C_{u\gamma}, C_{uG}\}$  and  $\{C_{u\gamma}, C_{uG}\}$  depending on whether the quarks with  $rr$  or  $pp$  flavor indices are closed. In this case, we have two four vectors, namely  $\vec{C}_{ur} = \{C_{u\gamma}, C_{uG}, C_{uu}^{V1,LR}, C_{uu}^{V8,LR}\}$  and  $\vec{C}_{up} = \{C_{u\gamma}, C_{uG}, C_{uu}^{V1,LR}, C_{uu}^{V8,LR}\}$ . Both cases involve an up-quark loop with flavor indices  $rr$  and  $pp$  respectively. The transformation matrix between the standard (after properly adjusting quark flavors in (4.20)) and JMS vectors  $\vec{C}_{ur}$  and  $\vec{C}_{up}$  is given by (4.29). In this case, in the original 2-loop ADM (4.22) one has to make replacements  $q_u \rightarrow q_u$  and  $q_d \rightarrow q_u$  which lead us to

$$\gamma_{\text{JMS}}^{ur} = \begin{pmatrix} \frac{8g_s^2}{3} & \frac{64eg_s}{9} & \frac{10eg_s^2 m_u}{9\pi^2} & \frac{40eg_s^2 m_u}{27\pi^2} \\ \frac{16eg_s}{3} & \frac{-19g_s^2}{3} & \frac{g_s^3 m_u}{6\pi^2} & \frac{-11g_s^3 m_u}{72\pi^2} \\ 0 & 0 & 0 & \frac{-8g_s^2}{3} \\ 0 & 0 & -12g_s^2 & -14g_s^2 \end{pmatrix}. \quad (4.32)$$

The  $\gamma_{\text{JMS}}^{up}$  is exactly same as  $\gamma_{\text{JMS}}^{ur}$ .

#### 4.4.3 $C_{pp}^{V1,LR}, C_{pp}^{V8,LR}$ onto dipoles

In this case, we have two four vectors, namely  $\vec{C}_{dr} = \{C_{d\gamma}, C_{dG}, C_{dd}^{V1,LR}, C_{dd}^{V8,LR}\}$  and  $\vec{C}_{dp} = \{C_{d\gamma}, C_{dG}, C_{dd}^{V1,LR}, C_{dd}^{V8,LR}\}$ . In the original 2-loop ADM (4.22) one has to make replacements  $q_u \rightarrow q_d$  and  $q_d \rightarrow q_d$ . This leads us to

$$\gamma_{\text{JMS}}^{dr} = \begin{pmatrix} \frac{8g_s^2}{3} & \frac{-32eg_s}{9} & \frac{-5eg_s^2 m_d}{9\pi^2} & \frac{-20eg_s^2 m_d}{27\pi^2} \\ \frac{-8eg_s}{3} & \frac{-19g_s^2}{3} & \frac{g_s^3 m_d}{6\pi^2} & \frac{-11g_s^3 m_d}{72\pi^2} \\ 0 & 0 & 0 & \frac{-8g_s^2}{3} \\ 0 & 0 & -12g_s^2 & -14g_s^2 \end{pmatrix}. \quad (4.33)$$

The  $\gamma_{\text{JMS}}^{dp}$  is exactly same as  $\gamma_{\text{JMS}}^{dr}$ .

All four-quark and dipole operators with bottom-quark in 5+3 WET												
$i \downarrow$	$\eta_i^j(\mu_{\text{low}}, \mu_{\text{ew}})$						$\eta_i^j(\mu_b, \mu_{\text{ew}})$					
	$C_{uG}$ <sub>11</sub>	$C_{u\gamma}$ <sub>11</sub>	$C_{dG}$ <sub>11</sub>	$C_{dG}$ <sub>22</sub>	$C_{d\gamma}$ <sub>11</sub>	$C_{d\gamma}$ <sub>22</sub>	$C_{\hat{G}}$	$C_{e\gamma}$ <sub>11</sub>	$C_{dG}$ <sub>33</sub>	$C_{d\gamma}$ <sub>33</sub>	$C_{uG}$ <sub>22</sub>	$C_{u\gamma}$ <sub>22</sub>
$[C_{dd}^{S1,RR}]_{3333}$	$4.6 \cdot 10^{-8}$	-	$9.8 \cdot 10^{-8}$	$2.0 \cdot 10^{-6}$	-	-	$-1.4 \cdot 10^{-4}$	-	$-2.6 \cdot 10^{-1}$	$1.2 \cdot 10^{-2}$	-	-
$[C_{dd}^{S8,RR}]_{3333}$	-	-	$-2.0 \cdot 10^{-8}$	$-4.1 \cdot 10^{-7}$	-	-	$3.0 \cdot 10^{-5}$	-	$5.5 \cdot 10^{-2}$	$1.4 \cdot 10^{-2}$	-	-
$[C_{dd}^{S1,RR}]_{1133}$	-	-	$2.6 \cdot 10^{-2}$	-	$3.6 \cdot 10^{-4}$	-	$1.3 \cdot 10^{-8}$	-	$2.4 \cdot 10^{-5}$	$1.4 \cdot 10^{-7}$	-	-
$[C_{dd}^{S8,RR}]_{1133}$	-	-	$8.9 \cdot 10^{-3}$	-	$-1.1 \cdot 10^{-3}$	-	-	-	$8.1 \cdot 10^{-6}$	$-1.2 \cdot 10^{-6}$	-	-
$[C_{dd}^{S1,RR}]_{2233}$	-	-	-	$2.6 \cdot 10^{-2}$	-	$3.6 \cdot 10^{-4}$	$2.6 \cdot 10^{-7}$	-	$4.8 \cdot 10^{-4}$	$2.7 \cdot 10^{-6}$	-	-
$[C_{dd}^{S8,RR}]_{2233}$	-	-	-	$8.9 \cdot 10^{-3}$	-	$-1.1 \cdot 10^{-3}$	$8.9 \cdot 10^{-8}$	-	$1.6 \cdot 10^{-4}$	$-2.4 \cdot 10^{-5}$	-	-
$[C_{dd}^{S1,RR}]_{1331}$	-	-	$-1.7 \cdot 10^{-1}$	-	$4.2 \cdot 10^{-3}$	-	$-8.5 \cdot 10^{-8}$	-	$-1.6 \cdot 10^{-4}$	$5.9 \cdot 10^{-6}$	-	-
$[C_{dd}^{S8,RR}]_{1331}$	-	-	$2.2 \cdot 10^{-2}$	-	$8.2 \cdot 10^{-3}$	-	$1.1 \cdot 10^{-8}$	-	$2.0 \cdot 10^{-5}$	$8.4 \cdot 10^{-6}$	-	-
$[C_{dd}^{S1,RR}]_{2332}$	-	-	-	$-1.7 \cdot 10^{-1}$	-	$4.2 \cdot 10^{-3}$	$-1.7 \cdot 10^{-6}$	-	$-3.2 \cdot 10^{-3}$	$1.2 \cdot 10^{-4}$	-	-
$[C_{dd}^{S8,RR}]_{2332}$	-	-	-	$2.2 \cdot 10^{-2}$	-	$8.2 \cdot 10^{-3}$	$2.2 \cdot 10^{-7}$	-	$4.0 \cdot 10^{-4}$	$1.7 \cdot 10^{-4}$	-	-
$[C_{ud}^{S1,RR}]_{1133}$	$2.6 \cdot 10^{-2}$	$-7.6 \cdot 10^{-4}$	-	-	-	-	-	-	$1.1 \cdot 10^{-5}$	$2.5 \cdot 10^{-8}$	-	-
$[C_{dd}^{S8,RR}]_{1133}$	-	-	$8.9 \cdot 10^{-3}$	-	$-1.1 \cdot 10^{-3}$	-	-	-	$8.1 \cdot 10^{-6}$	$-1.2 \cdot 10^{-6}$	-	-
$[C_{uddu}^{S1,RR}]_{1331}$	$-1.7 \cdot 10^{-1}$	$1.4 \cdot 10^{-2}$	-	-	-	-	$-4.0 \cdot 10^{-8}$	-	$-7.3 \cdot 10^{-5}$	$-8.1 \cdot 10^{-6}$	-	-
$[C_{uddu}^{S8,RR}]_{1331}$	$2.1 \cdot 10^{-2}$	$6.9 \cdot 10^{-3}$	-	-	-	-	-	-	$9.0 \cdot 10^{-6}$	$-7.5 \cdot 10^{-6}$	-	-
$[C_{ud}^{S1,RR}]_{2233}$	-	-	-	$-4.5 \cdot 10^{-8}$	-	-	$9.9 \cdot 10^{-5}$	-	$6.0 \cdot 10^{-3}$	$1.3 \cdot 10^{-5}$	$2.4 \cdot 10^{-2}$	$-3.2 \cdot 10^{-4}$
$[C_{ud}^{S8,RR}]_{2233}$	-	-	-	$-1.5 \cdot 10^{-8}$	-	-	$3.2 \cdot 10^{-5}$	-	$1.9 \cdot 10^{-3}$	$6.5 \cdot 10^{-4}$	$7.7 \cdot 10^{-3}$	$-1.4 \cdot 10^{-3}$
$[C_{uddu}^{S1,RR}]_{2332}$	-	-	$1.4 \cdot 10^{-8}$	$2.9 \cdot 10^{-7}$	-	-	$-6.5 \cdot 10^{-4}$	-	$-3.9 \cdot 10^{-2}$	$-4.3 \cdot 10^{-3}$	$-1.6 \cdot 10^{-1}$	$1.1 \cdot 10^{-2}$
$[C_{uddu}^{S8,RR}]_{2332}$	-	-	-	$-3.6 \cdot 10^{-8}$	-	-	$7.9 \cdot 10^{-5}$	-	$4.8 \cdot 10^{-3}$	$-4.0 \cdot 10^{-3}$	$1.9 \cdot 10^{-2}$	$7.5 \cdot 10^{-3}$
$[C_{uddu}^{V1,LR}]_{1331}$	$-5.0 \cdot 10^{-2}$	$1.1 \cdot 10^{-3}$	-	-	-	-	-	-	$-1.7 \cdot 10^{-6}$	$-2.3 \cdot 10^{-6}$	-	-
$[C_{uddu}^{V8,LR}]_{1331}$	$1.3 \cdot 10^{-2}$	$1.2 \cdot 10^{-2}$	-	-	-	-	-	-	$2.6 \cdot 10^{-6}$	$-5.5 \cdot 10^{-6}$	-	-
$[C_{dd}^{V1,LR}]_{1331}$	-	-	$-4.9 \cdot 10^{-2}$	-	$3.2 \cdot 10^{-3}$	-	-	-	$-3.6 \cdot 10^{-6}$	$4.1 \cdot 10^{-6}$	-	-
$[C_{dd}^{V8,LR}]_{1331}$	-	-	$1.4 \cdot 10^{-2}$	-	$1.2 \cdot 10^{-2}$	-	-	-	$5.7 \cdot 10^{-6}$	$5.6 \cdot 10^{-6}$	-	-
$[C_{dd}^{V1,LR}]_{2332}$	-	-	-	$-4.9 \cdot 10^{-2}$	-	$3.2 \cdot 10^{-3}$	$-3.9 \cdot 10^{-8}$	-	$-7.1 \cdot 10^{-5}$	$8.1 \cdot 10^{-5}$	-	-
$[C_{dd}^{V8,LR}]_{2332}$	-	-	-	$1.4 \cdot 10^{-2}$	-	$1.2 \cdot 10^{-2}$	$6.1 \cdot 10^{-8}$	-	$1.1 \cdot 10^{-4}$	$1.1 \cdot 10^{-4}$	-	-
$[C_{uddu}^{V1,LR}]_{2332}$	-	-	-	-	-	-	$-1.8 \cdot 10^{-4}$	-	$-8.6 \cdot 10^{-4}$	$-1.2 \cdot 10^{-3}$	$-4.5 \cdot 10^{-2}$	$2.9 \cdot 10^{-4}$
$[C_{uddu}^{V8,LR}]_{2332}$	-	-	-	-	-	-	$5.0 \cdot 10^{-5}$	-	$1.3 \cdot 10^{-3}$	$-2.7 \cdot 10^{-3}$	$1.3 \cdot 10^{-2}$	$1.2 \cdot 10^{-2}$
$[C_{dG}]_{33}$	$-2.2 \cdot 10^{-7}$	-	$-4.7 \cdot 10^{-7}$	$-9.5 \cdot 10^{-6}$	-	$-4.2 \cdot 10^{-8}$	$6.9 \cdot 10^{-4}$	-	$1.3 \cdot 10^0$	$3.2 \cdot 10^{-2}$	-	-
$[C_{d\gamma}]_{33}$	-	-	-	$-1.9 \cdot 10^{-7}$	-	-	$1.3 \cdot 10^{-5}$	-	$2.5 \cdot 10^{-2}$	$9.0 \cdot 10^{-1}$	-	-
	$C_{uG}$ <sub>11</sub>	$C_{u\gamma}$ <sub>11</sub>	$C_{dG}$ <sub>11</sub>	$C_{dG}$ <sub>22</sub>	$C_{d\gamma}$ <sub>11</sub>	$C_{d\gamma}$ <sub>22</sub>	$C_{\hat{G}}$	$C_{e\gamma}$ <sub>11</sub>	$C_{dG}$ <sub>33</sub>	$C_{d\gamma}$ <sub>33</sub>	$C_{uG}$ <sub>22</sub>	$C_{u\gamma}$ <sub>22</sub>

**Table 4:** Operator mixing of the bottom quark operators in 5 + 3 WET (1st column) onto dipole operators (2nd row) in 3+1 and 5+3 flavor WET is shown. Here the entries represent the quantity  $\eta_i^j(\mu_{\text{low}}, \mu_{\text{ew}})$ ,  $\mu_{\text{ew}} = 91.1876$  GeV,  $\mu_{\text{low}} = 2.0$  GeV. Entries below  $10^{-8}$  are dropped. Note that for the charm and bottom dipoles, we stop running at  $\mu = m_b = 4.18$  GeV.

#### 4.4.4 $C_{ee}^{V,LR}$ onto dipole

The leptonic  $C_{ee}^{V,LR}$  operator can break CP is  $p \neq r$ . In this case, we have two vectors, namely  $\vec{C}_{er} = \{C_{e\gamma}, C_{ee}^{V,LR}\}$  and  $\vec{C}_{ep} = \{C_{e\gamma}, C_{ee}^{V,LR}\}$ . One example of the 2-loop Feynman diagrams governing this mixing is given in diagram (e) of Fig. 3. In the 2-loop ADM (4.25) one has to make replacements  $q_u \rightarrow q_e$  and  $q_d \rightarrow q_e$ . However, since these are purely leptonic operators which exhibit only QED mixing we need to replace gluons in these diagrams with

photons. So we need to take out the color factors in the original result. We found that the 2-loop  $P$ -type diagrams (which are the only ones allowed for the pure leptonic operators) shown in Fig. 4 of [126] has a universal color factor  $C_F = (T^A T^A)_{ij} = \delta_{ij}(N^2 - 1)/2N$ .

Therefore, we need to divide the elements of ADM by this overall color factor  $C_F$ . With all these adjustments, we arrived at the RG equation for  $C_{pp}^{e\gamma}$

$$16\pi^2\mu(dC_{pp}^{e\gamma}/d\mu) = \frac{15e^3 m_r Q_e}{12\pi^2} C_{pp}^{e\gamma, LR}. \quad (4.34)$$

Trivially, the same RGE holds for  $C_{rr}^{e\gamma}$ .

All operators with charm-quark in 4+1 WET										
$\eta_i^j(\mu_{\text{low}}, \mu_{\text{ew}})$										
$i \downarrow$	$[C_{uG}]_{11}$	$[C_{u\gamma}]_{11}$	$[C_{dG}]_{11}$	$[C_{dG}]_{22}$	$[C_{d\gamma}]_{11}$	$[C_{d\gamma}]_{22}$	$C_{\tilde{G}}$	$[C_{e\gamma}]_{11}$	$[C_{uG}]_{22}$	$[C_{u\gamma}]_{22}$
$[C_{uu}^{S1,RR}]_{2222}$	-	-	-	-	-	-	$-3.7 \cdot 10^{-4}$	-	$-1.0 \cdot 10^{-1}$	$-7.0 \cdot 10^{-3}$
$[C_{uu}^{S8,RR}]_{2222}$	-	-	-	-	-	-	$8.5 \cdot 10^{-5}$	-	$2.3 \cdot 10^{-2}$	$-8.5 \cdot 10^{-3}$
$[C_{uu}^{S1,RR}]_{1122}$	$1.3 \cdot 10^{-2}$	$-8.8 \cdot 10^{-5}$	-	-	-	-	$9.2 \cdot 10^{-8}$	-	$2.5 \cdot 10^{-5}$	$-1.6 \cdot 10^{-7}$
$[C_{uu}^{S8,RR}]_{1122}$	$4.4 \cdot 10^{-3}$	$9.7 \cdot 10^{-4}$	-	-	-	-	$3.0 \cdot 10^{-8}$	-	$8.2 \cdot 10^{-6}$	$1.8 \cdot 10^{-6}$
$[C_{ud}^{S1,RR}]_{2211}$	-	-	$1.3 \cdot 10^{-2}$	-	$8.4 \cdot 10^{-5}$	-	$2.0 \cdot 10^{-7}$	-	$5.4 \cdot 10^{-5}$	$-9.5 \cdot 10^{-7}$
$[C_{ud}^{S8,RR}]_{2211}$	-	-	$4.0 \cdot 10^{-3}$	-	$1.1 \cdot 10^{-3}$	-	$5.9 \cdot 10^{-8}$	-	$1.6 \cdot 10^{-5}$	$-2.4 \cdot 10^{-6}$
$[C_{ud}^{S1,RR}]_{2222}$	-	-	-	$1.3 \cdot 10^{-2}$	-	$8.4 \cdot 10^{-5}$	$4.0 \cdot 10^{-6}$	-	$1.1 \cdot 10^{-3}$	$-1.9 \cdot 10^{-5}$
$[C_{ud}^{S8,RR}]_{2222}$	-	-	-	$4.0 \cdot 10^{-3}$	-	$1.1 \cdot 10^{-3}$	$1.2 \cdot 10^{-6}$	-	$3.3 \cdot 10^{-4}$	$-4.9 \cdot 10^{-5}$
$[C_{uddu}^{S1,RR}]_{2112}$	-	-	$-6.4 \cdot 10^{-2}$	-	$-6.1 \cdot 10^{-3}$	-	$-9.4 \cdot 10^{-7}$	-	$-2.6 \cdot 10^{-4}$	$1.7 \cdot 10^{-5}$
$[C_{uddu}^{S8,RR}]_{2112}$	-	-	$6.9 \cdot 10^{-3}$	-	$-4.9 \cdot 10^{-3}$	-	$1.0 \cdot 10^{-7}$	-	$2.7 \cdot 10^{-5}$	$9.0 \cdot 10^{-6}$
$[C_{uddu}^{S1,RR}]_{2222}$	-	-	-	$-6.4 \cdot 10^{-2}$	-	$-6.1 \cdot 10^{-3}$	$-1.9 \cdot 10^{-5}$	-	$-5.2 \cdot 10^{-3}$	$3.5 \cdot 10^{-4}$
$[C_{uddu}^{S8,RR}]_{2222}$	-	-	-	$6.9 \cdot 10^{-3}$	-	$-4.9 \cdot 10^{-3}$	$2.0 \cdot 10^{-6}$	-	$5.5 \cdot 10^{-4}$	$1.8 \cdot 10^{-4}$
$[C_{uu}^{S1,RR}]_{1221}$	$-6.4 \cdot 10^{-2}$	$-3.4 \cdot 10^{-3}$	-	-	-	-	$-4.4 \cdot 10^{-7}$	-	$-1.2 \cdot 10^{-4}$	$-6.3 \cdot 10^{-6}$
$[C_{uu}^{S8,RR}]_{1221}$	$7.2 \cdot 10^{-3}$	$-5.2 \cdot 10^{-3}$	-	-	-	-	$4.9 \cdot 10^{-8}$	-	$1.4 \cdot 10^{-5}$	$-9.8 \cdot 10^{-6}$
$[C_{uddu}^{V1,LR}]_{2112}$	-	-	$-1.3 \cdot 10^{-2}$	-	$-2.3 \cdot 10^{-3}$	-	$-1.7 \cdot 10^{-8}$	-	$-4.8 \cdot 10^{-6}$	$2.0 \cdot 10^{-6}$
$[C_{uddu}^{V8,LR}]_{2112}$	-	-	$4.3 \cdot 10^{-3}$	-	$-8.1 \cdot 10^{-3}$	-	$3.4 \cdot 10^{-8}$	-	$9.2 \cdot 10^{-6}$	$9.2 \cdot 10^{-6}$
$[C_{uddu}^{V1,LR}]_{2222}$	-	-	-	$-1.3 \cdot 10^{-2}$	-	$-2.3 \cdot 10^{-3}$	$-3.4 \cdot 10^{-7}$	-	$-9.4 \cdot 10^{-5}$	$4.0 \cdot 10^{-5}$
$[C_{uddu}^{V8,LR}]_{2222}$	-	-	-	$4.3 \cdot 10^{-3}$	-	$-8.1 \cdot 10^{-3}$	$6.7 \cdot 10^{-7}$	-	$1.8 \cdot 10^{-4}$	$1.8 \cdot 10^{-4}$
$[C_{uu}^{V1,LR}]_{1221}$	$-1.3 \cdot 10^{-2}$	$-3.3 \cdot 10^{-3}$	-	-	-	-	-	-	$-1.9 \cdot 10^{-6}$	$-6.1 \cdot 10^{-6}$
$[C_{uu}^{V8,LR}]_{1221}$	$4.5 \cdot 10^{-3}$	$-8.0 \cdot 10^{-3}$	-	-	-	-	$1.8 \cdot 10^{-8}$	-	$5.0 \cdot 10^{-6}$	$-8.3 \cdot 10^{-6}$
$[C_{u\gamma}]_{22}$	-	-	-	-	-	-	$-4.9 \cdot 10^{-4}$	-	$-1.4 \cdot 10^{-1}$	$8.7 \cdot 10^{-1}$
$[C_{uG}]_{22}$	-	-	-	-	-	-	$5.1 \cdot 10^{-3}$	-	$1.4 \cdot 10^0$	$-8.7 \cdot 10^{-2}$
$[C_{eu}^{S,RR}]_{1122}$	-	-	-	-	-	-	-	$-1.5 \cdot 10^{-4}$	-	$5.8 \cdot 10^{-8}$
$[C_{eu}^{T,RR}]_{1122}$	-	-	-	-	-	-	-	$7.4 \cdot 10^{-2}$	$1.5 \cdot 10^{-6}$	$-3.0 \cdot 10^{-5}$
	$[C_{uG}]_{11}$	$[C_{u\gamma}]_{11}$	$[C_{dG}]_{11}$	$[C_{dG}]_{22}$	$[C_{d\gamma}]_{11}$	$[C_{d\gamma}]_{22}$	$C_{\tilde{G}}$	$[C_{e\gamma}]_{11}$	$[C_{uG}]_{22}$	$[C_{u\gamma}]_{22}$

**Table 5:** Operator mixing of the charm quark operators in 4 + 1 WET (1st column) onto dipole operators (2nd row) in 3 + 1 and 4 + 1 flavor WET is shown. Here the entries represent the quantity  $\eta_i^j(\mu_{\text{low}}, \mu_{\text{ew}})$ ,  $\mu_{\text{ew}} = 91.1876$  GeV,  $\mu_{\text{low}} = 2.0$  GeV. Entries below  $10^{-8}$  are dropped.

## 4.5 Numerical solution for the RGEs

In this section, we provide the numerical solution to the RGEs, which allows us to quantify the impact of such effects on the low-energy operators that contribute to EDMs at the tree level. As we have learned in the previous subsections, 1-loop and 2-loop RG running effects and threshold effects cause operator mixing leading to the expansion of operator basis for the EDMs.

All semileptonic operators in 5+3 WET												
$i \downarrow$	$\eta_i^j(\mu_{\text{low}}, \mu_{\text{ew}})$						$\eta_i^j(\mu_b, \mu_{\text{ew}})$					
	$C_{uG}$ <sub>11</sub>	$C_{u\gamma}$ <sub>11</sub>	$C_{dG}$ <sub>11</sub>	$C_{dG}$ <sub>22</sub>	$C_{d\gamma}$ <sub>11</sub>	$C_{d\gamma}$ <sub>22</sub>	$C_{\bar{G}}$	$C_{e\gamma}$ <sub>11</sub>	$C_{dG}$ <sub>33</sub>	$C_{d\gamma}$ <sub>33</sub>	$C_{uG}$ <sub>22</sub>	$C_{u\gamma}$ <sub>22</sub>
$[C_{eu}^{S,RR}]_{1111}$	-	$5.8 \cdot 10^{-8}$	-	-	-	-	-	$-2.9 \cdot 10^{-7}$	-	-	-	-
$[C_{ed}^{S,RR}]_{1111}$	-	-	-	-	$-2.9 \cdot 10^{-8}$	-	-	$-1.5 \cdot 10^{-7}$	-	-	-	-
$[C_{ed}^{S,RR}]_{1122}$	-	-	-	-	-	$-2.9 \cdot 10^{-8}$	-	$-3.1 \cdot 10^{-6}$	-	-	-	-
$[C_{eu}^{S,RL}]_{1111}$	-	-	-	-	-	-	-	-	-	-	-	-
$[C_{ed}^{S,RL}]_{1111}$	-	-	-	-	-	-	-	-	-	-	-	-
$[C_{ed}^{S,RL}]_{1122}$	-	-	-	-	-	-	-	-	-	-	-	-
$[C_{eu}^{T,RR}]_{1111}$	$1.5 \cdot 10^{-6}$	$-3.0 \cdot 10^{-5}$	-	-	-	-	-	$1.4 \cdot 10^{-4}$	-	-	-	-
$[C_{ed}^{T,RR}]_{1111}$	-	-	$-5.8 \cdot 10^{-7}$	-	$-3.0 \cdot 10^{-5}$	-	-	$-1.5 \cdot 10^{-4}$	-	-	-	-
$[C_{ed}^{T,RR}]_{1122}$	-	-	-	$-5.8 \cdot 10^{-7}$	-	$-3.0 \cdot 10^{-5}$	-	$-3.0 \cdot 10^{-3}$	-	-	-	-
$[C_{eu}^{T,RR}]_{1122}$	-	-	-	-	-	-	-	$7.4 \cdot 10^{-2}$	-	-	$6.7 \cdot 10^{-7}$	$-2.6 \cdot 10^{-5}$
$[C_{eu}^{S,RR}]_{1122}$	-	-	-	-	-	-	-	$-1.5 \cdot 10^{-4}$	-	-	-	$4.0 \cdot 10^{-8}$
$[C_{ed}^{T,RR}]_{1133}$	-	-	-	-	-	-	-	$-1.1 \cdot 10^{-1}$	$-3.4 \cdot 10^{-7}$	$-2.6 \cdot 10^{-5}$	-	-
$[C_{ed}^{T,RR}]_{2211}$	-	-	$-1.2 \cdot 10^{-4}$	-	$-6.3 \cdot 10^{-3}$	-	-	-	-	-	-	-
$[C_{ed}^{T,RR}]_{2222}$	-	-	-	$-1.2 \cdot 10^{-4}$	-	$-6.3 \cdot 10^{-3}$	-	-	-	-	-	-
$[C_{ed}^{T,RR}]_{2233}$	-	-	-	-	-	-	$-3.8 \cdot 10^{-8}$	-	$-7.0 \cdot 10^{-5}$	$-5.4 \cdot 10^{-3}$	-	-
$[C_{ed}^{T,RR}]_{3311}$	-	-	$-2.0 \cdot 10^{-3}$	-	$-1.1 \cdot 10^{-1}$	-	-	-	-	-	-	-
$[C_{ed}^{T,RR}]_{3322}$	-	-	-	$-2.0 \cdot 10^{-3}$	-	$-1.1 \cdot 10^{-1}$	-	-	-	-	-	-
$[C_{ed}^{T,RR}]_{3333}$	-	-	-	-	-	-	$-6.4 \cdot 10^{-7}$	-	$-1.2 \cdot 10^{-3}$	$-9.0 \cdot 10^{-2}$	-	-
$[C_{eu}^{T,RR}]_{2211}$	$3.1 \cdot 10^{-4}$	$-6.3 \cdot 10^{-3}$	-	-	-	-	-	-	-	-	-	-
$[C_{eu}^{T,RR}]_{2222}$	-	-	-	-	-	-	$1.1 \cdot 10^{-6}$	-	-	-	$1.4 \cdot 10^{-4}$	$-5.3 \cdot 10^{-3}$
$[C_{eu}^{T,RR}]_{3311}$	$5.3 \cdot 10^{-3}$	$-1.1 \cdot 10^{-1}$	-	-	-	-	-	-	-	-	-	-
$[C_{eu}^{T,RR}]_{3322}$	-	-	-	-	-	-	$1.9 \cdot 10^{-5}$	-	-	-	$2.3 \cdot 10^{-3}$	$-9.0 \cdot 10^{-2}$
$[C_{ed}^{S,RR}]_{1133}$	-	-	-	-	-	-	-	$-8.1 \cdot 10^{-5}$	-	$-2.0 \cdot 10^{-8}$	-	-
$[C_{ed}^{S,RR}]_{2211}$	-	-	$-3.6 \cdot 10^{-8}$	-	$-6.0 \cdot 10^{-6}$	-	-	-	-	-	-	-
$[C_{ed}^{S,RR}]_{2222}$	-	-	-	$-3.6 \cdot 10^{-8}$	-	$-6.0 \cdot 10^{-6}$	-	-	-	-	-	-
$[C_{ed}^{S,RR}]_{2233}$	-	-	-	-	-	-	-	-	-	$-4.1 \cdot 10^{-6}$	-	-
$[C_{ed}^{S,RR}]_{3311}$	-	-	$-6.0 \cdot 10^{-7}$	-	$-1.0 \cdot 10^{-4}$	-	-	-	-	-	-	-
$[C_{ed}^{S,RR}]_{3322}$	-	-	-	$-6.0 \cdot 10^{-7}$	-	$-1.0 \cdot 10^{-4}$	-	-	-	-	-	-
$[C_{ed}^{S,RR}]_{3333}$	-	-	-	-	-	-	-	-	-	$-6.9 \cdot 10^{-5}$	-	-
$[C_{eu}^{S,RR}]_{2211}$	$-2.6 \cdot 10^{-7}$	$1.2 \cdot 10^{-5}$	-	-	-	-	-	-	-	-	-	-
$[C_{eu}^{S,RR}]_{2222}$	-	-	-	-	-	-	-	-	-	-	-	$8.2 \cdot 10^{-6}$
$[C_{eu}^{S,RR}]_{3311}$	$-4.4 \cdot 10^{-6}$	$2.0 \cdot 10^{-4}$	-	-	-	-	-	-	-	-	-	-
$[C_{eu}^{S,RR}]_{3322}$	-	-	-	-	-	-	$-1.6 \cdot 10^{-8}$	-	-	-	-	$1.4 \cdot 10^{-4}$
$[C_{ee}^{V,LR}]_{1221}$	-	-	-	-	-	-	-	$-2.0 \cdot 10^{-4}$	-	-	-	-
$[C_{ee}^{V,LR}]_{1331}$	-	-	-	-	-	-	-	$-3.2 \cdot 10^{-3}$	-	-	-	-
$[C_{ee}^{S,RR}]_{1221}$	-	-	-	-	-	-	-	$6.3 \cdot 10^{-4}$	-	-	-	-
$[C_{ee}^{S,RR}]_{1331}$	-	-	-	-	-	-	-	$1.1 \cdot 10^{-2}$	-	-	-	-
$[C_{ee}^{S,RR}]_{1122}$	-	-	-	-	-	-	-	$-1.3 \cdot 10^{-5}$	-	-	-	-
$[C_{ee}^{S,RR}]_{1133}$	-	-	-	-	-	-	-	$-2.2 \cdot 10^{-4}$	-	-	-	-

**Table 6:** Operator mixing of the semileptonic operators in 5 + 3 WET (1st column) onto dipole operators (2nd row) in 3+1 and 5+3 flavor WET is shown. Here the entries represent the quantity  $\eta_i^j(\mu_{\text{low}}, \mu_{\text{ew}})$ ,  $\mu_{\text{ew}} = 91.1876$  GeV,  $\mu_{\text{low}} = 2.0$  GeV. Entries below  $10^{-8}$  are dropped. Note that for the charm and bottom dipoles, we stop running at  $\mu = m_b = 4.18$  GeV.



In Tabs. 4, 5 and 6, we show the numerical values of the quantity

$$\eta_i^j(\mu_{low}, \mu_{ew}) = \frac{\text{Im}C_j(\mu_{low})}{\text{Im}C_i(\mu_{ew})} \quad (4.35)$$

for  $\mu_{low} = 2$  GeV and  $\mu_{ew} = 91$  GeV. In these tables, we focus mainly on heavy flavor operators, that do not generate EDMs at tree level. In this case,  $C_j(\mu_{low})$  stands for the WCs of the dipole and Weinberg operators that enter at tree-level to the EDM expressions. The  $C_i(\mu_{ew})$  represent the all other WET operators which mix with  $C_j(\mu_{low})$  via any of the mechanism discussed above. In the 4+1 and 5+3 theories we only show the operators that contain at least one heavy flavor fermion current. Running effects, in particular QCD running, are also important for light flavor operators, and they are fully accounted for in the master formulae that we provide in Section 5.

## 5 EDM Master Formulae in WET

In this section, we derive master formulae for the EDMs for various species such as electron (via the HfF, ThO and YbF precession frequencies), neutron, and proton as well as diamagnetic atoms such as Hg, Xe, and Ra in terms of WET WCs at the EW scale in the JMS basis. By matching the WET to SMEFT and HEFT these formulae can be used to get the EDMs predictions in a large class of UV scenarios with linear and non-linear realizations of EW symmetry breaking, respectively. The main strengths of these formulae are the systematic inclusion of short-distance effects due to RG running and matching and the inclusion of the heavy flavor for the quark and leptons which are novel.

Without loss of generality, the EDMs can be expressed as a linear function of WET WCs as

$$d_X = \sum_{I \in \text{dipoles}} \alpha_I^X(\mu_{ew}) C_I^{(5)}(\mu_{ew}) [\text{TeV}^{-1}] + \sum_{J \in 4f} \alpha_J^X(\mu_{ew}) C_J^{(6)}(\mu_{ew}) [\text{TeV}^{-2}], \quad (5.1)$$

here  $X = n, p$  or Hg, Xe, Ra and the indices  $I$  and  $J$  run over all contributing dipole and four-fermion operators in the  $n_f = 5 + 3$   $\Delta F = 0$  WET at the EW scale. The complete list of relevant operators can be found in Sec. 2. The coefficients  $\alpha_I$  encode the long-distance effects due to matrix elements and RG running at the 2-loop level as described in the previous section. These coefficients have units of  $e \text{ cm TeV}^2$  or  $e \text{ cm TeV}$  for the dim-6 and dim-5 WCs, respectively. The WCs in (5.1) have  $\text{TeV}^{-2}$  and  $\text{TeV}^{-1}$  units for dim-6 and dim-5 operators. This is indicated by the units in square brackets in Eq. (5.1). In this way, the overall units of  $d_X$  are  $e \text{ cm}$ . To obtain the EDMs in the  $\text{GeV}^{-1}$  units we need to divide the  $\alpha_I$  coefficients by a conversion factor according to  $\text{GeV}^{-1} = 6.52 \times 10^{-14} e \text{ cm}$ .

We can write very similar expressions for the frequencies for the electron EDM. In this case, the  $\alpha_I^X$  coefficients will have  $(\text{mrad/s})\text{TeV}^2$  or  $(\text{mrad/s})\text{TeV}$  units. The values for  $\alpha_I$  coefficients at the EW scale and their theoretical uncertainties for the HfF precession frequency, the Hg and neutron EDMs are given in Tab. 7, 8, 9 and 10. The master formulae for  $d_p$ ,  $\omega_{\text{ThO}}$  and  $\omega_{\text{YbF}}$  can be found in appendix A. We do not provide explicit master formulae for  $d_{\text{Xe}}$  and  $d_{\text{Ra}}$ , but they have been implemented in `flavio`.

$\alpha_I^{\text{HFF}}(\mu_{ew})$ for the $\omega_{\text{HFF}}$			
$n_f = 3 + 1$		$n_f = 5 + 3$	
$[C_{e\gamma}]_{11}$	$(-2.9 \pm 0.1) \cdot 10^{12}$	$[C_{eu}^{S,RR}]_{1122}$	$(9.2 \pm 0.3) \cdot 10^5$
$[C_{ee}^{S,RR}]_{1111}$	$(-2.7 \pm 0.1) \cdot 10^4$	$[C_{eu}^{T,RR}]_{1122}$	$(-3.8 \pm 0.2) \cdot 10^8$
$[C_{eu}^{S,RR}]_{1111}$	$(-2.6 \pm 0.2) \cdot 10^8$	$[C_{ed}^{S,RR}]_{1133}$	$(3.7 \pm 0.1) \cdot 10^5$
$[C_{ed}^{S,RR}]_{1111}$	$(-2.6 \pm 0.3) \cdot 10^8$	$[C_{ed}^{T,RR}]_{1133}$	$(4.8 \pm 0.2) \cdot 10^8$
$[C_{ed}^{S,RR}]_{1122}$	$(-1.9 \pm 0.1) \cdot 10^7$	$[C_{ee}^{S,RR}]_{1122}$	$(5.8 \pm 0.2) \cdot 10^4$
$[C_{eu}^{S,RL}]_{1111}$	$(-2.6 \pm 0.3) \cdot 10^8$	$[C_{ee}^{S,RR}]_{1133}$	$(1.3 \pm 0.0) \cdot 10^6$
$[C_{ed}^{S,RL}]_{1111}$	$(-2.6 \pm 0.2) \cdot 10^8$	$[C_{ee}^{S,RR}]_{1221}$	$(-2.8 \pm 0.1) \cdot 10^6$
$[C_{ed}^{S,RL}]_{1122}$	$(-1.9 \pm 0.1) \cdot 10^7$	$[C_{ee}^{S,RR}]_{1331}$	$(-5.5 \pm 0.2) \cdot 10^7$
$[C_{eu}^{T,RR}]_{1111}$	$(2.3 \pm 0.1) \cdot 10^8$	$[C_{ee}^{V,LR}]_{1221}$	$(9.1 \pm 0.4) \cdot 10^5$
$[C_{ed}^{T,RR}]_{1111}$	$(-1.2 \pm 0.0) \cdot 10^8$	$[C_{ee}^{V,LR}]_{1331}$	$(1.5 \pm 0.1) \cdot 10^7$
$[C_{ed}^{T,RR}]_{1122}$	$(-9.0 \pm 0.4) \cdot 10^7$		-

**Table 7:** Master formula for  $\omega_{\text{HFF}}$  in WET in the JMS basis at the EW scale. The  $\alpha_I^{\text{HFF}}$  coefficients have units of (mrad/s)TeV<sup>2</sup> and (mrad/s)TeV for the four-fermion and dipole operators, respectively. The 90% CL upper bound on  $\omega_{\text{HFF}}$  is 0.17 mrad/s.

## 5.1 Theoretical uncertainties

The theoretical uncertainties in the  $\alpha_I^X$  coefficients can stem from various sources such as the SM parameters and the matrix elements. The latter arise from both nuclear theory and hadronization uncertainties and, for most species, they are the dominant source. The uncertainties from atomic theory are in most cases better understood. As discussed in Section 3, the quoted hadronic and nuclear uncertainties provide at best a very rough estimate of the real theoretical uncertainty. In this respect, the field is less advanced compared to flavor physics, where, for several observables, lattice QCD matrix elements have been evaluated, or collider physics. Here we assume theoretical uncertainties to be Gaussian distributed. The estimate of the theoretical uncertainties is based on the random sampling of the input parameters and the evaluation of the standard deviation of the corresponding EDM observables.

## 5.2 $\omega_{\text{HFF}}$

In this subsection, we provide a master formula for  $\omega_{\text{HFF}}$  (mrad/s), which is sensitive to the electron EDM, see Tab. 7. Similar formulae for the  $\omega_{\text{ThO}}$  and  $\omega_{\text{YbF}}$  are given in App. A.

Recalling that the 90% CL upper bound on  $\omega_{\text{HFF}}$  is 0.17 mrad/s, we can immediately see that the scale of the operators that contribute at tree level, which comprises all the operators in the  $n_f = 3 + 1$  column of Table 7 with the exception of  $[C_{ee}^{S,RR}]_{1111}$ , has to be very high,  $\Lambda \sim 10^4$  TeV. Even for  $[C_{ee}^{S,RR}]_{1111}$ , which mixes onto  $C_{e\gamma}$  at one loop,  $\Lambda$  has to be close to 400 TeV. The  $n_f = 5 + 3$  column in Table 7 contains operators with electrons and heavy quarks or electrons and muons or taus. All these operators are very strongly constrained.

### 5.3 $d_{\text{Hg}}$

The master formulae for  $d_{\text{Hg}}$  are presented in Tab. 8 and Tab. 9 for the semileptonic and four-quark operators, respectively. From Table 9 we notice that for all the four-quark operators in Table 1, the central value of  $d_{\text{Hg}}$  is larger than the experimental bound, implying that, even in the worst case scenario, Hg EDM experiments probe four-quark scales of 1 TeV or larger. This is true even for four-quark operators with four heavy quarks, such as  $[C_{uddu}^{V1,LR}]_{2332}$  (with two  $b$  and two  $c$  quarks) or  $[C_{dd}^{S8,RR}]_{3333}$  (with four  $b$  quarks). The scale of light flavor operators needs in general to be much larger than the TeV. This picture is complicated by theoretical uncertainties, which are generally very large.

$\alpha_I^{\text{Hg}}(\mu_{ew})$ for the Hg EDM: SL operators		
$n_f = 3 + 1$	$n_f = 4 + 1$	$n_f = 5 + 3$
$[C_{eu}^{S,RR}]_{1111}$ $(8.3 \pm 1.5) \cdot 10^{-22}$	$[C_{eu}^{T,RR}]_{1122}$ -	$[C_{ed}^{T,RR}]_{1133}$ -
$[C_{ed}^{S,RR}]_{1111}$ $(-3.8 \pm 1.3) \cdot 10^{-22}$	$[C_{eu}^{S,RR}]_{1122}$ -	$[C_{ed}^{T,RR}]_{2211}$ $(-2.6 \pm 0.7) \cdot 10^{-25}$
$[C_{ed}^{S,RR}]_{1122}$ $(1.7 \pm 0.4) \cdot 10^{-23}$	-	$[C_{ed}^{T,RR}]_{2222}$ $(1.0 \pm 0.7) \cdot 10^{-27}$
$[C_{eu}^{S,RL}]_{1111}$ $(-3.8 \pm 1.4) \cdot 10^{-22}$	-	$[C_{ed}^{T,RR}]_{2233}$ -
$[C_{ed}^{S,RL}]_{1111}$ $(8.3 \pm 1.6) \cdot 10^{-22}$	-	$[C_{ed}^{T,RR}]_{3311}$ $(-4.8 \pm 1.4) \cdot 10^{-24}$
$[C_{ed}^{S,RL}]_{1122}$ $(1.7 \pm 0.4) \cdot 10^{-23}$	-	$[C_{ed}^{T,RR}]_{3322}$ $(1.9 \pm 1.3) \cdot 10^{-26}$
$[C_{eu}^{T,RR}]_{1111}$ $(-3.7 \pm 0.9) \cdot 10^{-23}$	-	$[C_{ed}^{T,RR}]_{3333}$ $(3.5 \pm 2.1) \cdot 10^{-31}$
$[C_{ed}^{T,RR}]_{1111}$ $(-2.4 \pm 0.6) \cdot 10^{-22}$	-	$[C_{eu}^{T,RR}]_{2211}$ $(5.0 \pm 8.0) \cdot 10^{-26}$
$[C_{ed}^{T,RR}]_{1122}$ $(1.7 \pm 0.6) \cdot 10^{-24}$	-	$[C_{eu}^{T,RR}]_{2222}$ $(-5.9 \pm 3.8) \cdot 10^{-31}$
-	-	$[C_{eu}^{T,RR}]_{3311}$ $(9.1 \pm 12.1) \cdot 10^{-25}$
-	-	$[C_{eu}^{T,RR}]_{3322}$ $(-9.9 \pm 5.7) \cdot 10^{-30}$
-	-	$[C_{ed}^{S,RR}]_{1133}$ -
-	-	$[C_{ed}^{S,RR}]_{2211}$ $(-2.6 \pm 0.6) \cdot 10^{-28}$
-	-	$[C_{ed}^{S,RR}]_{2222}$ $(1.0 \pm 0.6) \cdot 10^{-30}$
-	-	$[C_{ed}^{S,RR}]_{2233}$ -
-	-	$[C_{ed}^{S,RR}]_{3311}$ $(-5.2 \pm 1.4) \cdot 10^{-27}$
-	-	$[C_{ed}^{S,RR}]_{3322}$ $(2.0 \pm 1.3) \cdot 10^{-29}$
-	-	$[C_{ed}^{S,RR}]_{3333}$ -
-	-	$[C_{eu}^{S,RR}]_{2211}$ $(-8.9 \pm 5.2) \cdot 10^{-29}$
-	-	$[C_{eu}^{S,RR}]_{2222}$ -
-	-	$[C_{eu}^{S,RR}]_{3311}$ $(-1.8 \pm 1.0) \cdot 10^{-27}$
-	-	$[C_{eu}^{S,RR}]_{3322}$ -

**Table 8:** Master formula for  $d_{\text{Hg}}$  in terms of semileptonic WET operators in the JMS basis at the EW scale. The  $\alpha_I^{\text{Hg}}$  have units of  $e \text{ cm TeV}^2$ . The 90% CL upper bound on  $d_{\text{Hg}}$  is  $6.2 \times 10^{-30} e \text{ cm}$ . The entries below  $10^{-33}$  have been dropped.

$\alpha_I^{\text{Hg}}(\mu_{ew})$ for the Hg EDM					
$n_f = 3 + 1$		$n_f = 4 + 1$		$n_f = 5 + 3$	
$C_{\bar{G}}$	$(-2.4 \pm 3.9) \cdot 10^{-25}$	$[C_{uG}]_{22}$	$(-2.6 \pm 1.5) \cdot 10^{-24}$	$[C_{dG}]_{33}$	$(-3.8 \pm 2.6) \cdot 10^{-25}$
$[C_{dG}]_{11}$	$(5.0 \pm 28.3) \cdot 10^{-20}$	$[C_{u\gamma}]_{22}$	$(2.5 \pm 1.6) \cdot 10^{-25}$	$[C_{d\gamma}]_{33}$	$(-7.3 \pm 5.3) \cdot 10^{-27}$
$[C_{dG}]_{22}$	$(-6.7 \pm 4.9) \cdot 10^{-24}$	$[C_{uu}^{S1,RR}]_{2222}$	$(1.9 \pm 1.0) \cdot 10^{-28}$	$[C_{uddu}^{V1,LR}]_{1331}$	$(-1.4 \pm 7.4) \cdot 10^{-24}$
$[C_{uG}]_{11}$	$(4.1 \pm 32.9) \cdot 10^{-20}$	$[C_{uu}^{S8,RR}]_{2222}$	$(-4.3 \pm 2.6) \cdot 10^{-29}$	$[C_{uddu}^{V8,LR}]_{1331}$	$(3.2 \pm 21.5) \cdot 10^{-25}$
$[C_{d\gamma}]_{11}$	$(3.5 \pm 1.3) \cdot 10^{-20}$	$[C_{uu}^{S1,RR}]_{1122}$	$(5.9 \pm 46.4) \cdot 10^{-25}$	$[C_{dd}^{V1,LR}]_{1331}$	$(-1.6 \pm 7.4) \cdot 10^{-24}$
$[C_{d\gamma}]_{22}$	$(-1.3 \pm 0.8) \cdot 10^{-22}$	$[C_{uu}^{S8,RR}]_{1122}$	$(1.7 \pm 15.9) \cdot 10^{-25}$	$[C_{dd}^{V8,LR}]_{1331}$	$(9.5 \pm 20.4) \cdot 10^{-25}$
$[C_{u\gamma}]_{11}$	$(-9.4 \pm 21.8) \cdot 10^{-21}$	$[C_{ud}^{S1,RR}]_{2211}$	$(7.0 \pm 35.1) \cdot 10^{-25}$	$[C_{dd}^{V1,LR}]_{2332}$	$(-5.0 \pm 3.3) \cdot 10^{-28}$
$[C_{uddu}^{V1,LR}]_{1111}$	$(8.9 \pm 30.3) \cdot 10^{-24}$	$[C_{ud}^{S8,RR}]_{2211}$	$(2.6 \pm 12.5) \cdot 10^{-25}$	$[C_{dd}^{V8,LR}]_{2332}$	$(-1.8 \pm 1.1) \cdot 10^{-27}$
$[C_{uddu}^{V8,LR}]_{1111}$	$(1.4 \pm 5.3) \cdot 10^{-23}$	$[C_{ud}^{S1,RR}]_{2222}$	$(-1.2 \pm 0.6) \cdot 10^{-29}$	$[C_{dd}^{S1,RR}]_{3333}$	$(7.8 \pm 5.0) \cdot 10^{-29}$
$[C_{uddu}^{V1,LR}]_{11221}$	$(4.8 \pm 14.4) \cdot 10^{-24}$	$[C_{ud}^{S8,RR}]_{2222}$	$(-2.3 \pm 1.4) \cdot 10^{-28}$	$[C_{dd}^{S8,RR}]_{3333}$	$(-1.6 \pm 1.2) \cdot 10^{-29}$
$[C_{uddu}^{V8,LR}]_{11221}$	$(7.4 \pm 23.5) \cdot 10^{-24}$	$[C_{uddu}^{S1,RR}]_{2112}$	$(-3.1 \pm 15.0) \cdot 10^{-24}$	$[C_{dd}^{S1,RR}]_{1133}$	$(9.1 \pm 52.2) \cdot 10^{-25}$
$[C_{dd}^{V1,LR}]_{11221}$	$(-4.1 \pm 13.9) \cdot 10^{-24}$	$[C_{uddu}^{S8,RR}]_{2112}$	$(5.1 \pm 201.5) \cdot 10^{-26}$	$[C_{dd}^{S8,RR}]_{1133}$	$(2.6 \pm 14.4) \cdot 10^{-25}$
$[C_{dd}^{V8,LR}]_{11221}$	$(-6.2 \pm 20.0) \cdot 10^{-24}$	$[C_{uddu}^{S1,RR}]_{2222}$	$(1.1 \pm 0.6) \cdot 10^{-27}$	$[C_{dd}^{S1,RR}]_{2233}$	$(-5.6 \pm 3.5) \cdot 10^{-29}$
$[C_{uu}^{S1,RR}]_{1111}$	$(-5.9 \pm 21.7) \cdot 10^{-24}$	$[C_{uddu}^{S8,RR}]_{2222}$	$(8.5 \pm 6.3) \cdot 10^{-28}$	$[C_{dd}^{S8,RR}]_{2233}$	$(1.6 \pm 1.1) \cdot 10^{-28}$
$[C_{uu}^{S8,RR}]_{1111}$	$(1.8 \pm 5.6) \cdot 10^{-24}$	$[C_{uu}^{S1,RR}]_{1221}$	$(-2.4 \pm 15.3) \cdot 10^{-24}$	$[C_{dd}^{S1,RR}]_{1331}$	$(-5.7 \pm 34.0) \cdot 10^{-24}$
$[C_{dd}^{S1,RR}]_{1111}$	$(4.9 \pm 24.4) \cdot 10^{-24}$	$[C_{uu}^{S8,RR}]_{1221}$	$(2.7 \pm 14.9) \cdot 10^{-25}$	$[C_{dd}^{S8,RR}]_{1331}$	$(1.1 \pm 4.2) \cdot 10^{-24}$
$[C_{dd}^{S8,RR}]_{1111}$	$(-1.5 \pm 4.6) \cdot 10^{-24}$	$[C_{uddu}^{V1,LR}]_{2112}$	$(-5.5 \pm 22.3) \cdot 10^{-25}$	$[C_{dd}^{S1,RR}]_{2332}$	$(-6.4 \pm 4.7) \cdot 10^{-28}$
$[C_{dd}^{S1,RR}]_{2222}$	$(-4.4 \pm 2.8) \cdot 10^{-29}$	$[C_{uddu}^{V8,LR}]_{2112}$	$(-1.7 \pm 10.2) \cdot 10^{-25}$	$[C_{dd}^{S8,RR}]_{2332}$	$(-1.3 \pm 0.8) \cdot 10^{-27}$
$[C_{dd}^{S8,RR}]_{2222}$	$(-5.3 \pm 3.2) \cdot 10^{-29}$	$[C_{uddu}^{V1,LR}]_{2222}$	$(3.6 \pm 2.4) \cdot 10^{-28}$	$[C_{ud}^{S1,RR}]_{1133}$	$(7.7 \pm 61.1) \cdot 10^{-25}$
$[C_{dd}^{S1,RR}]_{1122}$	$(1.3 \pm 5.7) \cdot 10^{-24}$	$[C_{uddu}^{V8,LR}]_{2222}$	$(1.2 \pm 0.8) \cdot 10^{-27}$	$[C_{ud}^{S8,RR}]_{1133}$	$(2.6 \pm 13.2) \cdot 10^{-25}$
$[C_{dd}^{S8,RR}]_{1122}$	$(-3.7 \pm 14.2) \cdot 10^{-25}$	$[C_{uu}^{V1,LR}]_{1221}$	$(-3.6 \pm 21.9) \cdot 10^{-25}$	$[C_{uddu}^{S1,RR}]_{1331}$	$(-5.1 \pm 24.2) \cdot 10^{-24}$
$[C_{ud}^{S1,RR}]_{1221}$	$(1.1 \pm 4.1) \cdot 10^{-24}$	$[C_{uu}^{V8,LR}]_{1221}$	$(1.8 \pm 6.7) \cdot 10^{-25}$	$[C_{uddu}^{S8,RR}]_{1331}$	$(5.6 \pm 33.0) \cdot 10^{-25}$
$[C_{ud}^{S8,RR}]_{1221}$	$(-3.5 \pm 13.1) \cdot 10^{-25}$	-	-	$[C_{ud}^{S1,RR}]_{2233}$	$(-5.1 \pm 2.8) \cdot 10^{-29}$
$[C_{ud}^{S1,RR}]_{1111}$	$(-2.3 \pm 3.6) \cdot 10^{-25}$	-	-	$[C_{ud}^{S8,RR}]_{2233}$	$(-1.7 \pm 0.9) \cdot 10^{-29}$
$[C_{ud}^{S8,RR}]_{1111}$	$(7.0 \pm 10.8) \cdot 10^{-26}$	-	-	$[C_{uddu}^{S1,RR}]_{2332}$	$(3.3 \pm 2.0) \cdot 10^{-28}$
$[C_{ud}^{S1,RR}]_{1122}$	$(-1.4 \pm 5.1) \cdot 10^{-24}$	-	-	$[C_{uddu}^{S8,RR}]_{2332}$	$(-4.0 \pm 1.8) \cdot 10^{-29}$
$[C_{ud}^{S8,RR}]_{1122}$	$(4.5 \pm 18.1) \cdot 10^{-25}$	-	-	$[C_{uddu}^{V1,LR}]_{2332}$	$(9.3 \pm 4.7) \cdot 10^{-29}$
$[C_{ud}^{S1,RR}]_{1111}$	$(-2.4 \pm 3.8) \cdot 10^{-25}$	-	-	$[C_{uddu}^{V8,LR}]_{2332}$	$(-2.6 \pm 1.4) \cdot 10^{-29}$
$[C_{ud}^{S8,RR}]_{1111}$	$(7.0 \pm 10.6) \cdot 10^{-26}$	-	-	-	-
$[C_{uddu}^{S1,RR}]_{1221}$	$(-1.6 \pm 6.0) \cdot 10^{-24}$	-	-	-	-
$[C_{uddu}^{S8,RR}]_{1221}$	$(4.6 \pm 14.6) \cdot 10^{-25}$	-	-	-	-

**Table 9:** Master formula for  $d_{\text{Hg}}$  in WET in the JMS basis at the EW scale. The  $\alpha_I^{\text{Hg}}$  have units of  $e \text{ cm TeV}^2$  and  $e \text{ cm TeV}$  for the four-fermion and dipole operators, respectively. The 90% CL upper bound on  $d_{\text{Hg}}$  is  $6.2 \times 10^{-30} e \text{ cm}$ .

Table 8 provides a similar message for semileptonic operators, where one can extract strong constraints on operators such as  $[C_{eu}^{T,RR}]_{3311}$  (two  $\tau$  leptons and two  $u$  quarks) or  $[C_{ed}^{T,RR}]_{3311}$  (two  $\tau$  leptons and two  $d$  quarks). In this case, however, operators with both heavy leptons and heavy quarks are less constrained and their scale can drop below the TeV. This is for example the case of  $[C_{eu}^{T,RR}]_{2222}$  (with a naive scale of  $\Lambda \sim 0.3 \text{ TeV}$ , neglecting theoretical uncertainties) or  $[C_{eu}^{S,RR}]_{3322}$ , with naive scale below the electroweak.

#### 5.4 $d_n$

The master formula for the neutron EDM is presented in Tab. 10. As in the case of  $d_{\text{Hg}}$ , we notice that, if we neglect theoretical uncertainties, all four-quark operators in Table 1 need to have scales larger than the TeV.

$\alpha_I^n(\mu_{ew})$ for neutron EDM					
$n_f = 3 + 1$		$n_f = 4 + 1$		$n_f = 5 + 3$	
$C_{\tilde{G}}$	$(5.5 \pm 2.8) \cdot 10^{-22}$	$[C_{uG}]_{22}$	$(7.7 \pm 3.9) \cdot 10^{-21}$	$[C_{dG}]_{33}$	$(1.1 \pm 0.5) \cdot 10^{-21}$
$[C_{dG}]_{11}$	$(-3.7 \pm 1.8) \cdot 10^{-17}$	$[C_{u\gamma}]_{22}$	$(-7.4 \pm 3.4) \cdot 10^{-22}$	$[C_{d\gamma}]_{33}$	$(2.0 \pm 1.1) \cdot 10^{-23}$
$[C_{dG}]_{22}$	$(1.5 \pm 0.9) \cdot 10^{-20}$	$[C_{uu}^{S1,RR}]_{2222}$	$(-5.6 \pm 3.0) \cdot 10^{-25}$	$[C_{uddu}^{V1,LR}]_{1331}$	$(6.0 \pm 3.1) \cdot 10^{-22}$
$[C_{uG}]_{11}$	$(-1.9 \pm 0.9) \cdot 10^{-17}$	$[C_{uu}^{S8,RR}]_{2222}$	$(1.3 \pm 0.5) \cdot 10^{-25}$	$[C_{uddu}^{V8,LR}]_{1331}$	$(1.5 \pm 0.9) \cdot 10^{-22}$
$[C_{d\gamma}]_{11}$	$(-8.9 \pm 0.4) \cdot 10^{-17}$	$[C_{uu}^{S1,RR}]_{1122}$	$(-2.3 \pm 1.1) \cdot 10^{-22}$	$[C_{dd}^{V1,LR}]_{1331}$	$(8.1 \pm 6.4) \cdot 10^{-22}$
$[C_{d\gamma}]_{22}$	$(3.0 \pm 1.7) \cdot 10^{-19}$	$[C_{uu}^{S8,RR}]_{1122}$	$(-3.6 \pm 4.1) \cdot 10^{-23}$	$[C_{dd}^{V8,LR}]_{1331}$	$(-1.5 \pm 0.2) \cdot 10^{-21}$
$[C_{u\gamma}]_{11}$	$(2.5 \pm 0.2) \cdot 10^{-17}$	$[C_{ud}^{S1,RR}]_{2211}$	$(-4.8 \pm 2.6) \cdot 10^{-22}$	$[C_{dd}^{V1,LR}]_{2332}$	$(1.1 \pm 0.6) \cdot 10^{-24}$
$[C_{uddu}^{V1,LR}]_{1111}$	$(-4.3 \pm 2.4) \cdot 10^{-22}$	$[C_{ud}^{S8,RR}]_{2211}$	$(-2.8 \pm 0.7) \cdot 10^{-22}$	$[C_{dd}^{V8,LR}]_{2332}$	$(4.1 \pm 2.5) \cdot 10^{-24}$
$[C_{uddu}^{V8,LR}]_{1111}$	$(-6.6 \pm 3.7) \cdot 10^{-22}$	$[C_{ud}^{S1,RR}]_{2222}$	$(2.9 \pm 1.4) \cdot 10^{-26}$	$[C_{dd}^{S1,RR}]_{3333}$	$(-2.2 \pm 1.1) \cdot 10^{-25}$
$[C_{uddu}^{V1,LR}]_{1221}$	$(-9.0 \pm 4.7) \cdot 10^{-22}$	$[C_{ud}^{S8,RR}]_{2222}$	$(5.2 \pm 3.3) \cdot 10^{-25}$	$[C_{dd}^{S8,RR}]_{3333}$	$(4.6 \pm 2.5) \cdot 10^{-26}$
$[C_{uddu}^{V8,LR}]_{1221}$	$(-1.4 \pm 0.7) \cdot 10^{-21}$	$[C_{uddu}^{S1,RR}]_{2112}$	$(2.6 \pm 1.0) \cdot 10^{-21}$	$[C_{dd}^{S1,RR}]_{1133}$	$(-6.4 \pm 3.2) \cdot 10^{-22}$
$[C_{dd}^{V8,LR}]_{1221}$	$(-4.8 \pm 2.6) \cdot 10^{-22}$	$[C_{uddu}^{S8,RR}]_{2112}$	$(3.8 \pm 1.0) \cdot 10^{-22}$	$[C_{dd}^{S8,RR}]_{1133}$	$(-9.7 \pm 9.5) \cdot 10^{-23}$
$[C_{dd}^{S1,RR}]_{1221}$	$(-7.4 \pm 3.1) \cdot 10^{-22}$	$[C_{uddu}^{S1,RR}]_{2222}$	$(-2.5 \pm 1.5) \cdot 10^{-24}$	$[C_{dd}^{S8,RR}]_{2233}$	$(1.3 \pm 0.7) \cdot 10^{-25}$
$[C_{uu}^{S1,RR}]_{1111}$	$(1.1 \pm 0.5) \cdot 10^{-21}$	$[C_{uddu}^{S8,RR}]_{2222}$	$(-1.9 \pm 1.3) \cdot 10^{-24}$	$[C_{dd}^{S1,RR}]_{2233}$	$(-3.7 \pm 2.1) \cdot 10^{-25}$
$[C_{uu}^{S8,RR}]_{1111}$	$(-3.4 \pm 1.5) \cdot 10^{-22}$	$[C_{uu}^{S1,RR}]_{1221}$	$(8.3 \pm 4.2) \cdot 10^{-22}$	$[C_{dd}^{S8,RR}]_{1331}$	$(3.5 \pm 2.0) \cdot 10^{-21}$
$[C_{dd}^{S1,RR}]_{1111}$	$(5.7 \pm 3.1) \cdot 10^{-22}$	$[C_{uu}^{S8,RR}]_{1221}$	$(-2.5 \pm 0.4) \cdot 10^{-22}$	$[C_{dd}^{S1,RR}]_{1331}$	$(-1.3 \pm 0.3) \cdot 10^{-21}$
$[C_{dd}^{S8,RR}]_{1111}$	$(-1.8 \pm 0.9) \cdot 10^{-22}$	$[C_{ud}^{V1,LR}]_{2112}$	$(5.4 \pm 1.4) \cdot 10^{-22}$	$[C_{dd}^{S8,RR}]_{2332}$	$(1.4 \pm 0.8) \cdot 10^{-24}$
$[C_{dd}^{S1,RR}]_{2222}$	$(1.0 \pm 0.6) \cdot 10^{-25}$	$[C_{ud}^{V8,LR}]_{2112}$	$(7.2 \pm 0.5) \cdot 10^{-22}$	$[C_{dd}^{S1,RR}]_{2332}$	$(2.9 \pm 1.6) \cdot 10^{-24}$
$[C_{dd}^{S8,RR}]_{2222}$	$(1.2 \pm 0.6) \cdot 10^{-25}$	$[C_{uddu}^{V1,LR}]_{2222}$	$(-8.1 \pm 4.5) \cdot 10^{-25}$	$[C_{dd}^{S8,RR}]_{1133}$	$(-3.2 \pm 1.4) \cdot 10^{-22}$
$[C_{dd}^{S1,RR}]_{1122}$	$(1.2 \pm 0.7) \cdot 10^{-22}$	$[C_{uddu}^{V8,LR}]_{2222}$	$(-2.8 \pm 1.8) \cdot 10^{-24}$	$[C_{dd}^{S1,RR}]_{1133}$	$(-1.4 \pm 0.5) \cdot 10^{-22}$
$[C_{dd}^{S8,RR}]_{1122}$	$(-4.7 \pm 2.4) \cdot 10^{-23}$	$[C_{uu}^{V1,LR}]_{1221}$	$(6.3 \pm 7.9) \cdot 10^{-23}$	$[C_{dd}^{S8,RR}]_{1331}$	$(2.3 \pm 1.0) \cdot 10^{-21}$
$[C_{dd}^{S1,RR}]_{1221}$	$(2.5 \pm 1.0) \cdot 10^{-22}$	$[C_{uu}^{V8,LR}]_{1221}$	$(-2.6 \pm 0.3) \cdot 10^{-22}$	$[C_{dd}^{S1,RR}]_{1331}$	$(-5.8 \pm 11.6) \cdot 10^{-23}$
$[C_{dd}^{S8,RR}]_{1221}$	$(-7.8 \pm 2.0) \cdot 10^{-23}$	-	-	$[C_{dd}^{S8,RR}]_{2233}$	$(1.5 \pm 0.7) \cdot 10^{-25}$
$[C_{ud}^{S1,RR}]_{1111}$	$(4.2 \pm 2.1) \cdot 10^{-22}$	-	-	$[C_{dd}^{S1,RR}]_{2233}$	$(4.9 \pm 2.0) \cdot 10^{-26}$
$[C_{ud}^{S8,RR}]_{1111}$	$(-1.3 \pm 0.7) \cdot 10^{-22}$	-	-	$[C_{dd}^{S8,RR}]_{2332}$	$(-9.7 \pm 4.9) \cdot 10^{-25}$
$[C_{ud}^{S1,RR}]_{1122}$	$(2.6 \pm 1.4) \cdot 10^{-22}$	-	-	$[C_{dd}^{S1,RR}]_{2332}$	$(1.2 \pm 0.6) \cdot 10^{-25}$
$[C_{ud}^{S8,RR}]_{1122}$	$(-8.8 \pm 4.4) \cdot 10^{-23}$	-	-	$[C_{dd}^{S8,RR}]_{2332}$	$(-2.7 \pm 1.5) \cdot 10^{-25}$
$[C_{ud}^{S1,RR}]_{1111}$	$(4.2 \pm 2.2) \cdot 10^{-22}$	-	-	$[C_{uddu}^{V8,LR}]_{2332}$	$(7.5 \pm 3.6) \cdot 10^{-26}$
$[C_{ud}^{S8,RR}]_{1111}$	$(-1.3 \pm 0.7) \cdot 10^{-22}$	-	-	-	-
$[C_{ud}^{S1,RR}]_{1221}$	$(3.4 \pm 1.4) \cdot 10^{-22}$	-	-	-	-
$[C_{ud}^{S8,RR}]_{1221}$	$(-8.4 \pm 3.9) \cdot 10^{-23}$	-	-	-	-

**Table 10:** Master formula for  $d_n$  in WET in the JMS basis at the EW scale. The  $\alpha_I^n$  have units of  $e$  cm TeV<sup>2</sup> and  $e$  cm TeV for the four-fermion and dipole operators, respectively. The 90% CL upper bound on  $d_n$  is  $1.8 \times 10^{-26}$   $e$  cm.

## 6 Non-standard Higgs Couplings

In this section, we apply the master formulae derived so far to constrain possible non-standard Yukawa couplings of the Higgs boson. We consider the following Yukawa Lagrangian

$$\mathcal{L}_{\text{Yuk}}^{\text{eff}} = - \left( \sum_{i,j=d,s,b} y_{ij}^d \bar{d}_{L,i} d_{R,j} + \sum_{i,j=u,c,t} y_{ij}^u \bar{u}_{L,i} u_{R,j} + \sum_{i,j=e,\mu,\tau} y_{ij}^e \bar{e}_{L,i} e_{R,j} \right) h + h.c. \quad (6.1)$$

This Lagrangian can arise in two theoretical frameworks that can be used for describing non-standard couplings of the Higgs to quarks, lepton, and gauge bosons. In SMEFT,

gauge symmetry is linearly realized, the Higgs boson belongs to a  $SU_L(2)$  doublet and operators are organized according to their canonical dimension. In this framework, the SM Yukawa couplings arise at dim-4, they can always be chosen to be real and diagonal, and are determined by the quark and lepton masses. Non-standard Yukawa couplings arise at dim-6 and are given by the Lagrangian [17, 128, 129]

$$\begin{aligned} \mathcal{L}_h = & (D_\mu H)^\dagger (D^\mu H) - \lambda \left( H^\dagger H - \frac{1}{2} v^2 \right)^2 - \left[ \bar{Q} \hat{Y}_u u_R \tilde{H} + \bar{Q} \hat{Y}_d d_R H + \bar{L} \hat{Y}_e e_R H \right. \\ & \left. + (\bar{Q} C_{uH} u_R \tilde{H} + \bar{Q} C_{dH} d_R H + \bar{L} C_{eH} e_R H) (H^\dagger H) + h.c. \right]. \end{aligned} \quad (6.2)$$

In unitary gauge

$$H = \frac{1}{\sqrt{2}} (0, v + h)^T, \quad (6.3)$$

where  $h$  is the physical Higgs boson field.  $C_{fH}$ , for  $f = u, d, e$ , are the WC of dim-6 SMEFT operators. We can rewrite Eq. (6.2) in terms of mass matrices,  $M_f$ , and Yukawa interactions

$$M_u = \frac{v}{\sqrt{2}} \left( \hat{Y}_u + \frac{v^2}{2} C_{uH} \right), \quad y^u = \frac{1}{\sqrt{2}} \left( \hat{Y}_u + \frac{3}{2} v^2 C_{uH} \right) = \frac{M_u}{v} + \frac{v^2}{\sqrt{2}} C_{uH}, \quad (6.4)$$

$$M_d = \frac{v}{\sqrt{2}} \left( \hat{Y}_d + \frac{v^2}{2} C_{dH} \right), \quad y^d = \frac{1}{\sqrt{2}} \left( \hat{Y}_d + \frac{3}{2} v^2 C_{dH} \right) = \frac{M_d}{v} + \frac{v^2}{\sqrt{2}} C_{dH}, \quad (6.5)$$

$$M_e = \frac{v}{\sqrt{2}} \left( \hat{Y}_e + \frac{v^2}{2} C_{eH} \right), \quad y^e = \frac{1}{\sqrt{2}} \left( \hat{Y}_e + \frac{3}{2} v^2 C_{eH} \right) = \frac{M_e}{v} + \frac{v^2}{\sqrt{2}} C_{eH}. \quad (6.6)$$

Since at dim-6 the fermion masses and Yukawa couplings are proportional to different linear combinations of  $\hat{Y}_f$  and  $C_{fH}$ , once the mass matrices are diagonalized, the Yukawas are in general non-diagonal and complex.

The other possible theoretical framework is the Higgs Effective Field Theory (HEFT), in which gauge symmetry is realized non-linearly. In this case, the Higgs field  $h$  is a singlet under  $SU(2)_L$ , and the EFT provides a momentum expansion in  $Q/\Lambda$ . The LO HEFT Lagrangian is given by [18]

$$\begin{aligned} \mathcal{L}_{Uh} = & \frac{v^2}{4} \langle D_\mu U^\dagger D^\mu U \rangle (1 + F_U(h)) + \frac{1}{2} \partial_\mu h \partial^\mu h - V(h) \\ & - v \left[ \bar{Q} \left( \hat{Y}_u + \sum_{n=1}^{\infty} \hat{Y}_u^{(n)} \left( \frac{h}{v} \right)^n \right) U P_{+r} + \bar{Q} \left( \hat{Y}_d + \sum_{n=1}^{\infty} \hat{Y}_d^{(n)} \left( \frac{h}{v} \right)^n \right) U P_{-r} \right. \\ & \left. + \bar{L} \left( \hat{Y}_e + \sum_{n=1}^{\infty} \hat{Y}_e^{(n)} \left( \frac{h}{v} \right)^n \right) U P_{-\eta} + h.c. \right]. \end{aligned} \quad (6.7)$$

Here,  $F_U(h)$  and  $V(h)$  are arbitrary functions of the Higgs field

$$F_U(h) = \sum_{n=1}^{\infty} f_{U,n} \left( \frac{h}{v} \right)^n, \quad V(h) = v^4 \sum_{n=2}^{\infty} f_{V,n} \left( \frac{h}{v} \right)^n. \quad (6.8)$$

Also, the left and right-chiral fields are defined by  $Q = (u_L, d_L)^T$ ,  $L = (\nu_L, e_L)^T$ ,  $r = (u_R, d_R)^T$  and  $\eta = (\nu_R, e_R)^T$  and  $P_\pm = (1 \pm \tau_3)/2$ , with  $\tau$  Pauli matrices.  $U$  is a matrix

containing the Goldstone fields

$$U = \exp(2i\Phi/v), \quad \Phi = \phi^a \frac{\tau^a}{2} = \frac{1}{\sqrt{2}} \begin{pmatrix} \frac{\phi^0}{\sqrt{2}} & \phi^+ \\ \phi^- & -\frac{\phi^0}{\sqrt{2}} \end{pmatrix}, \quad (6.9)$$

and the action of covariant derivative on  $U$  is given by

$$D_\mu U = \partial_\mu U + igW_\mu U - ig'B_\mu U \frac{\tau_3}{2}. \quad (6.10)$$

The implications of (6.7) are that the  $hWW$  and  $hZZ$  couplings are decoupled from the  $W$  and  $Z$  masses. They are parameterized by a free coupling  $\kappa_V$ , with  $\kappa_V = 1$  in the SM. Similarly, the fermion masses and Yukawas are characterized by independent matrices, so that, as in the SMEFT, the Yukawa couplings are in general complex and non-diagonal. In this case, we have

$$M_f = v\hat{Y}_f, \quad y^f = \hat{Y}_f^{(1)}. \quad (6.11)$$

The main difference between the HEFT and SMEFT is that in HEFT the leading operator (as well as subleading operators) contain an arbitrary number of Higgs fields, while in SMEFT insertions of  $H^\dagger H$  are suppressed by  $\Lambda^2$  [18]. Thus, in HEFT, Yukawa couplings and fermion masses differ already at leading order.

## 6.1 Matching at the EW scale

Integrating out the Higgs boson at tree level leads to several four-fermion scalar operators with CPV WCs, if the Yukawa couplings are assumed to be complex [129].

$$\begin{aligned} [C_{dd}^{S1,RR}]_{ijkl}(\mu_{ew}) &= \frac{1}{2m_h^2} y_{ij}^d y_{kl}^d, & [C_{uu}^{S1,RR}]_{ijkl}(\mu_{ew}) &= \frac{1}{2m_h^2} y_{ij}^u y_{kl}^u, \\ [C_{ud}^{S1,RR}]_{ijkl}(\mu_{ew}) &= \frac{1}{m_h^2} y_{ij}^u y_{kl}^d, & [C_{ee}^{S,RR}]_{ijkl}(\mu_{ew}) &= \frac{1}{2m_h^2} y_{ij}^e y_{kl}^e, \\ [C_{ed}^{S,RR}]_{ijkl}(\mu_{ew}) &= \frac{1}{m_h^2} y_{ij}^e y_{kl}^d, & [C_{eu}^{S,RR}]_{ijkl}(\mu_{ew}) &= \frac{1}{m_h^2} y_{ij}^e y_{kl}^u, \\ [C_{ed}^{S,RL}]_{ijkl}(\mu_{ew}) &= \frac{1}{m_h^2} y_{ij}^e y_{lk}^{d*}, & [C_{eu}^{S,RL}]_{ijkl}(\mu_{ew}) &= \frac{1}{m_h^2} y_{ij}^e y_{lk}^{u*}, \\ [C_{dd}^{V1,LR}]_{ijkl}(\mu_{ew}) &= -\frac{1}{6m_h^2} y_{il}^d y_{jk}^{d*}, & [C_{dd}^{V8,LR}]_{ijkl}(\mu_{ew}) &= -\frac{1}{m_h^2} y_{il}^d y_{jk}^{d*}, \\ [C_{uu}^{V1,LR}]_{ijkl}(\mu_{ew}) &= -\frac{1}{6m_h^2} y_{il}^u y_{jk}^{u*}, & [C_{uu}^{V8,LR}]_{ijkl}(\mu_{ew}) &= -\frac{1}{m_h^2} y_{il}^u y_{jk}^{u*}, \\ [C_{uddu}^{V1,LR}]_{ijkl}(\mu_{ew}) &= -\frac{1}{6m_h^2} y_{il}^u y_{jk}^{d*}, & [C_{uddu}^{V8,LR}]_{ijkl}(\mu_{ew}) &= -\frac{1}{m_h^2} y_{il}^u y_{jk}^{d*}, \\ [C_{ee}^{V,LR}]_{ijkl}(\mu_{ew}) &= -\frac{1}{2m_h^2} y_{il}^e y_{jk}^{e*}. \end{aligned} \quad (6.12)$$

Here the matching scale  $\mu_{ew}$  can be set to  $m_h$ . Since EDMs can only constrain the imaginary parts of the WCs, they probe combinations of couplings such as

$$\text{Im}(y_{ij}^f y_{kl}^{f'}) = \text{Re}(y_{ij}^f) \text{Im}(y_{kl}^{f'}) + \text{Im}(y_{ij}^f) \text{Re}(y_{kl}^{f'}), \quad f, f' = u, d, e. \quad (6.13)$$

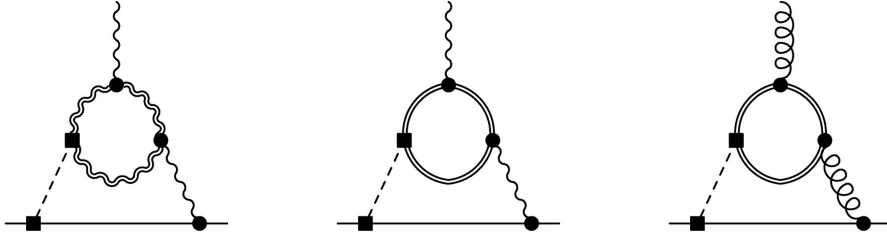


**Figure 4:** Two loop Barr-Zee diagrams contributing to  $\Delta F = 0$  dipole operators. Here plain lines denote quarks and leptons lighter than the electroweak scale, double lines the top quark and double wiggly lines the  $W$  boson. Insertions of the fermion Yukawa and of the  $hWW$  couplings are denoted by squares, while gauge couplings are denoted by dots.

In the SMEFT, the imaginary part of the Yukawa coupling can be non-zero only at dim-6, so that four-fermion operators become proportional to

$$\text{Im}(y_{ij}^f y_{kl}^{f'}) \Big|_{\text{SMEFT}} = \frac{m_f}{v} \delta_{ij} \text{Im}(y_{kl}^{f'}) + \frac{m_{f'}}{v} \delta_{kl} \text{Im}(y_{ij}^f) + \mathcal{O}\left(\frac{v^4}{\Lambda^4}\right). \quad (6.14)$$

In this case, flavor-violating couplings only contribute to EDMs at dim-8 and can be neglected. Both flavor-conserving and flavor-violating couplings contribute at leading order in the HEFT. In the following, we analyze the flavor-conserving and flavor-violating couplings separately. Eq. (6.12) is the initial condition for the renormalization group evolution. As discussed in Section 4, the renormalization group running of these operators below the EW scale results in contributions to four-fermion operators, and, in particular in the case of operators with heavy quarks and leptons, to quark and gluon dipole operators. All these contributions are included in the master formulae.

Beyond tree level, non-standard Yukawa couplings generate dipole contributions at one loop [24, 130]. These are proportional to the same combination of couplings in Eq. (6.12) and provide a next-to-leading logarithmic correction, which we can neglect.

At two loops, Barr-Zee diagrams [131] provide sizable contributions, and are sensitive to different combinations of Yukawa couplings. The diagrams are shown in Fig. 4. Integrating out the top-quark, Higgs boson, and  $W$ -boson at  $\mu_{ew}$  leads to contributions to the quark and lepton dipole operators  $C_{f\gamma}$  and to the quark chromo-dipole operator  $C_{qG}$

$$\begin{aligned} \text{Im}[C_{f\gamma}]_{ii}(\mu_{ew}) &= -12e \frac{\alpha}{(4\pi)^3} q_f q_t^2 \frac{1}{m_t} \left[ f(x_t) \text{Re}(y_{ii}^f) \text{Im}(y_{33}^u) + g(x_t) \text{Im}(y_{ii}^f) \text{Re}(y_{33}^u) \right] \\ &\quad + 2eq_f \frac{\alpha}{(4\pi)^3} \frac{1}{v} \kappa_V (3f(x_W) + 5g(x_W)) \text{Im}(y_{ii}^f), \end{aligned} \quad (6.15)$$

$$\text{Im}[C_{qG}]_{ii}(\mu_{ew}) = 2g_s \frac{\alpha_s}{(4\pi)^3} \frac{1}{m_t} [f(x_t) \text{Re}(y_{ii}^q) \text{Im}(y_{33}^u) + g(x_t) \text{Im}(y_{ii}^q) \text{Re}(y_{33}^u)], \quad (6.16)$$



where  $x_i = m_i^2/m_h^2$ , and  $q_i$  is the electric charge. The loop functions are given by

$$f(z) = \frac{z}{2} \int_0^1 dx \frac{1-2x(1-x)}{x(1-x)-z} \ln \frac{x(1-x)}{z}, \quad g(z) = \frac{z}{2} \int_0^1 dx \frac{1}{x(1-x)-z} \ln \frac{x(1-x)}{z}. \quad (6.17)$$

In the SMEFT,  $\kappa_V = 1$ , and we can set the real part of the Yukawa couplings to its dim-4 value. In the HEFT,  $\kappa_V$  is a free, real parameter, that needs to be extracted from data. In the HEFT, the loop and momentum expansions are tied by  $\Lambda = 4\pi v$  so that the contributions in Eq. (6.15) arise at NNLO. At this order, one would also expect contributions from dipole operators in the HEFT [18]. Since the Barr-Zee diagrams are finite, we can however consider them in isolation.

## 6.2 Constraints on flavor-violating Higgs couplings

First, we discuss the constraints on flavor-violating Higgs couplings. In the SMEFT interpretation, flavor-violating Higgs couplings do not contribute to EDM at dim-6. The bounds in this subsection are thus valid in the HEFT picture. It is instructive to have linearized formulae of the EDMs directly in terms of Higgs couplings. Since  $d_{\text{Hg}}$  and electron EDM impose strongest limits, we employ our EFT master formulae to obtain expressions for  $d_{\text{Hg}}$  and  $\omega_{\text{HFF}}$ . For  $d_{\text{Hg}}$ , we find

$$\begin{aligned} \frac{d_{\text{Hg}}}{[\text{ecm}]} \supset & \frac{(1.1 \pm 4.1) \cdot 10^{-24}}{(2 \times 0.125^2)} \text{Im}(y_{12}^d y_{21}^d) + \frac{(-5.7 \pm 34) \cdot 10^{-24}}{(2 \times 0.125^2)} \text{Im}(y_{13}^d y_{31}^d) \\ & + \frac{(-6.4 \pm 4.7) \cdot 10^{-28}}{(2 \times 0.125^2)} \text{Im}(y_{23}^d y_{32}^d) + \frac{(-2.4 \pm 15.3) \cdot 10^{-24}}{(2 \times 0.125^2)} \text{Im}(y_{12}^u y_{21}^u), \end{aligned} \quad (6.18)$$

while, for  $\omega_{\text{HFF}}$ , we have

$$\frac{\omega_{\text{HFF}}}{[\text{mrad/s}]} \supset \frac{(9.1 \pm 0.4) \cdot 10^5}{(2 \times 0.125^2)} \text{Im}(y_{12}^e y_{21}^e) + \frac{(1.5 \pm 0.1) \cdot 10^7}{(2 \times 0.125^2)} \text{Im}(y_{13}^e y_{31}^e). \quad (6.19)$$

Similarly, one can find expressions for the other EDM observables. Only a specific combination of the Higgs coupling can be probed with EDMs. To get an estimate of the upper bounds on these couplings one can compare the above expressions with the experimental limits, e.g. for  $|d_{\text{Hg}}| < 6.2 \times 10^{-30} e \text{ cm}$  and  $|\omega_{\text{HFF}}| < 0.17 \text{ mrad/s}$ .

We also perform a combined fit of FV Higgs couplings to all EDM observables ( $d_n$ ,  $d_{\text{Hg}}$ ,  $d_{\text{Xe}}$ ,  $d_{\text{Ra}}$ ,  $\omega_{\text{HFF}}$ ,  $\omega_{\text{YbF}}$ ,  $\omega_{\text{ThO}}$ ) using the current and future upper limits given in Tab. 2. For this purpose, we assume only one combination of the couplings to be non-zero at a time. The results are presented in Tab. 11 (column 2).

In column 3, we indicate the origin of the EDMs in terms of low-energy WET operators at  $\mu = 2 \text{ GeV}$ . At the EW scale, the scalar and vector operators are generated by integrating out the Higgs as shown in the matching relations (6.12). Some of these give a leading contribution to the EDMs through direct four-fermion matrix elements (see (3.37)-(3.40)) for the light flavors  $f, f' = u, d, s$ . 1-loop QCD and QED effects through the operator mixing onto dipoles are also present for the light flavors. However, for the heavier generations,  $c$  and  $b$ , the contribution to the EDMs arises solely due to operator mixing

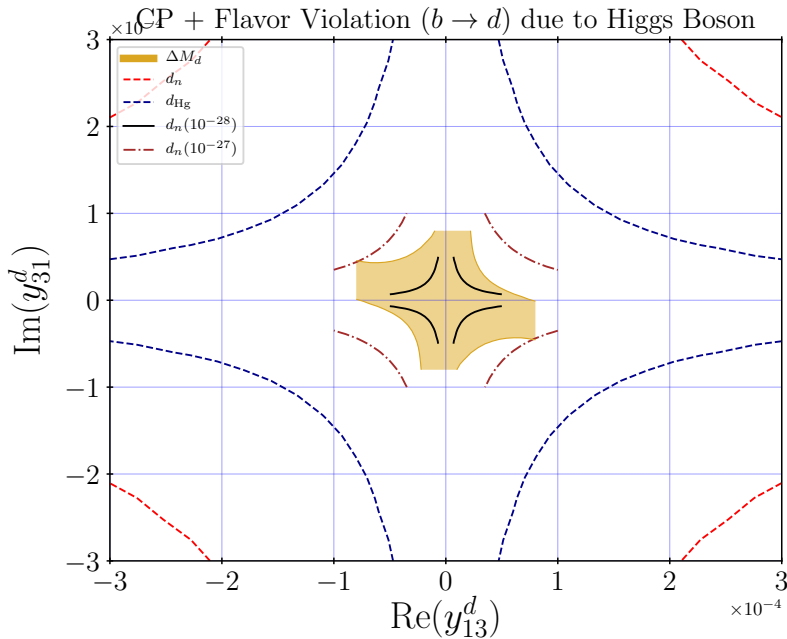


**Figure 5:** EDM and flavor constraints on the CP and flavor violating Higgs couplings. Note that the black line, brown and golden lines are truncated to increase the statistics.

at 1-loop level (see (4.1)-(4.3)). Apart from that, as shown in column 3, the Weinberg operator also contributes for the case of heavier generations due to threshold corrections of the  $b$  and  $c$  dipoles onto it at the  $m_b$  and  $m_c$  scales (see Eqs. (4.10) and (4.11)).

In Fig. 5 we show a comparison of the constraints from the EDMs and  $\Delta M_d$  on the CP + flavor violating down quark Higgs couplings in the  $bd$  sector. We see that current  $d_n$  and  $d_{Hg}$  bounds are weaker than the constraints from  $\Delta M_d$ . However, a neutron EDM bound at the level of  $10^{-27}$  e cm will be highly competitive with  $B-\bar{B}$  oscillations. For other sectors ( $bs$ ,  $sd$ , and  $uc$ ) the flavor bounds [132] are found to be stronger.

### 6.3 EDM constraints on flavor-conserving Higgs couplings

For the flavor-conserving Yukawas, we get contributions from the tree-level matching onto four-fermion, given in Eq. (6.12), and from the 2-loop Barr-Zee diagrams, in Eq. (6.15). Using these one can directly use the master formulae to obtain the EDMs in terms of the FC Yukawas, similar to the expressions in (6.18) and (6.19).

We note some unique features of BZ contributions, which are in contrast to the tree-level matching, associated with the particular combination of the Higgs couplings appearing in the matching relations. First, the BZ diagrams involve a top-quark Yukawa coupling which is correlated to the other quarks as well as leptonic Yukawas. Secondly, the BZ effects can also correlate fermion Yukawas to the  $W$ -Higgs couplings. These features are absent in the tree-level matching and therefore allow additional constraints on the FC Higgs couplings. Recall that, the EDMs through tree-level Higgs exchange (6.12) probe following

Generic FV Higgs couplings			
couplings	current limit	future limit	operators at hadronic scale
$\text{Im}(y_{12}^d y_{21}^d)$	$1.2 \cdot 10^{-7}$	$7.0 \cdot 10^{-9}$	$[C_{d\gamma(G)}]_{11,22}, [C_{dd}^{S1(8),RR}]_{1221}, [C_{dd}^{S1(8),RR}]_{1122}$
$\text{Im}(y_{13}^d y_{31}^d)$	$2.1 \cdot 10^{-8}$	$6.0 \cdot 10^{-10}$	$[C_{\tilde{G}}], [C_{d\gamma(G)}]_{11}$
$\text{Im}(y_{23}^d y_{32}^d)$	$1.5 \cdot 10^{-4}$	$1.4 \cdot 10^{-6}$	$[C_{\tilde{G}}], [C_{d\gamma(G)}]_{22}$
$\text{Im}(y_{12}^u y_{21}^u)$	$5.0 \cdot 10^{-8}$	$2.3 \cdot 10^{-9}$	$[C_{\tilde{G}}], [C_{u\gamma(G)}]_{11}$
$\text{Im}(y_{12}^e y_{21}^e)$	$1.1 \cdot 10^{-9}$	$1.1 \cdot 10^{-10}$	$[C_{e\gamma}]_{11}$
$\text{Im}(y_{13}^e y_{31}^e)$	$6.0 \cdot 10^{-11}$	$6.0 \cdot 10^{-12}$	$[C_{e\gamma}]_{11}$

**Table 11:** Current and future EDM constraints on the combinations of the generic flavor violating Higgs couplings (column 2) at  $1\sigma$  level. In the column 3, we also indicate the origin of EDM contributions at  $\mu = 2$  GeV. The matching scale is set to the Higgs mass.

combination of FC couplings

$$\text{Im}(y_{ii}^f y_{jj}^{f'}) = \text{Re}(y_{ii}^f) \text{Im}(y_{jj}^{f'}) + \text{Im}(y_{jj}^f) \text{Re}(y_{ii}^{f'}), \quad f, f' = u, d, e, \quad (6.20)$$

here  $f$  can be equal to  $f'$ . Therefore, for  $f = f'$  and  $i = j$ , one can also probe individual couplings (more precisely a combination of its Re and Im parts:  $\text{Re}(y_{ii}^f) \text{Im}(y_{ii}^f)$ ) in an uncorrelated manner to other couplings, under the assumption that only a single coupling is turned on. Overall, the tree-level and 2-loop BZ diagram effects can test very different parts of the low-energy Higgs effective coupling parameter space. In Tab. 12 we show upper bounds at  $1\sigma$  level on the various combinations of the generic FC Higgs couplings.

#### 6.4 LHC constraints on flavor-conserving Higgs couplings

Finally, we want to compare the bounds in Table 12 with complementary constraints from the LHC. Non-standard Yukawa couplings affect Higgs production and decay processes and are thus constrained by measurements of the Higgs properties at the LHC [133, 134]. For a given Higgs production mechanism,  $i \rightarrow H$ , followed by the decay of the Higgs to the final state  $f$ , the signal strength in the presence of non-standard interactions is defined as

$$\mu_{i \rightarrow H \rightarrow f} = \mu_i \mu_f = \left( 1 + \frac{\sigma_{i \rightarrow H}}{\sigma_{i \rightarrow H}^{\text{SM}}} \right) \frac{1 + \frac{\Gamma_{H \rightarrow f}}{\Gamma_{H \rightarrow f}^{\text{SM}}}}{1 + \frac{\Gamma_{\text{tot}}}{\Gamma_{\text{tot}}^{\text{SM}}}}, \quad (6.21)$$

where  $\sigma^{\text{SM}}$  and  $\sigma$  are, respectively, the production cross sections in the SM and the correction induced by non-standard interactions.  $\Gamma_{H \rightarrow f}^{\text{SM}}$  are the decay widths in the channel  $f$  and  $\Gamma_{\text{tot}}^{\text{SM}}$  the Higgs total width. In the SM, the Yukawas of the light  $u$ ,  $d$ , and  $s$  quarks are too small to significantly affect Higgs production and decay. Direct constraints on  $H \rightarrow c\bar{c}$  are sensitive to charm Yukawas about ten times larger than the SM expectation [135, 136], while the  $b$  and  $t$  Yukawas are compatible with the SM [133, 134]. In the HEFT, the quark masses and Yukawas are decoupled from each other. Light quark Yukawas can thus affect the Higgs production via the partonic processes  $\bar{q}q \rightarrow H$ , which falls in the same category

Generic FC Higgs couplings			
couplings	current limit	future limit	operators at hadronic scale
$\text{Im}(y_{11}^d y_{11}^d)$	$2.4 \cdot 10^{-8}$	$2.6 \cdot 10^{-9}$	$[C_{dd}^{S1(8),RR}]_{1111}, [C_{d\gamma(G)}]_{11}$
$\text{Im}(y_{22}^d y_{22}^d)$	$2.0 \cdot 10^{-3}$	$1.9 \cdot 10^{-5}$	$[C_{dd}^{S1(8),RR}]_{2222}, [C_{d\gamma(G)}]_{22}$
$\text{Im}(y_{33}^d y_{33}^d)$	$1.1 \cdot 10^{-3}$	$9.0 \cdot 10^{-6}$	$[C_{\tilde{G}}]$
$\text{Im}(y_{11}^u y_{11}^u)$	$2.6 \cdot 10^{-8}$	$1.6 \cdot 10^{-9}$	$[C_{uu}^{S1(8),RR}]_{1111}, [C_{u\gamma(G)}]_{11}$
$\text{Im}(y_{22}^u y_{22}^u)$	$4.0 \cdot 10^{-4}$	$3.5 \cdot 10^{-6}$	$[C_{\tilde{G}}]$
$\text{Im}(y_{11}^e y_{11}^e)$	$1.2 \cdot 10^{-7}$	$1.2 \cdot 10^{-8}$	$[C_{ee}^{S,RR}]_{1111}, [C_{e\gamma}]_{11}$

**Table 12:** Current and future EDM constraints on the combinations of the generic flavor conserving Higgs couplings at  $1\sigma$  level (to obtain 90%CL these numbers have to be multiplied by factor 1.6 ). In column 3, we also indicate the origin of leading contributions to the EDMs at  $\mu = 2\text{GeV}$ . It is worth mentioning that the EDMs can also probe other combinations of the Yukawa couplings which are not shown here. In that case, the scalar or vector operators with left-right chiralities are generated at the EW scale (see e.g. (6.12)). The electron EDM dominates the constraints on the leptonic and semileptonic operators. The matching scale is set to the Higgs mass.

at gluon fusion, and  $q\bar{q}^{(\prime)} \rightarrow HV$ , with  $V = W, Z$ . They also affect the decay signal strength by modifying the Higgs total width. The top Yukawa can be probed by the loop processes  $gg \rightarrow H$ ,  $H \rightarrow \gamma\gamma$ ,  $H \rightarrow \gamma Z$ , and, at tree level, via  $t\bar{t}H$  production.

At  $\sqrt{S} = 13$  TeV, the gluon fusion SM cross section is [137]

$$\sigma_{ggH}^{\text{SM}} = 48.58_{-3.27}^{+2.22} \pm 1.56 \text{ pb.}$$

where the cross-section is evaluated at the factorization and renormalization scales  $\mu_F = \mu_R = m_h/2$ . The first error includes the contribution of missing orders and EW corrections, while the second error denotes the PDF uncertainties.

Non-standard Yukawas affect the production cross-section in several ways. A nonstandard Yukawa coupling of the top quark affects gluon fusion production. The real part of the coupling simply rescales the SM contribution. In the large quark mass limit, the imaginary part of the top Yukawa coupling contributes to gluon fusion via the operator  $hG\tilde{G}$ . Neglecting  $\mathcal{O}(m_h^2/m_t^2)$  corrections and at leading order in QCD, the contribution of the imaginary part of the top Yukawa to the gluon fusion cross section is a factor of 9/4 larger than that of the real part. Higher order QCD corrections are different for scalar and pseudoscalar couplings, and the expression of the difference at NLO and NNLO can be found in Ref. [138, 139].

The contributions of light quarks with scalar and pseudoscalar Yukawas at NNLO in QCD have been computed in Ref. [140]. In this case, the cross-section is proportional to the absolute value of the Yukawa coupling, up to corrections proportional to  $m_q/m_h$ , which

we neglect. We write the production cross-section as

$$\begin{aligned} \sigma_{ggH} = & \left( (\text{Re } y_{33}^u)^2 + \frac{9}{4} (\text{Im } y_{33}^u)^2 \right) \frac{1}{|(y_{33}^u)_{\text{SM}}|^2} \sigma_{ggH}^{\text{SM}} + (\text{Im } y_{33}^u)^2 \Delta\sigma_{ggH} \\ & + \sum_{i=1}^3 \sigma_{ii}^d |y_{ii}^d|^2 + \sum_{i=1}^2 \sigma_{ii}^u |y_{ii}^u|^2, \end{aligned} \quad (6.22)$$

with the Yukawa couplings evaluated at the scale  $\mu = m_h$ . The results for  $\sigma_{q\bar{q}}$  at  $\sqrt{S} = 13$  TeV are summarized in Tab. 13. The central value of the cross-section is given at the scale  $\mu_F = \mu_R = m_h/2$ . The scale uncertainties are obtained by varying  $\mu = \mu_F = \mu_R$  between  $m_h/4$  and  $m_h$ , while the pdf and  $\alpha_s$  error was evaluated following the PDF4LHC21 recommendation [141], using 100 replicas in the PDF4LHC21\_mc\_pdfas PDF set.

$\sigma$ ( $10^3$ pb)	$\sigma_{11}^u$	$\sigma_{11}^d$	$\sigma_{22}^d$	$\sigma_{22}^u$	$\sigma_{33}^d$
central	120.0	83.3	31.7	12.6	3.9
scale	+2.7 -4.8	+1.9 -3.3	+0.8 -1.1	+0.5 -0.5	+0.2 -0.1
pdf	3.6	3.1	5.3	0.5	0.1
$\mu_{ggH}$	$[2.2, 2.8] \cdot 10^3$	$[1.5, 1.9] \cdot 10^3$	$[5.1, 8.2] \cdot 10^2$	$[2.3, 3.0] \cdot 10^2$	$[72, 91]$
$\sigma_{HV}$ (pb)	$\sigma_{11}^u$	$\sigma_{11}^d$	$\sigma_{22}^d$	$\sigma_{22}^u$	$\sigma_{33}^d$
$\sigma_{HW+}$	16.0	15.3	1.99	1.44	0.09
$\sigma_{HW-}$	8.35	8.50	1.53	1.69	0.06
$\sigma_{HZ}$	3.18	2.24	0.50	0.19	0.09
$\mu_{HW}$	158	154	22.8	20.3	0.97
$\mu_{HZ}$	106	75	17	6.37	3.02

**Table 13:** Contribution of non-standard light quark Yukawa couplings to the Higgs production cross section in the gluon fusion and HV channels.

The corrections to associated  $HW$  and  $HZ$  production induced by non-standard Yukawas were computed at NLO in QCD in Ref. [142]

$$\sigma_{HV} = \kappa_V \sigma_{HV}^{\text{SM}} + \sum_{i=1}^3 \sigma_{ii, HV}^d |y_{ii}^d|^2 + \sum_{i=1}^2 \sigma_{ii, HV}^u |y_{ii}^u|^2, \quad (6.23)$$

with [137]

$$\begin{aligned} \sigma_{HW+(\ell+\nu)}^{\text{SM}} &= 94.26_{-0.7\%}^{+0.5\%} \pm 1.8\% \text{ fb}, & \sigma_{HW-(\ell-\bar{\nu})}^{\text{SM}} &= 59.83_{-0.7\%}^{+0.4\%} \pm 2.0\% \text{ fb}, \\ \sigma_{HZ-(\ell+\ell-)}^{\text{SM}} &= 29.82_{-3.1\%}^{+3.8\%} \pm 1.6\% \text{ fb}. \end{aligned} \quad (6.24)$$

The theoretical uncertainties on the non-standard contributions to  $\sigma_{HW+}$ ,  $\sigma_{HW-}$  and  $\sigma_{HZ}$  were shown to be at the 10% level [142]. Since the HV channel gives weaker bounds and the theoretical uncertainties are small, we did not re-evaluate them in this work. For the corrections to the  $t\bar{t}H$  cross-section, we use

$$\mu_{t\bar{t}h} = \frac{(\text{Re } y_{33}^u)^2 + 0.4 (\text{Im } y_{33}^u)^2}{|(y_{33}^u)_{\text{SM}}|^2}. \quad (6.25)$$

The Yukawa also affect the Higgs decay into fermions. At NLO in QCD, the decay of a Higgs boson to two quarks is given by [143]

$$\Gamma(H \rightarrow q_j \bar{q}_j) = \frac{3m_h}{8\pi} |y_{jj}^q|^2 \left(1 + 5.67 \frac{\alpha_s}{\pi}\right) = (18.0 \text{ GeV}) |y_{jj}^q|^2. \quad (6.26)$$

The decay into two leptons has a similar expression, without the  $\mathcal{O}(\alpha_s)$  correction. For illustration, we use the signal strength measurements of the ATLAS experiment [133], set  $\kappa_V = 1$  and  $\text{Re} y_{33}^u$  to its SM value. The latter assumption is justified by analyses of the CP properties of the couplings of the Higgs boson to the top, which prefer a dominantly real coupling [144, 145]. With these assumptions, a combined fit to the Yukawas of the electron and of the  $u$ ,  $d$ ,  $s$ ,  $c$  and  $b$  quarks to ATLAS data yields

$$\begin{aligned} |y_{11}^e| &< 1.2 \cdot 10^{-2}, & |y_{11}^u| &< 6.4 \cdot 10^{-3}, & |y_{11}^d| &< 6.9 \cdot 10^{-3}, \\ |y_{22}^d| &< 7.1 \cdot 10^{-3}, & |y_{22}^u| &< 7.1 \cdot 10^{-3}, & & \end{aligned} \quad (6.27)$$

at the 90% confidence level, while, for the  $b$  quark, we have

$$0.90 \cdot 10^{-2} < |y_{33}^d| < 1.2 \cdot 10^{-2}. \quad (6.28)$$

The bounds are given on couplings at the renormalization scale  $\mu = m_h$ . For the  $u$  and  $d$  quarks, corrections to the production cross section and Higgs total width provide similar effects, while for  $s$ ,  $c$  and  $b$  quarks the dominant effect are the corrections to the Higgs partial and total widths. The data we use are only sensitive to the absolute values of the couplings.

We next perform a joint fit to the Higgs and EDM data in the HEFT framework, in which fermion masses and Yukawa are independent. In our fit, we fix  $\kappa_V$  and the real part of the top Yukawa coupling,  $\text{Re} y_{33}^u$ , to their SM model values. We then perform a simultaneous fit to the real parts of the  $e$ ,  $u$ ,  $d$ ,  $s$ ,  $c$  and  $b$  Yukawas and to one imaginary part at a time. We neglect theoretical errors on EDMs, so that the bounds give an indication of the full potential of EDMs experiments, but should be taken with some caution. If we include both the Barr-Zee and four-fermion contributions, at the 90% CL we find

$$\begin{aligned} |\text{Im} y_{11}^e| &< 1.2 \cdot 10^{-6}, & |\text{Im} y_{11}^u| &< 1.2 \cdot 10^{-6}, & |\text{Im} y_{11}^d| &< 1.7 \cdot 10^{-7}, \\ |\text{Im} y_{22}^d| &< 7.1 \cdot 10^{-3}, & |\text{Im} y_{22}^u| &< 7.1 \cdot 10^{-3}, & |\text{Im} y_{33}^d| &< 1.2 \cdot 10^{-2}. \end{aligned} \quad (6.29)$$

The 90% CL for the real part of the couplings corresponds to the ranges given in Eqs. (6.27) and (6.28). We see that for the  $e$ ,  $u$  and  $d$  Yukawas, the EDM bound on the imaginary part is much stronger than the bounds from Higgs observables in Eq. (6.27). For the  $s$ ,  $c$  and  $b$  quark, however, the bounds go back to what we obtained from the signal strengths. This is partially due to cancellations between the Barr-Zee (Eq. (6.15)) and four-fermion (Eq. (6.12)) contributions to EDMs, which can happen once we let the real part of the Yukawas deviate from its SM value.

## 6.5 SMEFT Interpretation

The Yukawa couplings in SMEFT are more constrained as compared to the HEFT. Since the leading non-standard effects to the Yukawa couplings are dim-6 (6.2), we can not have the double insertion of the Yukawas at this level. Hence, the contributions to the EDMs through flavor-violating Higgs couplings in Tab. 11 is essentially a dim-8 effect in the SMEFT power counting, because for the matching of  $[C_{ff}^{S1,RR}]_{ijjj}$  a double insertion of flavor-violating couplings is required. On the other hand, flavor-conserving CPV Yukawa couplings generate EDMs at dim-6 in SMEFT. In this case, one of the Yukawa has to be SM-like. Moreover, since the SM Yukawas are restricted to be real in the mass basis, one can directly constrain the individual CPV couplings from EDM observables unlike the generic case presented in Tab. 12.

Limiting to dim-6 effects in the SMEFT, the matching onto 4f WET operators can be obtained by setting one of the Yukawas in (6.12) to its SM value

$$y_{ii,SM}^d = \frac{m_{d_i}}{v}, \quad y_{ii,SM}^u = \frac{m_{u_i}}{v}, \quad y_{ii,SM}^e = \frac{m_{e_i}}{v}. \quad (6.30)$$

Moreover, in the BZ contributions (6.15) we also set  $\kappa_V = 1$ . The current limits on the CPV FC Higgs couplings are given in Tab. 14. For each case, we present two sets of results using the tree-level (4f) and 2-loop (BZ) matching. Also, in this case, we neglect theoretical errors. Once they are under better control, theoretical errors can straightforwardly be added to the analysis.

CPV FC Higgs couplings in SMEFT at $1\sigma$ level								
$d_n, \text{Hg, Xe, Ra}$								
matching	$\text{Im}(y_{11}^d)$	$\text{Im}(y_{22}^d)$	$\text{Im}(y_{33}^d)$	$\text{Im}(y_{11}^u)$	$\text{Im}(y_{22}^u)$	$\text{Im}(y_{11}^e)$	$\text{Im}(y_{22}^e)$	$\text{Im}(y_{33}^e)$
4f	$1.4 \cdot 10^{-5}$	$2.6 \cdot 10^{-3}$	$2.6 \cdot 10^{-3}$	$6.0 \cdot 10^{-6}$	$4.0 \cdot 10^{-3}$	–	–	–
BZ	$9.0 \cdot 10^{-8}$	$7.0 \cdot 10^{-4}$	$9.0 \cdot 10^{-3}$	$1.1 \cdot 10^{-7}$	$1.3 \cdot 10^{-3}$	–	–	–
$\omega_{\text{HfF}}, \omega_{\text{YbF}}, \omega_{\text{ThO}}$								
matching	$\text{Im}(y_{11}^d)$	$\text{Im}(y_{22}^d)$	$\text{Im}(y_{33}^d)$	$\text{Im}(y_{11}^u)$	$\text{Im}(y_{22}^u)$	$\text{Im}(y_{11}^e)$	$\text{Im}(y_{22}^e)$	$\text{Im}(y_{33}^e)$
4f	$4.0 \cdot 10^{-3}$	$4.0 \cdot 10^{-3}$	$2.0 \cdot 10^{-3}$	$9.0 \cdot 10^{-4}$	$8.0 \cdot 10^{-4}$	$2.6 \cdot 10^{-8}$	$1.6 \cdot 10^{-3}$	$1.0 \cdot 10^{-4}$
BZ	–	–	–	–	–	$1.5 \cdot 10^{-9}$	–	–
combined								
matching	$\text{Im}(y_{11}^d)$	$\text{Im}(y_{22}^d)$	$\text{Im}(y_{33}^d)$	$\text{Im}(y_{11}^u)$	$\text{Im}(y_{22}^u)$	$\text{Im}(y_{11}^e)$	$\text{Im}(y_{22}^e)$	$\text{Im}(y_{33}^e)$
4f + BZ	$9.0 \cdot 10^{-8}$	$7.0 \cdot 10^{-4}$	$1.8 \cdot 10^{-3}$	$1.0 \cdot 10^{-7}$	$7.0 \cdot 10^{-4}$	$1.5 \cdot 10^{-9}$	$1.6 \cdot 10^{-3}$	$1.0 \cdot 10^{-4}$

**Table 14:** The current limits on the CPV FC Yukawa couplings resulting due to tree-level and 2-loop Barr-Zee diagrams up to dim-6 level in SMEFT. The neutron, Hg, Xe, and Ra EDMs and the frequencies  $\omega_{\text{HfF}}, \omega_{\text{YbF}}, \omega_{\text{ThO}}$  are included in the fit. The real parts of the Yukawas are set to their SM values. The matching scale is set to the Higgs mass.

The imaginary part of the Yukawa couplings of the  $u$  and  $d$  quarks is predominantly constrained by the neutron and Hg EDMs, via the contributions arising from Barr-Zee diagrams. The constraints are very strong, and out of the reach of existing colliders. The  $s$

quark is also mostly constrained by hadronic EDMs. In this case, the bound is a factor of ten stronger than the constraints from Higgs observables discussed in Sec. 6.4, so that, once theoretical errors are considered, the LHC and EDM experiments can probe similar scales. The  $b$ -quark Yukawa is mostly constrained by the electron EDM. These contributions arise from first integrating out the Higgs and matching onto the scalar four-fermion operator  $[C_{ed}^{S,RR}]$ , which consequently runs into  $[C_{ed}^{T,RR}]$  and  $C_{e\gamma}$ . Finally, the  $c$ -quark Yukawa receive similar constraints from  $d_n$ ,  $d_{Hg}$  and  $\omega_{\text{HFF}}$ . For the  $c$  and  $b$  Yukawas, the indirect bounds on the Higgs couplings are complementary to the constraints resulting from the direct Higgs searches as presented in the previous section.

The bounds in Table 14 are of the same order of magnitude as those presented in Ref. [24]. The main difference is in the treatment of the RGE between the EW and  $\sim 2$  GeV scale. Ref. [24] ignored the role of four-fermion operators, which re-appeared as unresummed large logarithms of  $m_q/m_h$  in the matching coefficients. Our analysis is more similar to Ref. [28], which, for the  $b$  and  $c$  quarks, calculated the matching coefficients and the mixing between  $C_{e\gamma}$ ,  $[C_{eq}^{S,RR}]$  and  $[C_{eq}^{T,RR}]$  at one order higher than in our study. The bounds on  $y_{33}^d$  and  $y_{22}^u$  obtained in Ref. [28] are very close to those presented in Table 14.

## 7 Summary and Outlook

The inability of the SM to explain the origin of the baryon asymmetry in the Universe provides a strong motivation to search for new sources of CP violation beyond the phase of the CKM quark mixing matrix. Electric dipole moments of leptons, nucleons, atoms, and molecules are extremely sensitive probes of flavor-diagonal CP violation. Upcoming experiments have the potential to improve the bounds on the neutron EDM and on EDMs of diamagnetic atoms by at least one order of magnitude, while molecular experiments will further constrain the electron EDM and start to probe hadronic EDMs. As they could offer the first hints of BSM physics, it is important to develop robust tools for the model-independent interpretation of EDM experiments. In addition, identifying the detailed features of BSM physics from one or multiple observations in EDM experiments requires understanding their correlations with observables in other systems and at other energy scales. Effective Field Theories provide a natural framework to achieve these goals in a controlled and systematic way, with minimal reliance on specific BSM models. In this paper, we discuss EDMs in the Weak EFT and leverage EFT tools such as renormalization group evolution and matching at the heavy fermion thresholds to derive master formulae for EDMs in terms of the complete set of  $\Delta F = 0$  WET operators at the electroweak scale. This set includes both operators with light  $u$ ,  $d$ , and  $s$  quarks, which have nonvanishing nucleon matrix elements and thus contribute to EDM at “tree level”, but also operators with heavy  $b$  and  $c$  quarks and leptons of the second and third generations. Indeed we find that the great majority of CP-violating  $\Delta F = 0$  operators with heavy fermions mix into tree-level operators at leading or next to leading-log. EDM constraints are so strong that even in the case of operators that contribute at next-to-leading log (meaning two or even more loops) the operator scale has to be larger than 1 TeV. We now briefly summarize the main results of this paper.



- The main result of this paper is the master formulae for the Hf, ThO, and YbF precession frequencies, given in Tables 7 and 15, and for the neutron, proton, and Hg EDMs, in Tables 8, 9, 10 and 16. These formulae can be readily applied to EFTs at the electroweak scale (SMEFT or HEFT) or to BSM models by calculating the WET matching coefficients at the electroweak scale.

The coefficients  $\alpha_I^X(\mu_{ew})$  provided in these tables encode both short-distance effects, from the running between the electroweak scale  $\mu_{ew}$  and the low energy scales  $\mu_{low} = 2$  GeV (or the heavy fermion thresholds), and long-distance effects, from hadronic and nuclear matrix elements. Concerning the short-distance effects:

- We consider the full WET 1-loop anomalous dimension, which is sufficient to capture the LL contributions from scalar four-quark operators with two heavy and two light quarks ( $[C_{uu}^{S1(8),RR}]$ ,  $[C_{ud}^{S1(8),RR}]$ , and  $[C_{uddu}^{S1(8),RR}]$ ), scalar leptonic operators with two heavy and two light leptons ( $[C_{ee}^{S,RR}]$ ) and scalar and tensor semileptonic operators with light quarks and heavy leptons or light leptons and heavy quarks ( $[C_{eu(d)}^{T,RR}]$  and  $[C_{eu(d)}^{S,RR}]$ ). The 1-loop RGE and the 1-loop matching of heavy quark QCD dipoles onto the Weinberg three-gluon operator provide NLL contributions from four-quark scalar operators with four heavy quarks, and semileptonic scalar and tensor operators with heavy quarks and heavy leptons.
- The vector operators  $[C_{uu}^{V1(8),LR}]$ ,  $[C_{dd}^{V1(8),LR}]$ ,  $[C_{uddu}^{V1(8),LR}]$  and  $[C_{ee}^{V,LR}]$ , with two or four heavy fermions, do not generate LL contributions. For these operators, we identify NLL contributions by generalizing 2-loop anomalous dimensions originally derived for  $B \rightarrow X_s \gamma$  [127], and by considering the 1-loop matching at the heavy fermion threshold. After 2-loop running and 1-loop matching onto the  $b$  and  $c$  QCD dipole,  $[C_{uddu}^{V1(8),LR}]_{2332}$  generates a NNLL contribution to EDMs.

For the neutron, proton and diamagnetic atoms, the long distance piece of  $\alpha_I^X(\mu_{ew})$  is affected by large hadronic and nuclear uncertainties. Our master formulae use up-to-date available informations from Lattice QCD, QCD sum rules and chiral perturbation theory, and the implementation in the package `flavio` allows for the prompt updating of long-distance matrix elements, as soon as they become available.

As an example, we have applied the master formulae to study the constraints from EDMs on Higgs couplings. For flavor-violating Higgs couplings, we showed that, at the moment,  $\Delta F = 2$  observables provide stronger bounds. Future EDM experiments, however, will provide competitive constraints, especially in the  $bd$  sector. In the case of flavor conserving Yukawa couplings, we updated bounds on the imaginary part in two scenarios. In the HEFT scenario, in which the real part of the Yukawa is also a free parameter, we found that EDMs give the strongest bounds on the imaginary part of the  $e$ ,  $u$ , and  $d$  Yukawas, while Higgs observables dominate the bounds on the  $s$ ,  $c$  and  $b$  Yukawas. In the SMEFT scenario, in which, up to dimension-eight corrections, the real part of the Yukawa is fixed to its SM value, EDMs give by far the strongest bounds. In particular, the electron EDM gives the strongest bounds on the  $b$  and  $s$  Yukawas, neutron and mercury dominate the  $u$  and  $d$  bounds, and for the charm quark both contributions are important.

This work can be extended in several directions. First of all, we have in this paper relied on a logarithmic counting to organize the contributions to EDMs arising from the solution of the WET RGEs at one and two loops. This counting does not take into account the presence of small couplings, such as the QED coupling, for which the suppression from additional loops is not fully offset by the large logarithms. It is thus possible that higher loop corrections to matching and running, while formally subleading, will be numerically more important than the LL and NLL terms identified here, especially in those cases in which these effectively arise at three loops (e.g.  $[C_{uddu}^{V1(8),LR}]_{2332}$  or  $[C_{ud}^{S1(8),RR}]_{2233}$ ). Especially for applications to very sensitive observables as EDMs, it is thus important to extend the calculations of WET anomalous dimensions and threshold corrections to higher order.

Secondly, higher order corrections are necessary to constrain the few  $\Delta F = 0$  CP-violating operators that are not listed in Table 1. These include  $[C_{eu}^{S,RL}]_{1122}$ ,  $[C_{eu}^{S,RL}]_{1133}$  and all the entries with heavy leptons, for which it should be possible to generalize the 2-loop anomalous dimension for vector operators, and  $[C_{ee}^{S,RR}]_{ijjj}$  with  $i, j > 1$ . In addition, we find very weak constraints on  $\mu$ -charm and  $\tau$ -charm semileptonic operators ( $[C_{eu}^{T(S),RR}]_{2222}$ ,  $[C_{eu}^{T(S),RR}]_{3322}$ ) and  $\mu$ -bottom and  $\tau$ -bottom semileptonic operators ( $[C_{ed}^{T(S),RR}]_{2233}$  and  $[C_{ed}^{T(S),RR}]_{3333}$ ). For these classes, it will be important to find additional paths.

Finally, reducing the theoretical uncertainties is crucial to the success of the EDM program. This requires, in particular, to address the large hadronic and nuclear uncertainties that affect the master formulae provided in this paper. In future the theoretical uncertainties can be included in the fits using `smelli` program [146].

## Acknowledgements

We acknowledge several useful discussions with W. Dekens and M. Misiak. JK and EM are supported by the U.S. Department of Energy through the Los Alamos National Laboratory and by the Laboratory Directed Research and Development program of Los Alamos National Laboratory under project numbers 20220706PRD1 and 20240078DR. Los Alamos National Laboratory is operated by Triad National Security, LLC, for the National Nuclear Security Administration of U.S. Department of Energy (Contract No. 89233218CNA000001). We acknowledge support from the DOE Topical Collaboration “Nuclear Theory for New Physics,” award No. DE-SC0023663.

## A Additional Formulae

In this section, we provide some additional master formulae for the  $\omega_{\text{ThO}}$ ,  $\omega_{\text{YbF}}$  (15) and proton EDM (16).

$\alpha_I^{\text{ThO}}(\mu_{ew})$ for the $\omega_{\text{ThO}}$			
$n_f = 3 + 1$		$n_f = 5 + 3$	
$[C_{e\gamma}]_{11}$	$(9.9 \pm 2.1) \cdot 10^{12}$	$[C_{eu}^{S,RR}]_{1122}$	$(-3.2 \pm 0.6) \cdot 10^6$
$[C_{ee}^{S,RR}]_{1111}$	$(9.4 \pm 2.1) \cdot 10^4$	$[C_{eu}^{T,RR}]_{1122}$	$(1.3 \pm 0.3) \cdot 10^9$
$[C_{eu}^{S,RR}]_{1111}$	$(1.5 \pm 0.3) \cdot 10^9$	$[C_{ed}^{S,RR}]_{1133}$	$(-1.3 \pm 0.2) \cdot 10^6$
$[C_{ed}^{S,RR}]_{1111}$	$(1.5 \pm 0.3) \cdot 10^9$	$[C_{ed}^{T,RR}]_{1133}$	$(-1.7 \pm 0.3) \cdot 10^9$
$[C_{ed}^{S,RR}]_{1122}$	$(1.1 \pm 0.2) \cdot 10^8$	$[C_{ee}^{S,RR}]_{1122}$	$(-2.0 \pm 0.4) \cdot 10^5$
$[C_{eu}^{S,RL}]_{1111}$	$(1.5 \pm 0.3) \cdot 10^9$	$[C_{ee}^{S,RR}]_{1133}$	$(-4.4 \pm 0.7) \cdot 10^6$
$[C_{ed}^{S,RL}]_{1111}$	$(1.5 \pm 0.3) \cdot 10^9$	$[C_{ee}^{S,RR}]_{1221}$	$(9.9 \pm 2.0) \cdot 10^6$
$[C_{ed}^{S,RL}]_{1122}$	$(1.1 \pm 0.3) \cdot 10^8$	$[C_{ee}^{S,RR}]_{1331}$	$(1.9 \pm 0.4) \cdot 10^8$
$[C_{eu}^{T,RR}]_{1111}$	$(-8.7 \pm 1.6) \cdot 10^8$	$[C_{ee}^{V,LR}]_{1221}$	$(-3.2 \pm 0.6) \cdot 10^6$
$[C_{ed}^{T,RR}]_{1111}$	$(4.4 \pm 0.8) \cdot 10^8$	$[C_{ee}^{V,LR}]_{1331}$	$(-5.1 \pm 1.0) \cdot 10^7$
$[C_{ed}^{T,RR}]_{1122}$	$(3.1 \pm 0.5) \cdot 10^8$		-
$\alpha_I^{\text{YbF}}(\mu_{ew})$ for the $\omega_{\text{YbF}}$			
$n_f = 3 + 1$		$n_f = 5 + 3$	
$[C_{e\gamma}]_{11}$	$(1.6 \pm 0.1) \cdot 10^{12}$	$[C_{eu}^{S,RR}]_{1122}$	$(-5.2 \pm 0.4) \cdot 10^5$
$[C_{ee}^{S,RR}]_{1111}$	$(1.5 \pm 0.1) \cdot 10^4$	$[C_{eu}^{T,RR}]_{1122}$	$(2.1 \pm 0.2) \cdot 10^8$
$[C_{eu}^{S,RR}]_{1111}$	$(1.4 \pm 0.2) \cdot 10^8$	$[C_{ed}^{S,RR}]_{1133}$	$(-2.1 \pm 0.2) \cdot 10^5$
$[C_{ed}^{S,RR}]_{1111}$	$(1.4 \pm 0.2) \cdot 10^8$	$[C_{ed}^{T,RR}]_{1133}$	$(-2.7 \pm 0.2) \cdot 10^8$
$[C_{ed}^{S,RR}]_{1122}$	$(1.1 \pm 0.1) \cdot 10^7$	$[C_{ee}^{S,RR}]_{1122}$	$(-3.3 \pm 0.2) \cdot 10^4$
$[C_{eu}^{S,RL}]_{1111}$	$(1.4 \pm 0.2) \cdot 10^8$	$[C_{ee}^{S,RR}]_{1133}$	$(-7.1 \pm 0.5) \cdot 10^5$
$[C_{ed}^{S,RL}]_{1111}$	$(1.4 \pm 0.2) \cdot 10^8$	$[C_{ee}^{S,RR}]_{1221}$	$(1.6 \pm 0.1) \cdot 10^6$
$[C_{ed}^{S,RL}]_{1122}$	$(1.1 \pm 0.1) \cdot 10^7$	$[C_{ee}^{S,RR}]_{1331}$	$(3.1 \pm 0.2) \cdot 10^7$
$[C_{eu}^{T,RR}]_{1111}$	$(-1.3 \pm 0.1) \cdot 10^8$	$[C_{ee}^{V,LR}]_{1221}$	$(-5.1 \pm 0.4) \cdot 10^5$
$[C_{ed}^{T,RR}]_{1111}$	$(6.5 \pm 0.5) \cdot 10^7$	$[C_{ee}^{V,LR}]_{1331}$	$(-8.3 \pm 0.7) \cdot 10^6$
$[C_{ed}^{T,RR}]_{1122}$	$(5.1 \pm 0.4) \cdot 10^7$		-

**Table 15:** Master Formulae for  $\omega_{\text{ThO}}$  and  $\omega_{\text{YbF}}$  in WET in the JMS basis at the EW scale. The  $\alpha_I^{\text{ThO}}$  and  $\alpha_I^{\text{YbF}}$  have units of (mrad/s)TeV<sup>2</sup> and (mrad/s)TeV for the 4f and dipole operators, respectively. The 90% CL upper bound on  $\omega_{\text{ThO}}$  and  $\omega_{\text{YbF}}$  are 1.3mrad/s and 23.5mrad/s, respectively.

$\alpha_I^p(\mu_{ew})$ for proton EDM					
$n_f = 3 + 1$		$n_f = 4 + 1$		$n_f = 5 + 3$	
$C_{\tilde{G}}$	$(-7.6 \pm 3.8) \cdot 10^{-22}$	$[C_{uG}]_{22}$	$(-1.1 \pm 0.5) \cdot 10^{-20}$	$[C_{dG}]_{33}$	$(-1.5 \pm 0.8) \cdot 10^{-21}$
$[C_{dG}]_{11}$	$(2.1 \pm 1.0) \cdot 10^{-17}$	$[C_{u\gamma}]_{22}$	$(1.0 \pm 0.5) \cdot 10^{-21}$	$[C_{d\gamma}]_{33}$	$(-2.9 \pm 1.4) \cdot 10^{-23}$
$[C_{dG}]_{22}$	$(1.5 \pm 0.9) \cdot 10^{-20}$	$[C_{uu}^{S1,RR}]_{2222}$	$(7.8 \pm 3.9) \cdot 10^{-25}$	$[C_{uddu}^{V1,LR}]_{1331}$	$(-1.5 \pm 0.7) \cdot 10^{-21}$
$[C_{uG}]_{11}$	$(4.8 \pm 1.8) \cdot 10^{-17}$	$[C_{uu}^{S8,RR}]_{2222}$	$(-1.8 \pm 0.9) \cdot 10^{-25}$	$[C_{uddu}^{V8,LR}]_{1331}$	$(-8.1 \pm 2.0) \cdot 10^{-22}$
$[C_{d\gamma}]_{11}$	$(2.3 \pm 0.2) \cdot 10^{-17}$	$[C_{uu}^{S1,RR}]_{1122}$	$(5.7 \pm 2.9) \cdot 10^{-22}$	$[C_{dd}^{V1,LR}]_{1331}$	$(-6.1 \pm 3.7) \cdot 10^{-22}$
$[C_{d\gamma}]_{22}$	$(3.0 \pm 1.8) \cdot 10^{-19}$	$[C_{uu}^{S8,RR}]_{1122}$	$(3.8 \pm 8.2) \cdot 10^{-23}$	$[C_{dd}^{V8,LR}]_{1331}$	$(5.1 \pm 1.0) \cdot 10^{-22}$
$[C_{u\gamma}]_{11}$	$(-9.3 \pm 0.4) \cdot 10^{-17}$	$[C_{ud}^{S1,RR}]_{2211}$	$(2.9 \pm 1.3) \cdot 10^{-22}$	$[C_{dd}^{V1,LR}]_{2332}$	$(1.1 \pm 0.6) \cdot 10^{-24}$
$[C_{uddu}^{V1,LR}]_{1111}$	$(5.9 \pm 2.9) \cdot 10^{-22}$	$[C_{ud}^{S8,RR}]_{2211}$	$(1.2 \pm 0.4) \cdot 10^{-22}$	$[C_{dd}^{V8,LR}]_{2332}$	$(4.1 \pm 2.2) \cdot 10^{-24}$
$[C_{uddu}^{V8,LR}]_{1111}$	$(8.9 \pm 4.7) \cdot 10^{-22}$	$[C_{ud}^{S1,RR}]_{2222}$	$(1.5 \pm 1.4) \cdot 10^{-26}$	$[C_{dd}^{S1,RR}]_{2332}$	$(4.1 \pm 2.2) \cdot 10^{-24}$
$[C_{uddu}^{V1,LR}]_{1221}$	$(1.1 \pm 0.5) \cdot 10^{-21}$	$[C_{ud}^{S8,RR}]_{2222}$	$(5.1 \pm 2.8) \cdot 10^{-25}$	$[C_{dd}^{S1,RR}]_{3333}$	$(3.0 \pm 1.5) \cdot 10^{-25}$
$[C_{uddu}^{V8,LR}]_{1221}$	$(1.7 \pm 0.8) \cdot 10^{-21}$	$[C_{ud}^{S1,RR}]_{2112}$	$(-1.3 \pm 0.5) \cdot 10^{-21}$	$[C_{dd}^{S8,RR}]_{3333}$	$(-6.4 \pm 3.1) \cdot 10^{-26}$
$[C_{dd}^{V1,LR}]_{1221}$	$(5.1 \pm 2.7) \cdot 10^{-22}$	$[C_{uddu}^{S1,RR}]_{2112}$	$(-3.6 \pm 5.8) \cdot 10^{-23}$	$[C_{dd}^{S1,RR}]_{1133}$	$(3.8 \pm 1.9) \cdot 10^{-22}$
$[C_{dd}^{V8,LR}]_{1221}$	$(7.8 \pm 4.0) \cdot 10^{-22}$	$[C_{uddu}^{S8,RR}]_{2112}$	$(-2.4 \pm 1.5) \cdot 10^{-24}$	$[C_{dd}^{S8,RR}]_{1133}$	$(9.6 \pm 5.3) \cdot 10^{-23}$
$[C_{uu}^{S1,RR}]_{1111}$	$(-1.3 \pm 0.7) \cdot 10^{-21}$	$[C_{uu}^{S1,RR}]_{2222}$	$(-1.9 \pm 1.2) \cdot 10^{-24}$	$[C_{dd}^{S1,RR}]_{2233}$	$(1.3 \pm 0.8) \cdot 10^{-25}$
$[C_{uu}^{S8,RR}]_{1111}$	$(4.1 \pm 2.6) \cdot 10^{-22}$	$[C_{uu}^{S8,RR}]_{1221}$	$(-1.8 \pm 1.2) \cdot 10^{-21}$	$[C_{dd}^{S8,RR}]_{2233}$	$(-3.7 \pm 2.4) \cdot 10^{-25}$
$[C_{dd}^{S1,RR}]_{1111}$	$(-6.2 \pm 3.6) \cdot 10^{-22}$	$[C_{uu}^{S8,RR}]_{1221}$	$(8.3 \pm 1.3) \cdot 10^{-22}$	$[C_{dd}^{S1,RR}]_{1331}$	$(-2.3 \pm 1.1) \cdot 10^{-21}$
$[C_{dd}^{S8,RR}]_{1111}$	$(1.9 \pm 0.9) \cdot 10^{-22}$	$[C_{uu}^{V1,LR}]_{2112}$	$(-2.5 \pm 0.9) \cdot 10^{-22}$	$[C_{dd}^{S8,RR}]_{1331}$	$(5.2 \pm 1.6) \cdot 10^{-22}$
$[C_{dd}^{S1,RR}]_{2222}$	$(1.0 \pm 0.6) \cdot 10^{-25}$	$[C_{uu}^{V8,LR}]_{2112}$	$(-1.5 \pm 0.3) \cdot 10^{-22}$	$[C_{dd}^{S1,RR}]_{2332}$	$(1.5 \pm 0.9) \cdot 10^{-24}$
$[C_{dd}^{S8,RR}]_{2222}$	$(1.2 \pm 0.6) \cdot 10^{-25}$	$[C_{uu}^{V1,LR}]_{2222}$	$(-8.1 \pm 4.9) \cdot 10^{-25}$	$[C_{dd}^{S8,RR}]_{2332}$	$(2.9 \pm 1.7) \cdot 10^{-24}$
$[C_{dd}^{S1,RR}]_{1122}$	$(-1.4 \pm 0.9) \cdot 10^{-22}$	$[C_{uu}^{V8,LR}]_{2222}$	$(-2.8 \pm 1.6) \cdot 10^{-24}$	$[C_{ud}^{S1,RR}]_{1133}$	$(8.2 \pm 3.7) \cdot 10^{-22}$
$[C_{dd}^{S8,RR}]_{1122}$	$(5.1 \pm 2.3) \cdot 10^{-23}$	$[C_{uu}^{V1,LR}]_{1221}$	$(-2.9 \pm 18.4) \cdot 10^{-23}$	$[C_{ud}^{S8,RR}]_{1133}$	$(3.9 \pm 1.1) \cdot 10^{-22}$
$[C_{dd}^{S1,RR}]_{1221}$	$(-2.2 \pm 0.9) \cdot 10^{-22}$	$[C_{uu}^{V8,LR}]_{1221}$	$(9.4 \pm 0.6) \cdot 10^{-22}$	$[C_{ud}^{S1,RR}]_{1331}$	$(-6.2 \pm 2.5) \cdot 10^{-21}$
$[C_{dd}^{S8,RR}]_{1221}$	$(6.0 \pm 2.6) \cdot 10^{-23}$	-	-	$[C_{ud}^{S8,RR}]_{1331}$	$(-1.1 \pm 2.8) \cdot 10^{-22}$
$[C_{ud}^{S1,RR}]_{1111}$	$(-4.8 \pm 2.5) \cdot 10^{-22}$	-	-	$[C_{ud}^{S1,RR}]_{2233}$	$(-2.1 \pm 1.2) \cdot 10^{-25}$
$[C_{ud}^{S8,RR}]_{1111}$	$(1.5 \pm 0.8) \cdot 10^{-22}$	-	-	$[C_{ud}^{S8,RR}]_{2233}$	$(-6.8 \pm 3.3) \cdot 10^{-26}$
$[C_{ud}^{S1,RR}]_{1122}$	$(-3.0 \pm 1.7) \cdot 10^{-22}$	-	-	$[C_{ud}^{S1,RR}]_{2332}$	$(1.4 \pm 0.6) \cdot 10^{-24}$
$[C_{ud}^{S8,RR}]_{1122}$	$(1.1 \pm 0.5) \cdot 10^{-22}$	-	-	$[C_{ud}^{S8,RR}]_{2332}$	$(-1.7 \pm 0.9) \cdot 10^{-25}$
$[C_{uddu}^{S1,RR}]_{1111}$	$(-4.9 \pm 2.5) \cdot 10^{-22}$	-	-	$[C_{uddu}^{V1,LR}]_{2332}$	$(3.8 \pm 1.8) \cdot 10^{-25}$
$[C_{uddu}^{S8,RR}]_{1111}$	$(1.5 \pm 0.8) \cdot 10^{-22}$	-	-	$[C_{uddu}^{V8,LR}]_{2332}$	$(-1.0 \pm 0.5) \cdot 10^{-25}$
$[C_{uddu}^{S1,RR}]_{1221}$	$(-5.1 \pm 1.8) \cdot 10^{-22}$	-	-	-	-
$[C_{uddu}^{S8,RR}]_{1221}$	$(9.7 \pm 5.3) \cdot 10^{-23}$	-	-	-	-

**Table 16:** Master Formula for  $d_p$  in WET in the JMS basis at the EW scale. The  $\alpha_I^p$  have units of e-cm.TeV<sup>2</sup> and e-cm.TeV for the four-fermion and dipole operators, respectively.

## References

- [1] A. D. Sakharov, *Violation of CP Invariance, C asymmetry, and baryon asymmetry of the universe*, *Pisma Zh. Eksp. Teor. Fiz.* **5** (1967) 32–35.
- [2] M. B. Gavela, M. Lozano, J. Orloff, and O. Pene, *Standard model CP violation and baryon asymmetry. Part 1: Zero temperature*, *Nucl. Phys. B* **430** (1994) 345–381, [[hep-ph/9406288](#)].
- [3] M. B. Gavela, P. Hernandez, J. Orloff, and O. Pene, *Standard model CP violation and baryon asymmetry*, *Mod. Phys. Lett. A* **9** (1994) 795–810, [[hep-ph/9312215](#)].
- [4] M. B. Gavela, P. Hernandez, J. Orloff, O. Pene, and C. Quimbay, *Standard model CP violation and baryon asymmetry. Part 2: Finite temperature*, *Nucl. Phys. B* **430** (1994) 382–426, [[hep-ph/9406289](#)].
- [5] P. Huet and E. Sather, *Electroweak baryogenesis and standard model CP violation*, *Phys. Rev. D* **51** (1995) 379–394, [[hep-ph/9404302](#)].
- [6] I. B. Khriplovich, *Quark Electric Dipole Moment and Induced  $\theta$  Term in the Kobayashi-Maskawa Model*, *Phys. Lett. B* **173** (1986) 193–196.
- [7] A. Czarnecki and B. Krause, *Neutron electric dipole moment in the standard model: Valence quark contributions*, *Phys. Rev. Lett.* **78** (1997) 4339–4342, [[hep-ph/9704355](#)].
- [8] T. Mannel and N. Uraltsev, *Loop-Less Electric Dipole Moment of the Nucleon in the Standard Model*, *Phys. Rev. D* **85** (2012) 096002, [[arXiv:1202.6270](#)].
- [9] C.-Y. Seng, *Reexamination of The Standard Model Nucleon Electric Dipole Moment*, *Phys. Rev. C* **91** (2015), no. 2 025502, [[arXiv:1411.1476](#)].
- [10] M. Pospelov and A. Ritz, *Electric dipole moments as probes of new physics*, *Annals Phys.* **318** (2005) 119–169, [[hep-ph/0504231](#)].
- [11] T. Chupp, P. Fierlinger, M. Ramsey-Musolf, and J. Singh, *Electric Dipole Moments of the Atoms, Molecules, Nuclei and Particles*, [arXiv:1710.02504](#).
- [12] R. Alarcon et al., *Electric dipole moments and the search for new physics*, in *Snowmass 2021*, 3, 2022. [arXiv:2203.08103](#).
- [13] A. Buras, *Gauge Theory of Weak Decays*. Cambridge University Press, 6, 2020.
- [14] E. E. Jenkins, A. V. Manohar, and P. Stoffer, *Low-Energy Effective Field Theory below the Electroweak Scale: Operators and Matching*, *JHEP* **03** (2018) 016, [[arXiv:1709.04486](#)].
- [15] E. E. Jenkins, A. V. Manohar, and P. Stoffer, *Low-Energy Effective Field Theory below the Electroweak Scale: Anomalous Dimensions*, *JHEP* **01** (2018) 084, [[arXiv:1711.05270](#)].
- [16] W. Buchmuller and D. Wyler, *Effective Lagrangian Analysis of New Interactions and Flavor Conservation*, *Nucl. Phys.* **B268** (1986) 621–653.
- [17] B. Grzadkowski, M. Iskrzynski, M. Misiak, and J. Rosiek, *Dimension-Six Terms in the Standard Model Lagrangian*, *JHEP* **1010** (2010) 085, [[arXiv:1008.4884](#)].
- [18] G. Buchalla, O. Catà, and C. Krause, *Complete Electroweak Chiral Lagrangian with a Light Higgs at NLO*, *Nucl. Phys. B* **880** (2014) 552–573, [[arXiv:1307.5017](#)]. [Erratum: *Nucl.Phys.B* 913, 475–478 (2016)].

- [19] G. Buchalla, O. Cata, A. Celis, M. Knecht, and C. Krause, *Complete One-Loop Renormalization of the Higgs-Electroweak Chiral Lagrangian*, *Nucl. Phys. B* **928** (2018) 93–106, [[arXiv:1710.06412](#)].
- [20] I. B. Khriplovich and S. K. Lamoreaux, *CP violation without strangeness: Electric dipole moments of particles, atoms, and molecules*. 1997.
- [21] J. Engel, M. J. Ramsey-Musolf, and U. van Kolck, *Electric Dipole Moments of Nucleons, Nuclei, and Atoms: The Standard Model and Beyond*, *Prog. Part. Nucl. Phys.* **71** (2013) 21–74, [[arXiv:1303.2371](#)].
- [22] J. de Vries, E. Mereghetti, R. G. E. Timmermans, and U. van Kolck, *The Effective Chiral Lagrangian From Dimension-Six Parity and Time-Reversal Violation*, *Annals Phys.* **338** (2013) 50–96, [[arXiv:1212.0990](#)].
- [23] J. Brod, U. Haisch, and J. Zupan, *Constraints on CP-violating Higgs couplings to the third generation*, *JHEP* **11** (2013) 180, [[arXiv:1310.1385](#)].
- [24] Y. T. Chien, V. Cirigliano, W. Dekens, J. de Vries, and E. Mereghetti, *Direct and indirect constraints on CP-violating Higgs-quark and Higgs-gluon interactions*, *JHEP* **02** (2016) 011, [[arXiv:1510.00725](#)].
- [25] J. Brod, J. M. Cornell, D. Skodras, and E. Stamou, *Global constraints on Yukawa operators in the standard model effective theory*, *JHEP* **08** (2022) 294, [[arXiv:2203.03736](#)].
- [26] H. Bahl, E. Fuchs, S. Heinemeyer, J. Katzy, M. Menen, K. Peters, M. Saimpert, and G. Weiglein, *Constraining the CP structure of Higgs-fermion couplings with a global LHC fit, the electron EDM and baryogenesis*, *Eur. Phys. J. C* **82** (2022), no. 7 604, [[arXiv:2202.11753](#)].
- [27] E. Fuchs, M. Losada, Y. Nir, and Y. Viernik, *CP violation from  $\tau$ ,  $t$  and  $b$  dimension-6 Yukawa couplings - interplay of baryogenesis, EDM and Higgs physics*, *JHEP* **05** (2020) 056, [[arXiv:2003.00099](#)].
- [28] J. Brod, Z. Polonsky, and E. Stamou, *A Precise Electron EDM Constraint on CP-odd Heavy-Quark Yukawas*, [arXiv:2306.12478](#).
- [29] V. Cirigliano, W. Dekens, J. de Vries, and E. Mereghetti, *Constraining the top-Higgs sector of the Standard Model Effective Field Theory*, *Phys. Rev.* **D94** (2016), no. 3 034031, [[arXiv:1605.04311](#)].
- [30] K. Fuyuto and M. Ramsey-Musolf, *Top Down Electroweak Dipole Operators*, [arXiv:1706.08548](#).
- [31] Y. Ema, T. Gao, and M. Pospelov, *Improved indirect limits on charm and bottom quark EDMs*, *JHEP* **07** (2022) 106, [[arXiv:2205.11532](#)].
- [32] U. Haisch and G. Koole, *Beautiful and charming chromodipole moments*, *JHEP* **09** (2021) 133, [[arXiv:2106.01289](#)].
- [33] W. Dekens and J. de Vries, *Renormalization Group Running of Dimension-Six Sources of Parity and Time-Reversal Violation*, *JHEP* **05** (2013) 149, [[arXiv:1303.3156](#)].
- [34] V. Cirigliano, A. Crivellin, W. Dekens, J. de Vries, M. Hoferichter, and E. Mereghetti, *CP Violation in Higgs-Gauge Interactions: From Tabletop Experiments to the LHC*, *Phys. Rev. Lett.* **123** (2019), no. 5 051801, [[arXiv:1903.03625](#)].

- [35] U. Haisch and A. Hala, *Bounds on CP-violating Higgs-gluon interactions: the case of vanishing light-quark Yukawa couplings*, *JHEP* **11** (2019) 117, [[arXiv:1909.09373](#)].
- [36] S. Alioli, V. Cirigliano, W. Dekens, J. de Vries, and E. Mereghetti, *Right-handed charged currents in the era of the Large Hadron Collider*, *JHEP* **05** (2017) 086, [[arXiv:1703.04751](#)].
- [37] M. Endo and D. Ueda, *Nuclear EDM from SMEFT flavor-changing operator*, *JHEP* **04** (2020) 053, [[arXiv:1911.10805](#)].
- [38] S. Fajfer, J. F. Kamenik, N. Košnik, A. Smolkovič, and M. Tamaro, *New Physics in CP violating and flavour changing quark dipole transitions*, *JHEP* **10** (2023) 133, [[arXiv:2306.16471](#)].
- [39] J. Kley, T. Theil, E. Venturini, and A. Weiler, *Electric dipole moments at one-loop in the dimension-6 SMEFT*, *Eur. Phys. J. C* **82** (2022), no. 10 926, [[arXiv:2109.15085](#)].
- [40] D. M. Straub, *flavio: a Python package for flavour and precision phenomenology in the Standard Model and beyond*, [arXiv:1810.08132](#).
- [41] G. Buchalla, A. J. Buras, and M. E. Lautenbacher, *Weak decays beyond leading logarithms*, *Rev. Mod. Phys.* **68** (1996) 1125–1144, [[hep-ph/9512380](#)].
- [42] J. Aebischer, A. Crivellin, M. Fael, and C. Greub, *Matching of gauge invariant dimension-six operators for  $b \rightarrow s$  and  $b \rightarrow c$  transitions*, *JHEP* **05** (2016) 037, [[arXiv:1512.02830](#)].
- [43] W. Dekens and P. Stoffer, *Low-energy effective field theory below the electroweak scale: matching at one loop*, *JHEP* **10** (2019) 197, [[arXiv:1908.05295](#)].
- [44] J. Aebischer, J. Kumar, and D. M. Straub, *Wilson: a Python package for the running and matching of Wilson coefficients above and below the electroweak scale*, *Eur. Phys. J.* **C78** (2018), no. 12 1026, [[arXiv:1804.05033](#)].
- [45] J. Aebischer et al., *WCxf: an exchange format for Wilson coefficients beyond the Standard Model*, [arXiv:1712.05298](#).
- [46] R. D. Peccei and H. R. Quinn, *Constraints Imposed by CP Conservation in the Presence of Instantons*, *Phys. Rev.* **D16** (1977) 1791–1797.
- [47] R. D. Peccei and H. R. Quinn, *CP Conservation in the Presence of Instantons*, *Phys. Rev. Lett.* **38** (1977) 1440–1443.
- [48] J. Bühler and P. Stoffer, *One-loop matching of CP-odd four-quark operators to the gradient-flow scheme*, *JHEP* **08** (2023) 194, [[arXiv:2304.00985](#)].
- [49] **ACME** Collaboration, V. Andreev et al., *Improved limit on the electric dipole moment of the electron*, *Nature* **562** (2018), no. 7727 355–360.
- [50] T. S. Roussy et al., *An improved bound on the electron’s electric dipole moment*, *Science* **381** (2023), no. 6653 adg4084, [[arXiv:2212.11841](#)].
- [51] D. M. Kara, I. J. Smallman, J. J. Hudson, B. E. Sauer, M. R. Tarbutt, and E. A. Hinds, *Measurement of the electron’s electric dipole moment using YbF molecules: methods and data analysis*, *New J. Phys.* **14** (2012) 103051, [[arXiv:1208.4507](#)].
- [52] C. Abel et al., *Measurement of the Permanent Electric Dipole Moment of the Neutron*, *Phys. Rev. Lett.* **124** (2020), no. 8 081803, [[arXiv:2001.11966](#)].

- [53] W. C. Griffith, M. D. Swallows, T. H. Loftus, M. V. Romalis, B. R. Heckel, and E. N. Fortson, *Improved Limit on the Permanent Electric Dipole Moment of Hg-199*, *Phys. Rev. Lett.* **102** (2009) 101601, [[arXiv:0901.2328](#)].
- [54] N. Sachdeva et al., *New Limit on the Permanent Electric Dipole Moment of  $^{129}\text{Xe}$  using  $^3\text{He}$  Comagnetometry and SQUID Detection*, *Phys. Rev. Lett.* **123** (2019), no. 14 143003, [[arXiv:1902.02864](#)].
- [55] R. H. Parker et al., *First Measurement of the Atomic Electric Dipole Moment of  $^{225}\text{Ra}$* , *Phys. Rev. Lett.* **114** (2015), no. 23 233002, [[arXiv:1504.07477](#)].
- [56] T. Chupp and M. Ramsey-Musolf, *Electric Dipole Moments: A Global Analysis*, *Phys. Rev. C* **91** (2015), no. 3 035502, [[arXiv:1407.1064](#)].
- [57] G. Arrowsmith-Kron et al., *Opportunities for Fundamental Physics Research with Radioactive Molecules*, [arXiv:2302.02165](#).
- [58] **n2EDM** Collaboration, N. J. Ayres et al., *The design of the n2EDM experiment: nEDM Collaboration*, *Eur. Phys. J. C* **81** (2021), no. 6 512, [[arXiv:2101.08730](#)].
- [59] D. Wurm et al., *The PanEDM Neutron Electric Dipole Moment Experiment at the ILL*, *EPJ Web Conf.* **219** (2019) 02006, [[arXiv:1911.09161](#)].
- [60] J. W. Martin, *Current status of neutron electric dipole moment experiments*, *J. Phys. Conf. Ser.* **1643** (2020), no. 1 012002.
- [61] T. M. Ito et al., *Performance of the upgraded ultracold neutron source at Los Alamos National Laboratory and its implication for a possible neutron electric dipole moment experiment*, *Phys. Rev. C* **97** (2018), no. 1 012501, [[arXiv:1710.05182](#)].
- [62] J. Alexander et al., *The storage ring proton EDM experiment*, [arXiv:2205.00830](#).
- [63] B. Graner, Y. Chen, E. G. Lindahl, and B. R. Heckel, *Reduced Limit on the Permanent Electric Dipole Moment of Hg199*, *Phys. Rev. Lett.* **116** (2016), no. 16 161601, [[arXiv:1601.04339](#)]. [Erratum: *Phys.Rev.Lett.* 119, 119901 (2017)].
- [64] K. Kumar, Z.-T. Lu, and M. J. Ramsey-Musolf, *Working Group Report: Nucleons, Nuclei, and Atoms*, in *Workshop on Fundamental Physics at the Intensity Frontier*, pp. 159–214, 12, 2013. [arXiv:1312.5416](#).
- [65] C. Alexandrou, S. Bacchio, M. Constantinou, J. Finkenrath, K. Hadjiyiannakou, K. Jansen, G. Koutsou, and A. Vaquero Aviles-Casco, *Nucleon axial, tensor, and scalar charges and  $\sigma$ -terms in lattice QCD*, *Phys. Rev. D* **102** (2020), no. 5 054517, [[arXiv:1909.00485](#)].
- [66] W. Dekens, E. E. Jenkins, A. V. Manohar, and P. Stoffer, *Non-perturbative effects in  $\mu \rightarrow e\gamma$* , *JHEP* **01** (2019) 088, [[arXiv:1810.05675](#)].
- [67] J. Aebischer, W. Dekens, E. E. Jenkins, A. V. Manohar, D. Sengupta, and P. Stoffer, *Effective field theory interpretation of lepton magnetic and electric dipole moments*, *JHEP* **07** (2021) 107, [[arXiv:2102.08954](#)].
- [68] V. Cirigliano, K. Fuyuto, C. Lee, E. Mereghetti, and B. Yan, *Charged Lepton Flavor Violation at the EIC*, *JHEP* **03** (2021) 256, [[arXiv:2102.06176](#)].
- [69] M. Knecht and A. Nyffeler, *Resonance estimates of  $O(p^{*6})$  low-energy constants and QCD short distance constraints*, *Eur. Phys. J. C* **21** (2001) 659–678, [[hep-ph/0106034](#)].
- [70] V. Mateu and J. Portoles, *Form-factors in radiative pion decay*, *Eur. Phys. J. C* **52** (2007) 325–338, [[arXiv:0706.1039](#)].



- [71] O. Cata and V. Mateu, *Novel patterns for vector mesons from the large- $N(c)$  limit*, *Phys. Rev. D* **77** (2008) 116009, [[arXiv:0801.4374](#)].
- [72] **Muon (g-2) Collaboration**, G. W. Bennett et al., *An Improved Limit on the Muon Electric Dipole Moment*, *Phys. Rev. D* **80** (2009) 052008, [[arXiv:0811.1207](#)].
- [73] **Belle Collaboration**, K. Inami et al., *An improved search for the electric dipole moment of the  $\tau$  lepton*, *JHEP* **04** (2022) 110, [[arXiv:2108.11543](#)].
- [74] **Particle Data Group Collaboration**, R. L. Workman and Others, *Review of Particle Physics*, *PTEP* **2022** (2022) 083C01.
- [75] M. Hoferichter, J. Ruiz de Elvira, B. Kubis, and U.-G. Meißner, *Roy–Steiner-equation analysis of pion–nucleon scattering*, *Phys. Rept.* **625** (2016) 1–88, [[arXiv:1510.06039](#)].
- [76] **Flavour Lattice Averaging Group (FLAG) Collaboration**, Y. Aoki et al., *FLAG Review 2021*, *Eur. Phys. J. C* **82** (2022), no. 10 869, [[arXiv:2111.09849](#)].
- [77] S. Degenkolb, N. Elmer, T. Modak, M. Mühlleitner, and T. Plehn, *A Global View of the EDM Landscape*, [[arXiv:2403.02052](#)].
- [78] W. Dekens, J. de Vries, M. Jung, and K. K. Vos, *The phenomenology of electric dipole moments in models of scalar leptoquarks*, *JHEP* **01** (2019) 069, [[arXiv:1809.09114](#)].
- [79] R. Gupta, B. Yoon, T. Bhattacharya, V. Cirigliano, Y.-C. Jang, and H.-W. Lin, *Flavor diagonal tensor charges of the nucleon from (2+1+1)-flavor lattice QCD*, *Phys. Rev. D* **98** (2018), no. 9 091501, [[arXiv:1808.07597](#)].
- [80] T. Bhattacharya, V. Cirigliano, R. Gupta, E. Mereghetti, J.-S. Yoo, and B. Yoon, *Quark chromoelectric dipole moment operator on the lattice*, *Phys. Rev. D* **108** (2023), no. 7 074507, [[arXiv:2304.09929](#)].
- [81] M. Abramczyk, S. Aoki, T. Blum, T. Izubuchi, H. Ohki, and S. Syritsyn, *Lattice calculation of electric dipole moments and form factors of the nucleon*, *Phys. Rev. D* **96** (2017), no. 1 014501, [[arXiv:1701.07792](#)].
- [82] **SymLat Collaboration**, J. Kim, T. Luu, M. D. Rizik, and A. Shindler, *Nonperturbative renormalization of the quark chromoelectric dipole moment with the gradient flow: Power divergences*, *Phys. Rev. D* **104** (2021), no. 7 074516, [[arXiv:2106.07633](#)].
- [83] M. Pospelov and A. Ritz, *Neutron EDM from electric and chromoelectric dipole moments of quarks*, *Phys. Rev.* **D63** (2001) 073015, [[hep-ph/0010037](#)].
- [84] O. Lebedev, K. A. Olive, M. Pospelov, and A. Ritz, *Probing CP violation with the deuteron electric dipole moment*, *Phys. Rev. D* **70** (2004) 016003, [[hep-ph/0402023](#)].
- [85] K. Fuyuto, J. Hisano, and N. Nagata, *Neutron electric dipole moment induced by strangeness revisited*, *Phys. Rev. D* **87** (2013), no. 5 054018, [[arXiv:1211.5228](#)].
- [86] C.-Y. Seng, J. de Vries, E. Mereghetti, H. H. Patel, and M. Ramsey-Musolf, *Nucleon electric dipole moments and the isovector parity- and time-reversal-odd pion–nucleon coupling*, *Phys. Lett. B* **736** (2014) 147–153, [[arXiv:1401.5366](#)].
- [87] J. de Vries, E. Mereghetti, C.-Y. Seng, and A. Walker-Loud, *Lattice QCD spectroscopy for hadronic CP violation*, *Phys. Lett. B* **766** (2017) 254–262, [[arXiv:1612.01567](#)].
- [88] T. Bhattacharya, V. Cirigliano, R. Gupta, E. Mereghetti, and B. Yoon, *Dimension-5 CP-odd operators: QCD mixing and renormalization*, *Phys. Rev.* **D92** (2015), no. 11 114026, [[arXiv:1502.07325](#)].

- [89] E. Mereghetti, C. J. Monahan, M. D. Rizik, A. Shindler, and P. Stoffer, *One-loop matching for quark dipole operators in a gradient-flow scheme*, *JHEP* **04** (2022) 050, [[arXiv:2111.11449](#)].
- [90] D. A. Demir, M. Pospelov, and A. Ritz, *Hadronic EDMs, the Weinberg operator, and light gluinos*, *Phys. Rev.* **D67** (2003) 015007, [[hep-ph/0208257](#)].
- [91] U. Haisch and A. Hala, *Sum rules for CP-violating operators of Weinberg type*, *JHEP* **11** (2019) 154, [[arXiv:1909.08955](#)].
- [92] T. Bhattacharya, V. Cirigliano, R. Gupta, E. Mereghetti, and B. Yoon, *Calculation of neutron electric dipole moment due to the QCD topological term, Weinberg three-gluon operator and the quark chromoelectric moment*, *PoS LATTICE2021* (2022) 567, [[arXiv:2203.03746](#)].
- [93] V. Cirigliano, E. Mereghetti, and P. Stoffer, *Non-perturbative renormalization scheme for the CP -odd three-gluon operator*, *JHEP* **09** (2020) 094, [[arXiv:2004.03576](#)].
- [94] O. L. Crosas, C. J. Monahan, M. D. Rizik, A. Shindler, and P. Stoffer, *One-loop matching of the CP-odd three-gluon operator to the gradient flow*, *Phys. Lett. B* **847** (2023) 138301, [[arXiv:2308.16221](#)].
- [95] R. J. Crewther, P. Di Vecchia, G. Veneziano, and E. Witten, *Chiral Estimate of the Electric Dipole Moment of the Neutron in Quantum Chromodynamics*, *Phys. Lett. B* **88** (1979) 123. [Erratum: *Phys.Lett.B* 91, 487 (1980)].
- [96] J. Dragos, T. Luu, A. Shindler, J. de Vries, and A. Yousif, *Confirming the Existence of the strong CP Problem in Lattice QCD with the Gradient Flow*, *Phys. Rev. C* **103** (2021), no. 1 015202, [[arXiv:1902.03254](#)].
- [97] T. Bhattacharya, V. Cirigliano, R. Gupta, E. Mereghetti, and B. Yoon, *Contribution of the QCD  $\Theta$ -term to the nucleon electric dipole moment*, *Phys. Rev. D* **103** (2021), no. 11 114507, [[arXiv:2101.07230](#)].
- [98] C. M. Maekawa, E. Mereghetti, J. de Vries, and U. van Kolck, *The Time-Reversal- and Parity-Violating Nuclear Potential in Chiral Effective Theory*, *Nucl. Phys. A* **872** (2011) 117–160, [[arXiv:1106.6119](#)].
- [99] J. de Vries, E. Epelbaum, L. Girlanda, A. Gnech, E. Mereghetti, and M. Viviani, *Parity- and Time-Reversal-Violating Nuclear Forces*, *Front. in Phys.* **8** (2020) 218, [[arXiv:2001.09050](#)].
- [100] W. C. Haxton and E. M. Henley, *ENHANCED T VIOLATING NUCLEAR MOMENTS*, *Phys. Rev. Lett.* **51** (1983) 1937.
- [101] J. Engel, J. L. Friar, and A. C. Hayes, *Nuclear octupole correlations and the enhancement of atomic time reversal violation*, *Phys. Rev. C* **61** (2000) 035502, [[nucl-th/9910008](#)].
- [102] J. de Vries, E. Mereghetti, and A. Walker-Loud, *Baryon mass splittings and strong CP violation in SU(3) Chiral Perturbation Theory*, *Phys. Rev. C* **92** (2015), no. 4 045201, [[arXiv:1506.06247](#)].
- [103] V. Baluni, *CP Violating Effects in QCD*, *Phys. Rev. D* **19** (1979) 2227–2230.
- [104] M. Pospelov, *Best values for the CP odd meson nucleon couplings from supersymmetry*, *Phys. Lett. B* **530** (2002) 123–128, [[hep-ph/0109044](#)].
- [105] V. Cirigliano, W. Dekens, J. de Vries, and E. Mereghetti, *An  $\varepsilon'$  improvement from right-handed currents*, *Phys. Lett.* **B767** (2017) 1–9, [[arXiv:1612.03914](#)].

- [106] W. Dekens, J. de Vries, and S. Shain, *CP-violating axion interactions in effective field theory*, *JHEP* **07** (2022) 014, [[arXiv:2203.11230](#)].
- [107] V. Cirigliano, W. Dekens, M. Graesser, and E. Mereghetti, *Neutrinoless double beta decay and chiral SU(3)*, *Phys. Lett. B* **769** (2017) 460–464, [[arXiv:1701.01443](#)].
- [108] A. Nicholson et al., *Heavy physics contributions to neutrinoless double beta decay from QCD*, *Phys. Rev. Lett.* **121** (2018), no. 17 172501, [[arXiv:1805.02634](#)].
- [109] V. Spevak, N. Auerbach, and V. V. Flambaum, *Enhanced T odd P odd electromagnetic moments in reflection asymmetric nuclei*, *Phys. Rev. C* **56** (1997) 1357–1369, [[nucl-th/9612044](#)].
- [110] G. Barton, *Notes on the static parity nonconserving internucleon potential*, *Nuovo Cim.* **19** (1961) 512–527.
- [111] I. S. Towner and A. C. Hayes, *P, T violating nuclear matrix elements in the one meson exchange approximation*, *Phys. Rev. C* **49** (1994) 2391–2397, [[nucl-th/9402026](#)].
- [112] Y.-H. Song, R. Lazauskas, and V. Gudkov, *Nuclear electric dipole moment of three-body systems*, *Phys. Rev. C* **87** (2013), no. 1 015501, [[arXiv:1211.3762](#)].
- [113] Z. Yang, E. Mereghetti, L. Platter, M. R. Schindler, and J. Vanasse, *Electric dipole moments of three-nucleon systems in the pionless effective field theory*, *Phys. Rev. C* **104** (2021), no. 2 024002, [[arXiv:2011.01885](#)].
- [114] J. de Vries, A. Gnech, and S. Shain, *Renormalization of CP-violating nuclear forces*, *Phys. Rev. C* **103** (2021), no. 1 L012501, [[arXiv:2007.04927](#)].
- [115] M. Hubert and T. Fleig, *Electric dipole moments generated by nuclear Schiff moment interactions: A reassessment of the atoms Xe129 and Hg199 and the molecule TlF205*, *Phys. Rev. A* **106** (2022), no. 2 022817, [[arXiv:2203.04618](#)].
- [116] V. S. Prasanna, R. Mitra, and B. K. Sahoo, *Reappraisal of P, T-odd parameters from the improved calculation of electric dipole moment of 225Ra atom*, *J. Phys. B* **53** (2020), no. 19 195004.
- [117] V. F. Dmitriev and R. A. Sen'kov, *Schiff moment of the mercury nucleus and the proton dipole moment*, *Phys. Rev. Lett.* **91** (2003) 212303, [[nucl-th/0306050](#)].
- [118] K. Yanase, N. Shimizu, K. Higashiyama, and N. Yoshinaga, *Constraints on the nuclear Schiff moment from its correlation with electromagnetic properties*, [arXiv:2210.08498](#).
- [119] T. Fleig and M. Jung, *Model-independent determinations of the electron EDM and the role of diamagnetic atoms*, *JHEP* **07** (2018) 012, [[arXiv:1802.02171](#)].
- [120] T. Fleig and M. Jung,  *$\mathcal{P}, \mathcal{T}$ -odd interactions in atomic  $^{129}\text{Xe}$  and phenomenological applications*, *Phys. Rev. A* **103** (2021), no. 1 012807, [[arXiv:2009.07730](#)].
- [121] K. Gaul and R. Berger, *Global analysis of CP-violation in atoms, molecules and role of medium-heavy systems*, [arXiv:2312.08858](#).
- [122] K. Yanase, N. Yoshinaga, K. Higashiyama, and N. Yamanaka, *Electric dipole moment of  $^{199}\text{Hg}$  atom from P, CP-odd electron-nucleon interaction*, *Phys. Rev. D* **99** (2019), no. 7 075021, [[arXiv:1805.00419](#)].
- [123] J. Menendez, D. Gazit, and A. Schwenk, *Spin-dependent WIMP scattering off nuclei*, *Phys. Rev. D* **86** (2012) 103511, [[arXiv:1208.1094](#)].

- [124] J. S. M. Ginges and V. V. Flambaum, *Violations of fundamental symmetries in atoms and tests of unification theories of elementary particles*, *Phys. Rept.* **397** (2004) 63–154, [[physics/0309054](#)].
- [125] E. Braaten, C.-S. Li, and T.-C. Yuan, *The Evolution of Weinberg’s Gluonic CP Violation Operator*, *Phys. Rev. Lett.* **64** (1990) 1709.
- [126] M. Ciuchini, E. Franco, G. Martinelli, L. Reina, and L. Silvestrini, *Scheme independence of the effective Hamiltonian for  $b \rightarrow s\gamma$  and  $b \rightarrow sg$  decays*, *Phys. Lett.* **B316** (1993) 127–136, [[hep-ph/9307364](#)].
- [127] P. L. Cho and M. Misiak,  *$b \rightarrow s$  gamma decay in  $SU(2)_L \times SU(2)_R \times U(1)$  extensions of the Standard Model*, *Phys. Rev. D* **49** (1994) 5894–5903, [[hep-ph/9310332](#)].
- [128] W. Buchmüller, R. Rückl, and D. Wyler, *Leptoquarks in Lepton - Quark Collisions*, *Phys. Lett.* **B191** (1987) 442–448. [Erratum: *Phys. Lett.* **B448**, 320(1999)].
- [129] S. Hamoudou, J. Kumar, and D. London, *Dimension-8 SMEFT matching conditions for the low-energy effective field theory*, *JHEP* **03** (2023) 157, [[arXiv:2207.08856](#)].
- [130] J. Hisano, K. Tsumura, and M. J. S. Yang, *QCD Corrections to Neutron Electric Dipole Moment from Dimension-six Four-Quark Operators*, *Phys. Lett.* **B713** (2012) 473–480, [[arXiv:1205.2212](#)].
- [131] S. M. Barr and A. Zee, *Electric Dipole Moment of the Electron and of the Neutron*, *Phys. Rev. Lett.* **65** (1990) 21–24. [Erratum: *Phys. Rev. Lett.* **65**, 2920(1990)].
- [132] G. Blankenburg, J. Ellis, and G. Isidori, *Flavour-Changing Decays of a 125 GeV Higgs-like Particle*, *Phys. Lett. B* **712** (2012) 386–390, [[arXiv:1202.5704](#)].
- [133] **ATLAS** Collaboration, G. Aad et al., *A detailed map of Higgs boson interactions by the ATLAS experiment ten years after the discovery*, *Nature* **607** (2022), no. 7917 52–59, [[arXiv:2207.00092](#)]. [Erratum: *Nature* **612**, E24 (2022)].
- [134] **CMS** Collaboration, A. Tumasyan et al., *A portrait of the Higgs boson by the CMS experiment ten years after the discovery.*, *Nature* **607** (2022), no. 7917 60–68, [[arXiv:2207.00043](#)].
- [135] **ATLAS** Collaboration, G. Aad et al., *Direct constraint on the Higgs-charm coupling from a search for Higgs boson decays into charm quarks with the ATLAS detector*, *Eur. Phys. J. C* **82** (2022) 717, [[arXiv:2201.11428](#)].
- [136] **CMS** Collaboration, A. Tumasyan et al., *Search for Higgs Boson and Observation of Z Boson through their Decay into a Charm Quark-Antiquark Pair in Boosted Topologies in Proton-Proton Collisions at  $s=13$  TeV*, *Phys. Rev. Lett.* **131** (2023), no. 4 041801, [[arXiv:2211.14181](#)].
- [137] **LHC Higgs Cross Section Working Group** Collaboration, D. de Florian et al., *Handbook of LHC Higgs Cross Sections: 4. Deciphering the Nature of the Higgs Sector*, [[arXiv:1610.07922](#)].
- [138] C. Anastasiou and K. Melnikov, *Pseudoscalar Higgs boson production at hadron colliders in NNLO QCD*, *Phys. Rev. D* **67** (2003) 037501, [[hep-ph/0208115](#)].
- [139] R. V. Harlander and W. B. Kilgore, *Production of a pseudoscalar Higgs boson at hadron colliders at next-to-next-to leading order*, *JHEP* **10** (2002) 017, [[hep-ph/0208096](#)].

- [140] R. V. Harlander and W. B. Kilgore, *Higgs boson production in bottom quark fusion at next-to-next-to leading order*, *Phys. Rev. D* **68** (2003) 013001, [[hep-ph/0304035](#)].
- [141] **PDF4LHC Working Group** Collaboration, R. D. Ball et al., *The PDF4LHC21 combination of global PDF fits for the LHC Run III*, *J. Phys. G* **49** (2022), no. 8 080501, [[arXiv:2203.05506](#)].
- [142] S. Alioli, W. Dekens, M. Girard, and E. Mereghetti, *NLO QCD corrections to SM-EFT dilepton and electroweak Higgs boson production, matched to parton shower in POWHEG*, *JHEP* **08** (2018) 205, [[arXiv:1804.07407](#)].
- [143] M. Spira, *Higgs Boson Production and Decay at Hadron Colliders*, *Prog. Part. Nucl. Phys.* **95** (2017) 98–159, [[arXiv:1612.07651](#)].
- [144] **CMS** Collaboration, A. M. Sirunyan et al., *Measurements of  $t\bar{t}H$  Production and the CP Structure of the Yukawa Interaction between the Higgs Boson and Top Quark in the Diphoton Decay Channel*, *Phys. Rev. Lett.* **125** (2020), no. 6 061801, [[arXiv:2003.10866](#)].
- [145] **ATLAS** Collaboration, G. Aad et al., *CP Properties of Higgs Boson Interactions with Top Quarks in the  $t\bar{t}H$  and  $tH$  Processes Using  $H \rightarrow \gamma\gamma$  with the ATLAS Detector*, *Phys. Rev. Lett.* **125** (2020), no. 6 061802, [[arXiv:2004.04545](#)].
- [146] J. Aebischer, J. Kumar, P. Stangl, and D. M. Straub, *A Global Likelihood for Precision Constraints and Flavour Anomalies*, [arXiv:1810.07698](#).